INVOLVEMENT OF COLLAPSIN RESPONSE MEDIATOR PROTEIN 2

IN POSTTRAUMATIC SPROUTING IN ACQUIRED EPILEPSY

Sarah Marie Wilson

Accepted by the Graduate Faculty, of Indiana University, in partial
fulfillment of the requirements for the degree of Doctor of Philosophy.

_____

Gerry S. Oxford, Ph.D., Chair

_____

Rajesh Khanna, Ph.D.

Doctoral Committee

_____

Joanna Jen, M.D.,Ph.D.

_____

Zao C. Xu, M.D., Ph.D.

March 17, 2014

_____

Xiaoming Jin, Ph.D.

© 2014

Sarah Marie Wilson

DEDICATION

This thesis is dedicated to my parents for always pushing me to achieve my goals and to my husband for his unwavering support.

Sarah Marie Wilson

INVOLVEMENT OF COLLAPSIN RESPONSE MEDIATOR PROTEIN 2 IN

POSTTRAUMATIC SPROUTING IN ACQUIRED EPILEPSY

Posttraumatic epilepsy, the development of temporal lobe epilepsy (TLE) following traumatic brain injury, accounts for 20% of symptomatic epilepsy. Reorganization of mossy fibers within the hippocampus is a common pathological finding of TLE. Normal mossy fibers project into the CA3 region of the hippocampus where they form synapses with pyramidal cells. During TLE, mossy fibers are observed to innervate the inner molecular layer where they synapse onto the dendrites of other dentate granule cells, leading to the formation of recurrent excitatory circuits. To date, the molecular mechanisms contributing to mossy fiber sprouting are relatively unknown.

Recent focus has centered on the involvement of tropomycin-related kinase receptor B (TrkB), which culminates in glycogen synthase kinase 3β (GSK3β) inactivation. As the neurite outgrowth promoting collapsin response mediator protein 2 (CRMP2) is rendered inactive by GSK3β phosphorylation, events leading to inactivation of GSK3β should therefore increase CRMP2 activity. To determine the involvement of CRMP2 in mossy fiber sprouting, I developed a novel tool ((S)-LCM) for selectively targeting the ability of CRMP2 to enhance tubulin polymerization. Using (S)-LCM, it was demonstrated that increased neurite outgrowth following GSK3β inactivation is CRMP2 dependent. Importantly, TBI led to a decrease in GSK3β-phosphorylated CRMP2 within 24 hours which was secondary to the inactivation of GSK3β. The loss of

GSK3β-phosphorylated CRMP2 was maintained even at 4 weeks post-injury, despite the transience of GSK3β-inactivation.

Based on previous work, it was hypothesized that activity-dependent mechanisms may be responsible for the sustained loss of CRMP2 phosphorylation. Activity-dependent regulation of GSK3β-phosphorylated CRMP2 levels was observed that was attributed to a loss of priming by cyclin dependent kinase 5 (CDK5), which is required for subsequent phosphorylation by GSK3β. It was confirmed that the loss of GSK3β-phosphorylated CRMP2 at 4 weeks post-injury was likely due to decreased phosphorylation by CDK5. As TBI resulted in a sustained increase in CRMP2 activity, I attempted to prevent mossy fiber sprouting by targeting CRMP2 *in vivo* following TBI. While (*S*)-LCM treatment dramatically reduced mossy fiber sprouting following TBI, it did not differ significantly from vehicle-treated animals. Therefore, the necessity of CRMP2 in mossy fiber sprouting following TBI remains unknown.

Gerry S. Oxford, Ph.D.

TABLE OF CONTENTS

LIST OF TABLES

LIST OF FIGURES

FIGURE CONTRIBUTIONS

Figure 3.10. (*S*)- LCM does not alter slow inactivation of voltage-gated sodium channels

Electrophysiology performed by Xiao-Fang Yang of the Khanna Laboratory

Figure 4.3. Increased neurite outgrowth following OGD is CRMP2-dependent

Experiments performed with the assistance of the Xu Laboratory.

Figure 5.7 Effects of targeting CRMP2 *in vivo* on mossy fiber sprouting

Scoring of TIMM-stained sections was assisted by Rajesh Khanna, Ph.D. and Erik

Dustrude of the Khanna Laboratory

LIST OF ABBREVIATIONS

TLE	Temporal Lobe Epilepsy
AED	Antiepileptic Drug
GABA	Gamma-Aminobutyric Acid
TBI	Traumatic Brain Injury
SE	Status Epillepticus
GCL	Granule Cell Layer
PCL	Pyramidal Cell Layer
IML	Inner Molecular Layer
DH	Dentate Hilus
DG	Dentate Gyrus
TTX	Tetrodotoxin
cAMP	cyclic Adenosine Monophosphate
GAD	Glutamic Acid Decarboxylase
EPSC	Excitatory Post-Synaptic Current
EPSP	Excitatory Post-Synaptic Potential
mTOR	mammalian Target of Rapamycin
BDNF	Brain-Derived Neurotrophic Factor
Trk	Tropomycin-related Kinase Receptor
mRNA	messenger RNA
GSK	Glycogen Synthase Kinase
Akt	Protein Kinase B
PI3K	Phosphoinositide 3-Kinase
MAP	Microtubule-Associated Protein
NCAM	Neuronal Cell Adhesion Molecule
CRMP	Collapsin Response Mediator Protein
GTP	Guanosine Triphosphate
CDK5	Cyclin-Dependent Protein Kinase
CaMK	Calcium/calmodulin-Dependent Protein Kinase
ROCK	Rho-associated Protein Kinase
FYN	Tyrosine-protein Kinase FYN

PP	Protein Phosphatase
LCM	Lacosamide
VGSC	Voltage-gated Sodium Channel
RT	Room Temperature
HEPES	(4-(2-hydroxyethyl)-1-piperazineethanesulfonic acid)
EGFP	Enhanced Green Fluorescent Protein
MST	Microscale Thermophoresis
TBST	Tris-buffered Saline with Tween-20
siRNA	Small Interfering RNA
SDS-PAGE	Sodium Dodecyl Sulfate Polyacrylamide Gel Electrophoresis
PSD	Post-synaptic Density
GFAP	Glial Fibrillary Acid Protein
NF	Neurofilament
DAPI	4',6-diamido-2-phenylindole
PBS	Phosphate-buffered Saline
BSA	Bovine Serum Albumin
CAD	Catecholamine A-Differentiated
PVDF	Polyvinylidene Fluoride
HRP	Horseradish Peroxidase
OGD	Oxygen Glucose Deprivation
DIV	Days *In Vitro*
BSS	Balanced Salt Solution
CCI	Controlled Cortical Impact
DMSO	Dimethyl Sulfoxide
AUC	Area Under the Curve
SEM	Standard Error of the Mean
ANOVA	Analysis of Variance
PKC	Protein Kinase C
EEG	Electroencephalogram
PDK1	Phosphoinositide-dependent Kinase
PIP3	Phopshotidylinositol (3,4,5)-trisphosphate

CHAPTER 1. INTRODUCTION

1.1. Temporal Lobe Epilepsy: A Progressive, Acquired Phenomenon

Background

Nearly 2.3 million people in the United States alone are burdened by epilepsy (CDC, 2012), a neurological condition classified by spontaneously recurring seizures (Goddard et al., 1969), with an estimated 150,000 more diagnosed each year (Hirtz et al., 2007, (IOM), 2012). Outside of the United States, worldwide prevalence may reach as high as 6% in undeveloped countries (Burneo et al., 2005, Carpio and Hauser, 2009). It is estimated that nearly half of epilepsy cases are classified as complex partial seizures, the majority of which originate from foci within the temporal lobe (Hauser and Kurland, 1975, Manford et al., 1992a, b, Larner, 1995, Panayiotopoulos, 2005). While early symptoms of temporal lobe epilepsy (TLE) are well controlled with currently available anti-epileptic treatment strategies, as the disease progresses as many as 30% of patients develop medically-intractable seizures (Willmore, 1992, Wieser and Hane, 2004, Loscher and Schmidt, 2011). The basis of this advancement to an intractable state is likely to stem from the progressive nature of the disease rather than issues of pharmacological tolerance (Sutula, 2004). Unfortunately, while recent advances in antiepileptic drugs (AEDs) have reduced the risk of serious contraindications associated with first and second generation AEDs, they have not proven to be more efficacious in the treatment and/or prevention of epilepsy symptoms (Rogawski and Loscher, 2004b, a, Loscher and Schmidt, 2011, O'Dell et al., 2012). The lack of advancement in the treatment of TLE may be attributed to gaps in understanding of the mechanisms underlying its etiology.

Investigation of post-mortem tissue samples from TLE patients has highlighted various anatomical changes occurring within the hippocampus that may provide a

2

framework for understanding potential mechanisms (Margerison and Corsellis, 1966, de Lanerolle et al., 1989, Masukawa et al., 1989, Represa et al., 1989, Sutula et al., 1989, Geddes et al., 1990, Houser, 1990, Houser et al., 1990, Babb, 1991, Babb et al., 1991, McDonald et al., 1991, Masukawa et al., 1992). The most common pathological finding is the occurrence of hippocampal sclerosis, characterized by fibrous gliosis and overall atrophy of the hippocampal formation. These changes likely stem from selective loss of pyramidal cells within subregions CA1, CA3, and the hilus, that are not observed within the CA2 subregion or the granule cell layer (Margerison and Corsellis, 1966). Microscopic changes include alterations in excitatory and inhibitory neurotransmitter receptor expression, levels of peptidergic signaling molecules, and dramatic reorganization of both dendritic and axonal projections. Regional increases in ionic glutamate receptors have been observed within subregions CA1 and CA3, the entorhinal cortex, and the dentate gyrus (Represa et al., 1989, Geddes et al., 1990, McDonald et al., 1991). Alternatively, expression of GABA$_A$ receptors was decreased within subregions CA1 and CA4 (McDonald et al., 1991). Decreases in somatostatin and neuropeptide Y immunoreactivity within the hilus suggest an overall loss of inhibitory interneurons within this region (de Lanerolle et al., 1989, Robbins et al., 1991). Perhaps in compensation of this loss, synaptic reorganization of spared GABAergic and peptidergic interneurons was also observed (de Lanerolle et al., 1989, Masukawa et al., 1989). A more dramatic example of circuit reorganization was observed in the axons of dentate granule cells. Axon collaterals from these cells were observed aberrantly innervating the supragranular layer of the dentate gyrus (Sutula et al., 1989, Houser, 1990, Babb et al., 1991, Masukawa et al., 1992). Importantly, the majority of these observations are

recapitulated in animal models of TLE (Sutula et al., 1988, Mello et al., 1993, Frotscher et al., 2006). However, the contribution of these gross hippocampal alterations to the initiation and/or progression of TLE is not well understood. Epilepsy, as a whole, is a complex, progressive disorder (Larner, 1995, Sutula, 2004). As such, its mechanistic foundation is unlikely to be ascribed to one underlying factor. It is logical to assume that many of the aforementioned changes, in combination with one another, attribute to the manifestation of TLE and its symptoms. In fact, seizures may not simply be symptomatic expressions, but rather, contributing factors in the perpetuation of the disease (Goddard et al., 1969, Sutula, 2004).

In many patients, TLE is initiated by a traumatic event such as traumatic brain injury (TBI), febrile seizures, status epilepticus (SE), tumors, stroke, or infection (Kharatishvili and Pitkanen, 2010, Yang et al., 2010b, O'Dell et al., 2012). These events are often followed by an asymptomatic latency period lasting upwards of 10 years prior to the development of spontaneous recurring seizures (de Lanerolle et al., 2003, Sharma et al., 2007, Yang et al., 2010b). That these arguably diverse insults can lead to a similar phenotype suggests the possibility of shared epileptogenic mechanisms. Posttraumatic epilepsy (PTE), the development of TLE following TBI, accounts for 20% of symptomatic epilepsy (Agrawal et al., 2006). The risk of developing epilepsy following TBI is directly related to the severity of the injury, with relative risk increasing as much as 29-fold following severe TBI (Herman, 2002). While it is difficult to predict whether an individual will develop epilepsy following injury, key risk factors include skull fracture, dural penetration, intracranial hematoma, and prolonged loss of consciousness (Jennett and Lewin, 1960, Annegers et al., 1998, Asikainen et al., 1999, Englander et al.,

2003). While it has been suggested that the initial neuronal injury is the underlying cause of progressive syndromes such as epilepsy (Mathern et al., 1996, Mathern et al., 2002), the prevailing theory proposes that the initial injury is a "self-limiting" event that leads to slowly evolving secondary changes (Sutula, 2004). This secondary damage refers to neurodegeneration, neurogenesis, gliosis, demyelination, vascular damage, axonal sprouting, and angiogenesis (Reilly, 2001, Thompson et al., 2005, Pitkanen and McIntosh, 2006), which, in combination, may alter neuronal circuits and render them vulnerable to spontaneous synchronization (Sutula, 2004). Emphasis has recently been placed on identifying potential prophylactic intervention strategies that, when given following TBI, may prevent the development of PTE. Unfortunately, classical AEDs do not appear to have an anti-epileptogenic effect when administered following TBI in humans (Temkin, 2009). Additionally, spontaneous seizures occurring more than 1 week following injury are rarely used as outcome measures in preclinical TBI trails (Pitkänen and Lukasiuk, 2009). Therefore, much of the recent advancements have come from studies employing animal models.

<u>Animal Models</u>

The first animal model of TLE, developed in 1969, was based on the theory that seizures are self-perpetuating (Goddard et al., 1969). The model involves repeated subconvulsant current injections into the limbic structures, such as the amygdala or the hippocampus. At first, the injections cause no behavioral response. However, with repeated injections the previously subconvulsant currents elicit class V behavioral seizures, characterized by generalized tonic-clonic activity with loss of postural tone (Racine, 1972). This process is known as "kindling" (Goddard et al., 1969), and remains a popular model for studies of

epileptogenesis. Another commonly used model involves induction of limbic SE through either electrical stimulation or the use of chemical agents, followed by sustained electrographic discharges in limbic structures (Turski et al., 1983, Turski et al., 1984, Mazarati and Sankar, 2006, Mazarati et al., 2006). This model involves three distinct stages: (1) an hours-long episode of sustained SE, (2) a days to weeks-long asymptomatic latent period, and (3) gradual development and progressive increase of spontaneously recurring seizures (Dudek et al., 2002, Dudek et al., 2006). Interestingly, the evolution of spontaneous seizures following SE mirrors behavioral and electrographic milestones of kindling (Dudek et al., 2006). As the last stage is often permanent, this model is exceptionally appropriate for modeling a chronic epileptic state following an apparent latent period, as seen in human patients. While a variety of models exist for studying TBI in rodents, only a few of them have been characterized for the study of PTE (Pitkanen et al., 2006). Most TBI models fall into one of the following categories: focal injury models, diffuse brain injury models, or mixed models of focal and diffuse injury (Cernak, 2005, Morales et al., 2005). In these models, spontaneous injury-related seizures can be observed within the early phase (< 1wk) following injury (Nilsson et al., 1994, Williams et al., 2005, Kharatishvili et al., 2006, Williams et al., 2006). During this phase, increasing hyperexcitability is also observed within the hippocampus (Lowenstein et al., 1992, Coulter et al., 1996, Toth et al., 1997, Reeves et al., 2000, Santhakumar et al., 2001, Akasu et al., 2002, Witgen et al., 2005, Tran et al., 2006, Griesemer and Mautes, 2007). More convincing evidence of epileptogenesis is found during the late phase (> 1 wk) followng injury (Pitkänen et al., 2009). Hyperexcitability appears to be chronically maintained within the cortex and hippocampus (Santhakumar et al., 2001). A reduction

in the response threshold to proconvulsant stimuli is also observed several weeks following injury (Golarai et al., 2001, Statler et al., 2008). Most importantly, the emergence of spontaneous seizures can be observed starting at 7 weeks following injury (D'Ambrosio et al., 2004, D'Ambrosio et al., 2005, Kharatishvili et al., 2006). Within 1 year, it was estimated that epileptogenesis occurred in 40-50% of the animals receiving severe, non-penetrating TBI (Kharatishvili et al., 2006). Recent work suggests focal injury models are more likely to promote epileptogenesis (Volman et al., 2011). Histological analysis following TBI in these models yields changes reminiscent of those found in human TLE patients (Golarai et al., 2001, Thompson et al., 2005, Kharatishvili et al., 2006, Pitkanen et al., 2006, Pitkanen and McIntosh, 2006, Statler et al., 2008, Hunt et al., 2009). One of the more striking alterations consistently observed following injury is the aberrant sprouting of the dentate mossy fibers.

1.2. Mossy Fiber Sprouting

Background

Projecting through the hilus to the proximal dendrites of pyramidal cells within the CA3 subregion, the unmyelinated axonal projections of dentate granule cells are collectively referred to as mossy fibers (Golgi, 1886, Ramón y Cajal, 1893). By linking dentate granule cells with CA3 pyramidal cells, these projections form the second link in the hippocampal trisynaptic pathway that also includes the perforant path and the Schaffer collaterals, linking the entorhinal cortex to the dentate granule cells and the CA3 pyramidal cells to the CA1 pyramidal cells, respectively (Andersen et al., 1969). In addition to forming synaptic connections with CA3 pyramidal cells, collateral branches also synapse with a variety of neurons within the hilus, including interneurons (Blackstad

and Kjaerheim, 1961). In depth analysis reveals that a single mossy fiber makes approximately 120-150 excitatory synaptic connections with hilar interneurons, 7-12 large terminal contacts with hilar mossy cells, and 11-18 connections with the dendrites of CA3 pyramidal cells (Claiborne et al., 1986, Acsady et al., 1998). Mossy fibers are predominantly glutamatergic (Gutiérrez et al., 2003); however, they have also been observed to release the opioid peptide dynorphin as well as the inhibitory neurotransmitter GABA (Walker et al., 2001). Aberrant growth of the mossy fiber collaterals into the inner molecular layer is frequently observed in animal models on TLE, as well as in post-mortem tissue samples from human TLE patients (Figure 1.1) (Sutula et al., 1988, Sutula et al., 1989, Houser, 1990, Babb et al., 1991, Masukawa et al., 1992, Mello et al., 1993, Frotscher et al., 2006). The extent of aberrant mossy fiber sprouting is easily identified due to their high amount of chelatable zinc which can be visualized via a silver-sulfide staining method (Timm, 1958, Zimmer, 1973). Interestingly, mossy fiber sprouting can be elicited in response to TBI, status epilepticus, and repeated seizure activity (Sutula et al., 1988, Represa et al., 1989, Steward, 1992, Sutula et al., 1998, Golarai et al., 2001).

Lesion-induced sprouting

The hippocampus in general is particularly sensitive to CNS injury (Colicos et al., 1996, Yakovlev et al., 1997). In the case of TBI, injury to neuronal circuits can come directly from the injury, as in the case of penetrating injuries, or indirectly through axonal shearing and stretching that occurs with acceleration and deceleration of the brain (Povlishock and Katz, 2005). Circuit reorganization following injury is thought to be a
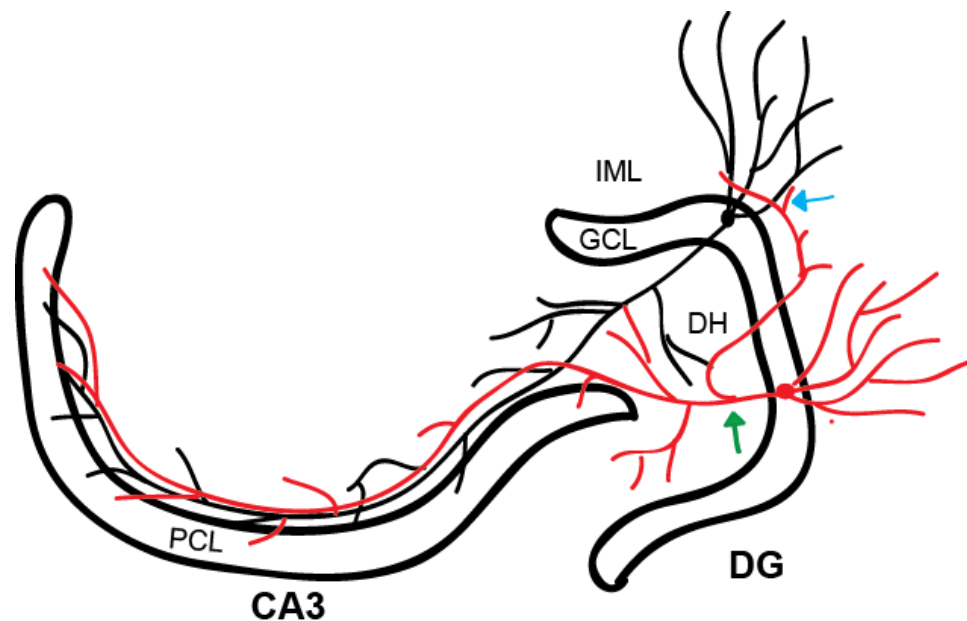
Figure 1.1. Representation of mossy fiber sprouting. A typical granule cell (black) extends apical dendrites from the soma in the granule cell layer (GCL) into the inner molecular layer (IML). Granule cells axons project through the hilus (DH) to synapse on pyramidal cells within the pyramidal cell layer (PCL) of the CA3 region, forming the mossy fiber projection. During mossy fiber sprouting (red), axon collaterals of dentate granule cells branch within the DH (green arrow) and extend into the IML where they form synapses with the dendrites of other granule cells (blue arrow).

compensatory mechanism, through which the lost functions of damaged regions are potentially restored by uninjured regions (Xerri et al., 1998, Ramirez, 2001). The functions of the damaged regions are potentially compensated for by homologous regions of the contralateral hemisphere, spared regions of the ipsilateral hemisphere, or lower-level structures (Stein, 1998). Post-lesion sprouting is classified as either homotypic or heterotypic in nature (Ramirez, 2001). Homotypic reorganization involves sprouting of pathways that share functional characteristics with the injured pathway, such as shared neurotransmitter systems. Conversely, heterotypic sprouting involves pathways dissimilar to that of the injured pathway. While injury-induced reorganization may lead to some restoration of function, changes in circuitry may also prove to be detrimental. It has been proposed that the balance between compensatory and maladaptive sprouting may lie within the degree of homotypic compared to heterotypic sprouting (Ramirez, 2001). While homotypic sprouting is generally associated with functional recovery, consequences of heterotypic sprouting can range from beneficial to detrimental. This relationship is further expanded by the principles of isomorphism, synergism, and dissonance (Steward, 1982, Sabel, 1999). The principle of isomorphism states that the probability that sprouting will contribute to functional recovery increases as a function of the similarity between the compensating and injured pathways. The principle of synergism suggests that probability that heterotypic sprouting will contribute to functional recovery increases as a function of the similarity between the outcome of sprouted afferent activity and that of the original, injured pathway. As the inverse of synergism, the principle of dissonance proposes that the probability that heterotypic

sprouting will be detrimental increases as a function of the dissimilarity in the outcome of heterotypic afferent activity and that of the original, injured pathway.

Lesion-induced sprouting can be observed throughout the hippocampus. Transection of the Schaffer collaterals both in hippocampal explant cultures as well as *in vivo* leads to an increase in the number and length of axon collaterals branching within CA3 and extending into CA1 (McKinney et al., 1997, Dinocourt et al., 2006, Aungst et al., 2013). The increase in axonal sprouting and extension is spatially and temporally correlated with an increase in immunoreactivity for growth associated protein-43 (GAP-43) within these regions. Injury to the entorhinal cortex leads to a 20-30% widening of the commissural/associational (C/A) projections due to either expansion of C/A terminal field or extension of granule cell basal dendrites (Lynch et al., 1973, Storm-Mathisen, 1974, Lynch et al., 1976, Goldowitz and Cotman, 1980, Laurberg and Zimmer, 1981, West, 1984. Injuries leading to deafferentiation of dentate granule cells can induce sprouting of the mossy fiber projections {Laurberg, 1981 #47, Schauwecker and McNeill, 1995, Styren et al., 1995). In some cases, the sprouted mossy fibers have been observed to aberrantly synapse with dendrites of other granule cells, potentially creating a recurrent circuit (Frotscher and Zimmer, 1983). These studies also demonstrated that mossy fiber sprouting can be induced by damage to the CA3 subregion. Lesion-induced sprouting was first affiliated with epilepsy disorders by Messenheimer and Steward (Messenheimer et al., 1979). Areas within the hippocampus that demonstrate high propensity for plasticity and structural reorganization are important for kindling.

<u>Mossy fiber sprouting in TLE</u>

Induction of TLE in rodent models typically leads to two distinct alterations to the mossy fiber pathway: sprouting of mossy fiber axon collaterals and the formation of basal dendrites on dentate granule cells (Nadler et al., 1980, Spigelman et al., 1998). Mossy fiber sprouting is consistently observed following chemically-induced SE, reaching its peak approximately 2-3 months post-insult (Okazaki et al., 1995, Sutula et al., 1998, Wenzel et al., 2000, Lew and Buckmaster, 2011). In human tissue samples, the degree of mossy fiber sprouting is thought to be dependent on the stage of TLE (Mathern et al., 1995a, Mathern et al., 1995b). Biocytin labeling of individual dentate granule cells confirmed that mossy fiber axons bifurcate within the hilus and aberrantly project into the inner molecular layer where they are likely to contact the dendrites of other granule cells. Electron microscopy has revealed that sprouted mossy fibers form a variety of new synapses, with a single mossy fiber forming an estimated 500 new synapses (Buckmaster et al., 2002). Within the inner molecular layer of animal and human samples, synapses are formed between mossy fiber terminals and granule cell dendrites as well as inhibitory interneurons (Isokawa et al., 1993, Buckmaster et al., 2002, Frotscher et al., 2006). Quantitative analysis revealed that the majority of new synapses formed are asymmetric, with synapses between mossy fibers and inhibitory interneurons accounting for less than 5% (Buckmaster et al., 2002, Cavazos et al., 2003). It is unknown if what appears to be preferential synaptogenesis is truly selective or if it is simply opportunistic, given the loss of inhibitory interneurons in TLE. Interestingly, while sprouted mossy fiber collaterals expand within the granule layer and the inner molecular layer, labeling of individual granule cells suggests they do not overlap with dendrites of the original granule cell

(Buckmaster et al., 2002). Therefore, the presence of autapses within the recurrent circuit is unlikely (Koyama and Ikegaya, 2004). While innervation of the inner molecular layer is the most prominent example of mossy fiber plasticity, collateral extension within the hilus, as well as, expansion of the terminal field within the CA3 subregion has been observed (Represa and Ben-Ari, 1992, Sutula et al., 1998, Buckmaster and Dudek, 1999, Holmes et al., 1999). Additionally, TLE-induced plasticity is not limited to mossy fiber axons. Sprouting and extension has also been observed in granule cell dendrites and within CA1 projections (Spigelman et al., 1998, Buckmaster and Dudek, 1999, Esclapez et al., 1999, Ribak et al., 2000, Smith and Dudek, 2001).

In models where TLE is initiated by SE, it was debated whether mossy fiber sprouting was a consequence of the macroscopic damage induced by SE or of the seizures elicited by sustained SE (Sutula, 2002). The presence of mossy fiber sprouting in kindling models supports the hypothesis that seizure activity is important for structural reorganization in TLE. Sprouting of mossy fiber collaterals into the inner molecular layer can be observed after only a few seizures and progresses with repeated stimulations (Cavazos et al., 1991). Similar to the reorganization elicited following lesion or SE, mossy fiber sprouting in kindled animals is permanent. In general, seizure-induced mossy fiber reorganization can be seen in genetic models of epilepsy, following repeated electroconvulsant seizures, and systemic administration of chemoconvulsant agents (Stanfield, 1989, Golarai et al., 1992, Qiao and Noebels, 1993, Holmes et al., 1998, Gombos et al., 1999, Holmes et al., 1999, Vaidya et al., 1999). In hippocampal explant cultures, hyperexcitation by the $GABA_A$ receptor antagonist picrotoxin was sufficient to induce mossy fiber sprouting (Koyama et al., 2004). This reorganization of hippocampal

circuits in response to seizure activity is not surprising. Plasticity on the neuronal or whole circuit level has been observed following repeated activation of pathways within the limbic, brain stem, cortical, and subcortical regions of many species (Sutula, 2004). As circuit reorganization is observed as a direct result of injury or seizure activity, mossy fiber sprouting in TLE is likely attributed to a combination of the two factors. It is logical to hypothesize that early phases of mossy fiber sprouting may be a direct result of injury-related mechanisms. Additionally, as the initial injury is thought to lead to episodes of neuronal synchronization (Sutula, 2004), later phases of mossy fiber sprouting may be attributed to activity-dependent mechanisms associated with epileptiform activity. Indeed, individual mossy fibers have been shown to exhibit activity-dependent plasticity (De Paola et al., 2003, Galimberti et al., 2006).

Activity dependence

Given the abnormal level of neuronal activity associated with seizures, it is not surprising that activity dependent processes have been implicated in epileptogenesis. Blocking neuronal activity with tetrodotoxin (TTX) prevents the development of hyperexcitability in a neocortical injury model of epileptogenesis (Graber and Prince, 1999, Graber and Prince, 2004). The induction and maintenance of epileptiform activity in hippocampal slice models were also observed to be activity-dependent (Karr and Rutecki, 2008). Activity-dependent release of neurotrophic factors has also been observed in animal models of TLE (Aloyz et al., 1999).

While many of the proposed contributing factors of TLE demonstrate some activity-dependence, of particular interest is synaptic plasticity and network reorganization. Activity-dependent neurite outgrowth has long been attributed to focal

14

changes in intracellular calcium concentration (Cohan and Kater, 1986, Connor, 1986, Fields et al., 1990, Schilling et al., 1991). The growth promoting aspect of activity is constrained within a small range of calcium concentrations, outside of which retraction and growth cone collapse can occur, suggesting the process is tightly regulated (Kater et al., 1988, Dubinsky et al., 1989, van Pelt et al., 1996). Such regulation allows for a reciprocal relationship between outgrowth and network connectivity (Van Ooyen et al., 1995). Mechanistic studies have suggested that the rise in intracellular calcium necessary to promote growth may be attributed to calcium influx through N-methyl-D-aspartate receptors, L-type voltage-gated calcium channels, or both (Kocsis et al., 1994, Wayman et al., 2006). Regardless of the initial route of calcium entry, preventing its secondary mobilization from intracellular stores abolishes the growth promoting effects of depolarization-induced activity (Kocsis et al., 1994). Other than strict calcium dependence, the specific mechanisms underlying activity-dependent outgrowth are relatively unknown. Second messenger systems, especially those responsive to changes in intracellular calcium such as cAMP, have been suggested to play a role (Mattson et al., 1988). Additionally, inhibitors of transcription have also been used to suggest that transcription – most likely of growth promoting genes – may be an important step linking activity to cytoskeletal dynamics (Solem et al., 1995). Additional studies also suggest the importance of kinase cascades (Solem et al., 1995, Wayman et al., 2006).

Functional consequences

The impact of mossy fiber sprouting on network activity is highly debated, and may depend on type and number of post-synaptic targets (Sutula, 2002). Synapse formation between sprouted mossy fibers and granule cells dendrites should form

15

recurrent excitatory circuits, whereas synapses formed with inhibitory interneurons may enhance overall inhibition (Tauck and Nadler, 1985). Therefore, mossy fiber sprouting could lead to two functionally distinct outcomes. Enhanced inhibition may compensate for hippocampal hyperexcitability and work to suppress the propagation of epileptiform events (Sloviter, 1991, 1992, Buhl et al., 1996, Kotti et al., 1997). However, the percent increase in the number of synapses with inhibitory interneurons in TLE is only 16%, compared to the near 475% increase in synapses formed on granule cell dendrites (Claiborne et al., 1986, Acsady et al., 1998, Buckmaster et al., 2002). Therefore, the novel formation of recurrent excitatory circuits may have more functional significance. The functional contribution of mossy fiber sprouting is further confounded by the finding that seizure activity increases the expression of GABA and its synthesizing enzyme glutamic acid decarboxylase-67 (GAD-67) within mossy fiber terminals (Gutierrez and Heinemann, 2001, Ramirez and Gutierrez, 2001, Gomez-Lira et al., 2002, Gutierrez, 2002). However, mossy fibers have also been shown to release zinc under these circumstances, which leads to inhibition of GABA receptors (Buhl et al., 1996, Coulter et al., 1996, Shumate et al., 1998). Therefore, the significance of GABA transmission at sprouted mossy fiber terminals is still debated. Some evidence from TLE patient samples supports the hypothesis that mossy fiber reorganization contributes to hippocampal hyperexcitability and, to some extent, epileptogenesis. Correlations have been made between surgical removal of sprouting-prone hippocampal regions and decreases in seizure activity in human patients (Sutula et al., 1989), yet this evidence is circumstantial at best. More convincingly, electrophysiological recordings of resected tissue revealed hyperexcitable responses of dentate granule cells following perforant path or mossy fiber

stimulation (Masukawa et al., 1989). Additional correlations have been drawn between the extent of mossy fiber sprouting and abnormal antidromic field responses in a subset of TLE patients (Masukawa et al., 1992).

Animal models of TLE induced by SE, kindling, or injury have allowed for more in-depth investigation of the consequences of mossy fiber sprouting on hippocampal networks. Similar to studies of human tissue, loose correlations have been drawn between the duration and complexity of evoked multispike field potentials and the extent of mossy fiber sprouting in rodents (Tauck and Nadler, 1985). Additionally, granule cell hyperexcitability following hilar stimulation is temporally correlated with mossy fiber sprouting (Wuarin and Dudek, 1996), and single stimulation of the perforant path led to an increased number of population spikes, followed by prolonged field sinks accompanied by irregular population spikes indicative of epileptiform activity (Patrylo et al., 1999). Therefore, input from the entorhinal cortex may potentially be converted into epileptiform activity within the mossy fiber pathways (Koyama and Ikegaya, 2004). Inward current sinks have been observed within the inner molecular layer of fully but not partially kindled rats, spatially corresponding to the terminal field of sprouted mossy fibers (Golarai and Sutula, 1996). This finding suggests that novel synapses formed between sprouted mossy fibers and granule cell dendrites are likely functional, which is essential to the hypothesis that mossy fiber sprouting leads to the formation of recurrent excitatory circuits. Interestingly, many studies reveal increased local circuit excitation and epileptiform activity via increases in evoked and spontaneous EPSCs as well as spontaneous burst discharges that are only visible under conditions of decreased inhibition (Cronin et al., 1992, Patrylo and Dudek, 1998, Molnar and Nadler, 1999,

Okazaki et al., 1999, Patrylo et al., 1999, Lynch and Sutula, 2000, Wuarin and Dudek, 2001). It has also been suggested that during baseline activity levels, recurrent excitatory networks are functionally silent. However, following high frequency stimulation, granule cells have been shown to synchronize (Feng et al., 2003). Neuronal synchronization is thought to underlie much of the epileptic process. The synchronization of granule cells is only observed in the presence of mossy fiber sprouting, thereby, connecting this structural reorganization with the most basic epileptic phenomenon.

More direct evidence for the existence of recurrent excitatory circuits in TLE comes from elegant studies involving focal application of glutamate via microdrops or photolysis of caged glutamate. Granule cell EPSPs were evoked following focal application of glutamate within the granule and inner molecular layer at long and variable latencies from the recorded cell (Wuarin et al., 1992, Wuarin and Dudek, 2001). Unfortunately, these studies do not allow one to definitively conclude that granule cells are monosynaptically connected. However, using the dual patch clamp technique, Scharfman and colleagues demonstrated the formation of mutual synaptic connections among granule cells following seizure-induced mossy fiber sprouting (Scharfman et al., 2003). Given the multitude of potentially maladaptive changes occurring duing TLE, the question still remains if the development of recurrent excitation within the hippocampus can be solely attributed to structural reorganization. Results from lesion-based studies suggest that injury-induced sprouting and reorganization is sufficient to cause hyperexcitability and, in some cases, epileptiform activity. Transection of the Schaffer collaterals in hippocampal explant cultures led to an increase in the frequency of spontaneous EPSPs that correlated with increased axon sprouting and growth of CA3

pyramidal cells (McKinney et al., 1997, Aungst et al., 2013). Stimulus-pair recordings in these cells demonstrated that the probability that any CA3 pyramidal cell was monosynaptically connected to another CA3 pyramidal cell was increased by 27% following injury. Additionally, field stimulation of the CA3 subregion led to prominent polysynaptic depolarizing responses lasting over 500 ms in lesioned cultures. This phenomenon was not attributed to decreased inhibition, suggesting the spread of excitation throughout the CA3 pyramidal cells was increased as a result of formation and extension of axon collaterals. A small percentage of lesioned slices also exhibited classical epileptiform burst discharges.

Despite evidence that mossy fiber sprouting can lead to the formation of recurrent excitatory circuits, there has been skepticism that it directly contributes to epileptogenesis. Several studies have failed to detect a relationship between mossy fiber sprouting and the development or frequency of spontaneous recurring seizures in animal models (Longo and Mello, 1998, 1999, Pitkanen et al., 2000, Nissinen et al., 2001). Additionally, results gained from selective destruction of dentate granule cells by the neurotoxin colchicine during entorhinal kindling suggested that the dentate gyrus is not essential for hippocampal kindling (Dasheiff and McNamara, 1982, Frush et al., 1986, Sutula et al., 1986). Prevailing theories supporting the importance of mossy fiber sprouting suggest that the formation of recurrent excitatory circuits by aberrantly sprouted mossy fibers may contribute to epileptogenesis under circumstances where other abnormalities, such as decreased inhibition, are also present (Sutula, 2002). It has also been suggested that while mossy fiber sprouting may not be a direct cause of epileptogenesis, its presence may contribute to the chronic progression of TLE (Koyama

and Ikegaya, 2004). In support of this hypothesis, the presence of mossy fiber sprouting seemed to increase the severity of spontaneous seizures (Zhang et al., 2002). Kainate priming prior to the induction of SE in animal models of TLE, prevents mossy fiber sprouting without affecting the development of spontaneous recurrent seizures. This finding is consistent with the hypothesis that mossy fiber sprouting is not involved in epileptogenesis. However, the severity of spontaneous seizures was exacerbated in non-primed animals with extensive mossy fiber sprouting compared to the primed animals that did not exhibit mossy fiber sprouting. Therefore it was the conclusion of this study that the presence of mossy fiber sprouting may intensify the major symptoms of TLE.

1.3. Mechanisms of mossy fiber sprouting

Background

As the mechanisms underlying mossy fiber sprouting are relatively unknown, few studies have been able to employ pharmacological strategies to target mossy fiber sprouting. Therefore, it can be difficult to draw conclusions from the aforementioned studies that are more than strong correlations. One strategy that has proven to be effective in altering mossy fiber sprouting *in vivo* is the inhibitor of mTOR signaling, rapamycin (Buckmaster et al., 2009). The mammalian target of rapamycin (mTOR), a serine/threonine protein kinase, participates in a multitude of intracellular signaling cascades involved in neuronal processes such as differentiation, synaptic plasticity, ion channel expression, axonal growth, dendritic arborization, and survival (Tang et al., 2002, Jaworski et al., 2005, Wullschleger et al., 2006, Abe et al., 2010, Wong, 2010, Galanopoulou et al., 2012). Unfortunately, the results of these studies appear to be in contradiction with one another. It was first demonstrated that administration of 6 mg/kg

rapamycin given to mice every other day following pilocarpine-induced SE reduced both mossy fiber sprouting and the frequency of spontaneous seizures (Zeng et al., 2009). However, when a lower dose of 3 mg/kg of rapapmycin was given to rats every day following kainic acid-induced SE, mossy fiber sprouting was again reduced yet the frequency of spontaneous seizures was not affected (Buckmaster and Lew, 2011). In a distantly-related study, rats that had already developed spontaneous recurring seizures following pilocarpine-induced SE and treated with 5 mg/kg rapamycin every other day demonstrated reduced frequency of spontaneous seizures (Huang et al., 2010). Another report details the effect of rapamycin on the electrophysiological correlates of epilepsy in hippocampal slices. In this study, 6 mg/kg rapamycin was given daily for 6 days, starting 24 hr following pilocarpine-induced SE. After 6 days of treatment, rapamycin was then administered every other day for up to 2 months. Mossy fiber sprouting was reduced following rapamycin treatment. Single cell and field recordings from the dentate gyrus revealed that rapamycin prevented many electrophysiological alterations associated with TLE, including the repetitive firing of population spikes following antidromic stimulation (Tang et al., 2012). Using a much higher dose of rapamycin, the Buckmaster group demonstrated that while mossy fiber sprouting was completely ablated by 10 mg/kg rapamycin given daily following pilocarpine-induced SE, the frequency of spontaneous seizures was not affected (Heng et al., 2013). Up until this point, seizure frequency was determined by video observation and thereby limited to behavioral seizures alone. Recent work employs continuous video-EEG monitoring to detect spontaneous seizures in mice following TBI (Guo et al., 2013). Along with preventing mossy fiber sprouting, daily administration of 6 mg/kg rapamycin after TBI reduced the percentage of animal

21

that developed spontaneous recurring seizures by ~37%. Of the animals that did develop seizures, rapamycin treatment was associated with a reduction in seizure frequency.

It is possible that the contradicting results presented in these studies are attributed to differences in the TLE model, methods of outcome measurement, dosage/regimen, or species used. However, as rapamycin is involved in a myriad of normal and pathological processes, its manipulation may be too broad to allow for conclusions to be drawn between two specific phenomena. Therefore, a selective method for targeting mossy fiber sprouting is essential in order to definitively conclude that it is contributing to epileptogenesis. The development of such a tool requires the understanding of molecular mechanisms underlying mossy fiber sprouting. One theory proposes that the events following injury that lead to mossy fiber sprouting and reorganization may mirror those during development. Mossy fiber guidance during development involves two distinct processes (Koyama et al., 2002). Initially, mossy fibers are guided by the presence of chemoattractants from the CA3 region as well as chemorepellants from the CA1 region. There is also evidence of chemorepellants from the entorhinal cortex that prevent mossy fibers from innervating the granule and inner molecular layers (Holtmaat et al., 2003). Mossy fibers are then thought to use contact guidance cues, allowing them to fasciculate with other mossy fibers. Aberrant sprouting of mossy fibers in TLE is also viewed as a two-step process (Koyama and Ikegaya, 2004). The first step is the initial branching of collaterals within the hilus. The second step involves extension of the sprouted collaterals and backward guidance into the inner molecular layer. It is unknown if separate mechanisms are responsible for these processes. In terms of guidance into the inner molecular layer, there is some evidence that the chemorepulsive cue that normally

22

prevents mossy fiber innervation in that region is lost in models of TLE (Holtmaat et al., 2003). Stellate cells projecting to the dentate gyrus from the entorhinal cortex provide a gradient of the chemorepellant Sema3A within the inner molecular layer, which is downregulated following status epilepticus. Since contact guidance is typically bi-directional, in the absence of the chemorepulsive cues from the entorhinal cortex, mossy fibers are free to enter the inner molecular layer. The question remains as to what initiates the sprouting of mossy fiber collaterals? One possibility is that sprouting is triggered by the release of extracellular signaling molecules either in response to the initial insult or seizure activity itself. To identify which signaling molecules may be involved, the following criteria must be satisfied: production and release of the molecule is regulated by injury or seizure activity and its release must induce structural and functional changes that, in turn, result in hyperexcitability (He et al., 2002).

BDNF

Interestingly, mRNA levels of the neurotrophin brain-derived neurotrophic factor (BDNF) are elevated in the hippocampus, and more specifically, in dentate granule cells of TLE patients (Mathern et al., 1997). BDNF activates tropomycin-related kinase receptors (Trks), initiating phosphorylation cascades involved in differentiation, cell survival, and synaptic plasticity (Kaplan and Miller, 2000). Pyramidal cells within the hippocampus express high levels of TrkB receptors (Huang and Reichardt, 2001). Importantly, cultured dentate granule cells display functional TrkB activity and application of BDNF leads to axon branching (Patel and McNamara, 1995, Lowenstein and Arsenault, 1996a, b). Increased levels of BDNF expression and corresponding activation of the TrkB receptor are observed within granule cell somas and mossy fiber

axons following insults often association with TLE, such as TBI, status epilepticus, and transient global ischemia (Yang et al., 1996, Hu et al., 1999, Oyesiku et al., 1999, Grundy et al., 2000, Hu et al., 2000, Griesbach et al., 2002, Hu et al., 2004, Heinrich et al., 2011). Other evidence suggests that seizure activity alone may be sufficient to induce increased BDNF expression and activation of TrkB. Limbic seizures lead to increased levels of BDNF mRNA and protein within the dentate gyrus *in vivo* which appeared to peak 24-48 hours following induction (Isackson et al., 1991, Nawa et al., 1995, Yan et al., 1997, Elmer et al., 1998, Vezzani et al., 1999, Katoh-Semba et al., 2001). Along these lines, increases in BDNF expression and activation of TrkB are observed during kindling (Binder et al., 1999a, He et al., 2002). As previously mentioned, hyperexcitation of hippocampal explant cultures can lead to mossy fiber sprouting. Interestinglu, regions corresponding to the mossy fiber sprouting also demonstrate elevated levels of BDNF in these slices (Koyama et al., 2004). Increased BDNF and TrkB activation are also observed to correspond to regions of GAP43 expression following Schaffer collateral transection in explant cultures (Dinocourt et al., 2006, Aungst et al., 2013). These studies provide evidence that increases in BDNF expression and subsequent activation of the TrkB receptor correspond temporally and spatially with injury and seizure-induced sprouting. However, mossy fiber sprouting and hyperexcitability must be directly linked with BDNF in order for it be considered as a potential candidate.

Application of BDNF on cultured dentate granule cells causes a concentration dependent increase in axon branching which is prevented by blockade of the TrkB receptor (Koyama et al., 2004). Similarly, chronic activation of TrkB receptors leads to increased axonal sprouting and excitability within hippocampal slice cultures (Schwyzer

et al., 2002). Interestingly, chronic infusion of BDNF into the rodent hippocampus is sufficient to lead to motor seizures and increased sensitivity to the pro-convulsant pilocarpine (Scharfman et al., 2002). Similar results were observed in transgenic mice overexpressing BDNF (Croll et al., 1999). Additionally, increased TrkB activity is associated with increased rate of epileptogenesis in mice (Heinrich et al., 2011). Conversely, decreased epileptiform spiking was observed following SE in transgenic mice overexpressing a truncated, dominant negative TrkB receptor (Lahteinen et al., 2002). Intraventricular infusion of antibodies against the TrkB, but not TrkA or TrkC receptors, decreased epileptogenesis during kindling, once again confirming the specificity of this phenomenon (Binder et al., 1999b). While kindling was only marginally impaired in BDNF +/- and BDNF -/- mice, conditional deletion of the TrkB receptor completely prevented its development (Kokaia et al., 1995, He et al., 2004). These findings provide a clear link between TrkB signaling and epileptogenesis. Insight from hippocampal slice cultures may illuminate BDNF/TrkB's involvement in mossy fiber sprouting and how it may contribute to epileptogenesis. Decreased TrkB activity, either via knockdown or small molecule inhibition, prevents sprouting or impairs the development of hyperexcitability following Schaffer collateral transection (Dinocourt et al., 2006, Aungst et al., 2013). The most convincing evidence for a direct link between BNDF signaling, mossy fiber spouting, and the development of hyperexcitability comes from the work of Koyama and colleagues. BDNF-containing beads placed in the hilus of hippocampal slice cultures were sufficient to induce mossy fiber sprouting and aberrant innervation of the inner molecular layer which was blocked by TrkB inhibition (Koyama et al., 2004). Hilar microstimulation in BDNF bead-containing but not control slices

elicited paroxysmal depolarization shifts reminiscent of interictal spikes typically recorded by electroencephalogram. These depolarization shifts, considered as the basis for epileptiform activity, are typified by sustained elevation of the resting potential above normal threshold levels, accompanied by action potential bursts (Ayala et al., 1973, Dichter and Ayala, 1987). Therefore, exogenous BDNF is sufficient to induce mossy fiber sprouting which led to the formation of recurrent excitatory circuits in hippocampal slices.

GSK3β

Downstream of TrkB activation, phosphoinositide 3 kinase (PI3K) intitiates the phosphorylation and activation of protein kinase B, also known as Akt (Alessi et al., 1996, Bhave et al., 1999). Evidence of increased Akt activation within the hippocampus, as well as other regions, has been observed following many insults that often predispose for TLE, such as TBI (Zhang et al., 2006, Zhao et al., 2012), hypoxia-ischemia (Ouyang et al., 1999, Namura et al., 2000, Janelidze et al., 2001, Noshita et al., 2001, Yano et al., 2001, Endo et al., 2006, Li et al., 2008, Xiong et al., 2012), and SE ((Lopes et al., 2012). Interestingly, Akt is also involved in mTOR signaling (Wu and Hu, 2010). That rapamycin reduces mossy fiber sprouting provides further support for the involvement of Akt and its substrates in this process. Upon activation, Akt phosphorylates and inactivates glycogen synthase kinase 3 beta (GSK3β) (Cross et al., 1995). Corresponding to changes in Akt activity, levels of phosphorylated (inactive) GSK3β are increased following TBI (Shapira et al., 2007, Dash et al., 2011, Zhao et al., 2012), hypoxia-ischemia (Sasaki et al., 2001, Endo et al., 2006, Xiong et al., 2012), and SE (Lee et al., 2012). Intriguingly, preventing GSK3β inactivation following the induction of SE, also

reduced mossy fiber sprouting (Lee et al., 2012). This result suggests that inactivation of GSK3β may be a crucial step along the TrkB signaling cascade responsible for mediating mossy fiber sprouting.

Originally identified for its role in glycogen metabolism, it is now known that the tonically active kinase aids in the regulation of a variety of neuronal functions. For example, phosphorylation by GSK3β regulates the activity of transcription factors involved in cell proliferation and growth, synaptic plasticity, and cell death (Boyle et al., 1991, Struthers et al., 1991, Wang et al., 1994, Davis et al., 1996, Karin et al., 1997, Silva et al., 1998, Bevilaqua et al., 1999, Shaywitz and Greenberg, 1999). GSK3β is also well known for its role in cytoskeletal dynamics via regulation microtubule associated proteins such as tau, MAP1B, MAP2, NCAM, and neurofilament proteins, whose function is determined by phosphorylation state (Mackie et al., 1989, Guan et al., 1991, Hanger et al., 1992, Mandelkow et al., 1992, Berling et al., 1994, Guidato et al., 1996, Sánchez et al., 1996, García-Pérez et al., 1998, Lucas et al., 1998). One particular substrate that may be of importance in microtubule dynamics is the intracellular phosphoprotein collapsin response mediator protein 2 (CRMP2) (Figure 1.2).

1.4. Collapsin Response Mediator Protein 2 (CRMP2)

Background

CRMP2, also known as DPYSL2/DRP2, Unc-33, Ulip, or TUC2, was first identified as a mediator of axon growth and guidance in chick dorsal root ganglia (Goshima et al., 1995), with analogs later identified in *Caenorhabditis elegans*, *Drosophila melongaster*, rodents, and humans (Hedgecock et al., 1985, Geschwind and Hockfield, 1989, Minturn et al., 1995, Byk et al., 1996, Kitamura et al., 1999, Morris et

27
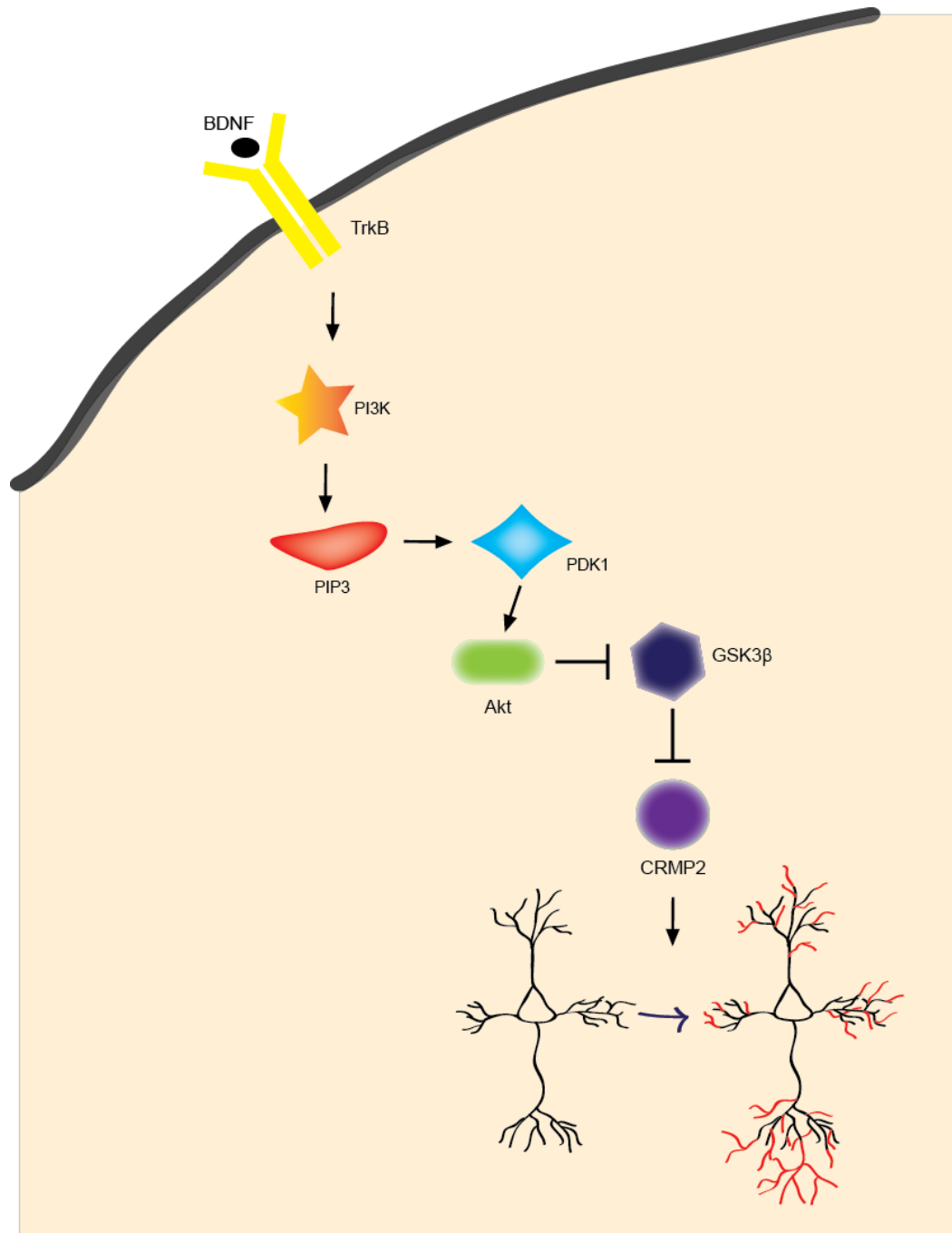
Figure 1.2. Signaling cascade potentially involved in mossy fiber sprouting.
Activation of the growth factor receptor TrkB by the binding of BDNF leads to the
activation of Akt through the depicted pathway. Akt inactivates GSK3β, thereby
increasing the amount of active CRMP2 available to promote neurite outgrowth.
(BDNF: brain-derived neurotrophic factor; TrkB: tropomycin-related kinase receptor
B; PI3K: phosphoinositide 3-kinase; PIP3: phopshotidylinositol (3,4,5)-trisphosphate;
PDK1: phosphoinositide-dependent kinase; Akt: protein kinase B; GSK3β: glycogen
synthase kinase 3β; CRMP2: collapsin response mediator protein 2)

al., 2012). CRMP2 is widely expressed within both the central and peripheral nervous systems (Goshima et al., 1995), as well as in fibroblasts and T cells (Vincent et al., 2005, Vuaillat et al., 2008). Five structurally similar proteins (CRMP1-5) comprise the mammalian CRMP family, with CRMP2 being the most well-studied (Fukada et al., 2000, Schmidt and Strittmatter, 2007). Resolution of the CRMP2 structure revealed a "bilobed-lung" configuration that is believed to be shared by all CRMPs as it was also observed following crystallization of CRMP1 (Deo et al., 2004, Stenmark et al., 2007). Intriguingly, CRMP family members are known to form hetero- and homotetramers, with the latter being less likely as many CRMP protein demonstrate lower affinity for itself compared to other family members (Wang and Strittmatter, 1997, Yoneda et al., 2012). While the presumed native configuration for CRMPs is tetrameric, the impact of oligomerization on CRMP function is unknown and likely depends on the composition of the tetramer. As CRMP2 is the most widely expressed of all family members (Wang and Strittmatter, 1996), many tetramers likely contain at least one CRMP2 monomer. Canonical functions of CRMP2 include axonogenesis, neurite outgrowth, migration, and neuronal polarity (Inagaki et al., 2001, Nishimura et al., 2003, Yoshimura et al., 2005). It is now known that CRMP2 also participates, mainly through trafficking, in protein endocytosis and vesicle recycling, synaptic assembly, calcium channel regulation, and neurotransmitter release (Hensley et al., 2011, Khanna et al., 2012). Many of these functions require an interaction between CRMP2 and multiple binding partners. For example, CRMP2's involvement in cytoskeletal dynamics requires interactions with proteins such as tubulin, actin, and vimentin (Fukata et al., 2002, Vincent et al., 2005, Vuaillat et al., 2008). Interactions with the motor proteins kinesin and dynein suggest

that CRMP2 may play an important role in trafficking, linking these proteins to their cargo packets (Nishimura et al., 2003, Kawano et al., 2005, Kimura et al., 2005, Lykissas et al., 2007, Arimura et al., 2009, Rahajeng et al., 2010). Through interactions with both voltage- and ligand-gated calcium channels, CRMP2 is involved in synapse dynamics both pre- and post-synaptically (Al-Hallaq et al., 2007, Brittain et al., 2009, Chi et al., 2009, Brittain et al., 2012). Many other interactions have been observed whose functional impact are not well understood, such as the Ras-GAP Neurofibromin and the calcium sensing protein, calmodulin (Xu et al., 1990, Zhang et al., 2009).

Post-translational regulation

Along with o-glycosylation, sumoylation, and proteolysis, CRMP2 is phosphorylated by numerous kinases (Arimura et al., 2000, Brown et al., 2004, Cole et al., 2004, Arimura et al., 2005, Yoshimura et al., 2005, Cole et al., 2006, Lykissas et al., 2007, Hou et al., 2009, Uchida et al., 2009, Varrin-Doyer et al., 2009). As knowledge progresses, it appears that many of CRMP2's functions are regulated by phosphorylation, especially its canonical functions. CRMP2 promotes neurite outgrowth by two distinct mechanisms: (1) binding and transporting tubulin dimers from the soma to distal projections (Fukata et al., 2002, Kimura et al., 2005) and (2) stabilizing the growing end of the microtubule by promoting the inherent GTPase activity of tubulin (Chae et al., 2009). Phosphorylation by GSK3β, cyclin dependent kinase 5 (CDK5), Rho-associated protein kinase (ROCK), calcium/calmodulin-dependent protein kinase II(CaMKII), or the tyrosine protein kinase, FYN, renders CRMP2 inactive, promoting neurite retraction and growth cone collapse (Arimura et al., 2000, Brown et al., 2004, Cole et al., 2004, Arimura et al., 2005, Uchida et al., 2005, Yoshimura et al., 2005, Cole et al., 2006, Hou

et al., 2009, Uchida et al., 2009). Specifically, GSK3β phosphorylates CRMP2 at threonines 509, 514, and 518, thereby reducing its affinity for tubulin (Yoshimura et al., 2005). As there is no strict consensus motif, GSK3β substrate recognition can be complex, often requiring prior phosphorylation (priming) at a serine slightly c-terminal to the GSK3β site(s) (DePaoli-Roach, 1984, Fiol et al., 1988). This type of hierarchical phosphorylation allows for complex regulation at multiple levels. In the case of CRMP2, it must be first be phosphorylated at serine 522 by the serine/threonine kinase CDK5 in order to be phosphorylated by GSK3β (Yoshimura et al., 2005, Cole et al., 2006). Sequential phosphorylation of CRMP2 by CDK5 and GSK3β has been demonstrated for many facets of CRMP2 function, most importantly, neurite outgrowth (Brown et al., 2004, Uchida et al., 2005). Elegant studies by the Ohshima and Goshima groups suggest that changes in the phosphorylation state of CRMP2 may allow for dynamic regulation of outgrowth and branching patterns, as phosphorylation by CDK5 is necessary for proper bifurcation of CA1 apical dendrites as well as organization of dendritic fields (Yamashita et al., 2012, Niisato et al., 2013). As phosphorylation at S522, T509, T514, and/or T518 renders CRMP2 unable to promote neurite outgrowth, dephosphorylation of those residues should activate CRMP2, thereby increasing neurite outgrowth. Indeed dephophsphorylation of GSK3β sites by either protein phosphatases 1 (PP1) and 2A (PP2A) enhance neurite outgrowth *in vitro* (Cole et al., 2008, Zhu et al., 2010, Astle et al., 2011).

Potential involvement in TLE

The inactivation of GSK3β that is observed following TBI, SE, and hypoxia-ischemia may lead to an overall decrease in the level of phosphorylated (inactive) CRMP2, thereby promoting neurite outgrowth. Therefore, the structural reorganization

that is seen in these models and often associated with TLE, may potentially be attributed to increased CRMP2 activity. Indeed, hypophophshorylation of CRMP2 has been observed following hypoxia-ischemia (Zhou et al., 2008, Sato et al., 2011), validating CRMP2 as the potential link connecting inactivation of GSK3β to insult induced structural plasticity. However, the multifunctional nature of CRMP2 provides a complex hurdle in determining its contribution to specific phenomena. The roles of CRMP2 within the nervous system are as varied as they are numerous (Khanna et al., 2012). Therefore, broad manipulations such as genetic knockdown are unlikely to yield valid information on specific CRMP2-dependent processes. The ability to selectively target the capacity of CRMP2 to promote neurite outgrowth is necessary in order to definitively determine the involvement of CRMP2 in TLE.

1.5. *(R)* Lacosamide

Background

It has been suggested that a novel antiepileptic drug, Lacosamide (Vimpat®) (R-N-benzyl 2-acetamido-3-methoxypropionamide) (*(R)*-LCM) binds and impairs the ability of CRMP2 to promote neurite outgrowth; however, this is somewhat controversial. *(R)*-LCM is a first in class AED approved by the United States Food and Drug Administration and the European Medicines Agency for adjunctive treatment of partial-onset epilepsy with or without secondary generalization in adults (for review see (Biton, 2012)). *(R)*-LCM was first identified as the lead compound in a class of functionalized amino acids demonstrating antiepileptic properties in the maximal electroshock model (Cortes et al., 1985, Choi et al., 1996).

Mechanism of action

Despite its success in both pre-clinical and clinical studies, the mechanism by which *(R)*-LCM alleviated seizure activity remained unknown (Duncan and Kohn, 2005). Radioligand displacement studies attempted to identify a target for *(R)*-LCM within the central nervous system. While the ability of *(R)*-LCM to weakly displace H^3-Batrachotoxin indicated some level of binding to voltage-gated sodium channels (VGSCs), *(R)*-LCM treatment did not affect steady state gating kinetics or current density (Errington et al., 2006). It was ultimately determined that *(R)*-LCM reduces excitability through selective enhancement of VGSC slow inactivation (Errington et al., 2008). It was hypothesized that this unique method of action would allow for discrimination between steady-state and aberrantly increased levels of firing. *(R)*-LCM derivatives were employed as affinity baits in an attempt to identify any additional targets within the central nervous system (Beyreuther et al., 2007, Park et al., 2009, Park et al., 2010). The results of these studies suggested that, aside from the voltage-gated sodium channel, *(R)*-LCM may also target CRMP2.

Controversy

The first evidence supporting the interaction can be found in the preclinical report published by Beyreuther and colleagues on behalf of Shwarz Biosciences (Beyreuther et al., 2007). Direct evidence supporting their claims that CRMP2 is a target of *(R)*-LCM can be found within a patent application filed by three of the authors: Beyreuther, Stohr, and Freitag (Beyreuther et al., 2009). The most convincing data within the application are the radioligand binding studies where they demonstrated competitive and specific binding of $[^{14}C]$-*(R)*-LCM to crude fractions isolated from Xenopus Oocytes transfected

with CRMP2, as well as rat brain membranes. These studies reported a Kd-value lower than 5 μM. Importantly, radioligand binding could be competed off with an excess of cold, unlabeled *(R)*-LCM. Additionally, no specific binding was reported from control Oocyte fractions not containing CRMP2. Based on these results, along with others supporting the interaction of CRMP2 and *(R)*-LCM, the application states the following: "CRMP2 is therefore regarded as a target of *(R)*-LCM in the nervous system in epilepsy, pain, essential tremor, dyskinesias, amyotrophic lateral sclerosis, schizophrenia, and other disease conditions" (Beyreuther et al., 2009). Affinity-bait capture of CRMP2 by *(R)*-LCM has been demonstrated in three separate reports (Park et al., 2009, Park et al., 2010, Wang et al., 2010a). Furthermore, *in silico* docking was used to identify putative binding sites for *(R)*-LCM within the CRMP2 protein. The technique uses the known structure of the target protein (CRMP2) to predict the structure of the intermolecular complex when bound to a ligand (*(R)*-LCM) (for review see (Sousa et al., 2006)). A total of 100 runs were carried out over the surface of the CRMP2 protein to yield five pockets capable of coordinating *(R)*-LCM binding. Interestingly, it was observed that CRMP2 expression levels can influence the ability of *(R)*-LCM to transition voltage-gated sodium channels to the slow-inactivated state in a neuronal cell line. Site-directed mutagenesis of key residues within the previously identified binding pockets on CRMP2 prevented the impact of CRMP2-overexpression on modulation of VGSC slow inactivation by *(R)*-LCM.

Evidence for a direct interaction between *(R)*-LCM and CRMP2 was disputed in a 2012 report by Wolff and colleagues (Wolff et al., 2012). Previous radioligand binding studies reported a Kd of ~5μM; however these employed [^{14}C] *(R)*-LCM which was

34

reported to have low specific radioactivity, limiting further binding studies. Therefore, Wolff and colleagues used [³H] *(R)*-LCM, whose specific activity was 1000 fold higher than that of [¹⁴C] *(R)*-LCM. No specific binding was observed in fractions taken from rat cortex, hippocampus, striatum, or cerebellum that were incubated with 300 nM [³H] *(R)*-LCM. To maximize CRMP2 levels, fractions were taken from CRMP2-expressing oocytes and incubated with 969 nM [³H] *(R)*-LCM. Still, no specific binding was observed. CRMP2 expressed in Cos-7 cells was sequestered by coupling to SPA beads prior to incubation with 600 nM [³H] *(R)*-LCM. Again, no specific binding was reported. Surface plasmon resonance studies revealed no detectable interaction between immobilized CRMP2 and *(R)*-LCM, ranging in concentration from 0.39-100 µM. Based on the lack of specific binding in this report, the authors infer that any effects of *(R)*-LCM on CRMP2, or vice versa, must be indirect in nature. The authors suggest that results gleaned from affinity bait studies do not provide direct evidence that CRMP2 is a target of *(R)*-LCM. As the structure of the ligand required modification (addition of Affinity Bait and Chemical Rreporter moieties), the observed interaction may be a result of an altered receptor interaction profile. Additionally, the authors refute the existence of *(R)*-LCM binding pockets, identified by *in silico* docking, within the CRMP2 protein. They report, based on personal communication with a colleague, the co-crystallization of CRMP2 in the presence of *(R)*-LCM did not reveal a specific binding site. While evidence suggests that CRMP2 may be a target of *(R)*-LCM, it was unclear if this interaction would impact the function of CRMP2. If *(R)*-LCM were able to selectively target CRMP2-mediated neurite outgrowth, it would be an extremely valuable tool in understanding the contribution of CRMP2 in mossy fiber sprouting.

<u>Impact on epileptogenesis</u>

As epileptogenesis is thought to involve changes in neuronal excitability, as well as, network reorganization, the ability of *(R)*-LCM to potentially target not only activity, but also structural plasticity may afford efficacy in the prevention of epileptogenesis, where so many classical antiepileptics have failed. However, the anti-epileptogenic potential of *(R)*-LCM relies heavily on the assumption that the relationship between aberrant sprouting and epileptogenesis is causal in nature. As the majority of AEDs are not disease-modifying, they do not alter kindling acquisition. However, work by Brandt and colleagues demonstrated that *(R)*-LCM treatment could hinder the progression of kindling (Brandt et al., 2006). Rats were kindled by once-daily stimulation of the amygdala 0.5 hrs following intra-peritoneal injection of 3, 10, or 30 mg/kg *(R)*-LCM. Both the severity of seizures and duration of after-discharges elicited by each current injection were decreased in animals treated with 10 or 30 mg/kg *(R)*-LCM. Additionally, *(R)*-LCM treatment led to a ~90% increase in the number of stimulations required for kindling. In fact, while all of the vehicle-treated rats were successfully kindled, only 8/10 and 7/10 rats reached kindled status in the 10 and 30 mg/kg treatment groups, respectively. To determine if the effect of *(R)*-LCM was long-lasting, after 22-23 days of stimulation rats were allowed a 2.5 month washout period, during which they received no current injections. All rats were able to be rekindled within 4 stimulations, regardless of prior *(R)*-LCM treatment. This outcome can be explained in a variety of ways. Of the rats used for the washout experiments, 7/10 *(R)*-LCM treated rats and 10/10 vehicle treated rats had reached kindled status, which by definition insinuates that all rats underwent class V seizures in response to the same current injection. Therefore, as the

36

seizure severity was relatively conserved across treatment groups, differences following a treatment-free washout period were unlikely. For this reason, previous work involving washout periods following amygdala stimulations excluded animals which had reached kindled status prior to washout (Loscher et al., 1998). In these studies, which identified potential anti-epileptogenic properties of the AED levetiracitam, the rate of kindling following washout was slower in previously exposed animals. Once kindling was obtained, however, focal seizure threshold was not different from controls. Therefore it is possible that while the kindling model provides a framework for anti-epileptogenic intervention, once kindling status has been reached the opportunity for prophylaxis may have passed. Alternatively, as *(R)*-LCM lowers excitability by enhancing sodium channel slow-inactivation, treatment directly prior to stimulation may have simply dampened the response to the current injections, thereby impeding the kindling process.

(R)-LCM treatment was associated with a dose-dependent decrease in the number of spontaneous recurrent seizures 6 weeks following induction of status epilepticus (Wasterlain et al., 2011). As the development of spontaneous recurring seizures is dependent upon successful, sustained status epilepticus, it is possible that the reduction of seizures is a direct result of *(R)*-LCM interfering with the induction process. Therefore, a second group of animals received *(R)*-LCM treatment 40 minutes following perforant path stimulation. While all of the vehicle-treated animals demonstrated SRS, they were only observed in 3 of 9 *(R)*-LCM-treated animals. Interestingly, of the animals that did develop SRS, there was no difference in the number of seizures across groups, suggesting that the development of SRS may be an all or nothing process. That late *(R)*-LCM

treatment was able to prevent the development of SRS in 67% of animals suggests that *(R)*-LCM may have some anti-epileptogenic potential.

The ability of *(R)*-LCM to alter injury-induced increases in connectivity was investigated using the undercut (neocortical isolation) model of posttraumatic epileptogenesis. In this model, axon sprouting has been demonstrated by morphological reconstruction of axons of the layer V pyramidal neurons (Salin et al., 1995) and by functional mapping of excitatory synaptic connectivity using laser scanning photostimulation of caged glutamate (Jin et al., 2006). Animals received daily *(R)*-LCM treatments for 1 week following surgery, upon which time the animals were allowed to for an additional week. While field potential recordings did not reveal a difference in the frequency of evoked epileptiform events, the mean amplitude of the recordings was significantly lower in *(R)*-LCM treated animals.   Importantly, electrophysiological recordings from layer V pyramidal neurons revealed a decrease in the frequency of spontaneous excitatory post-synaptic currents. A decrease in frequency without a change in the amplitude or kinetics (rise time, decay time, constant, and ½ width of events) is indicative of a decrease in the number of synaptic connections.   Indeed glutamate uncaging studies demonstrated a decrease in excitatory connectivity following *(R)*-LCM treatment (Figure 1.3). As animals had undergone a 1-week washout period prior to all recordings, these results suggest that *(R)*-LCM may have had a disease-modifying effect following neocortical isolation.

As previously mentioned, TBI is a common instigator of acquired epilepsy. Mice receiving closed-head TBI were treated with *(R)*-LCM 30 minutes following injury and continuing twice daily for 3 days. *(R)*-LCM treatment was associated with a decrease in
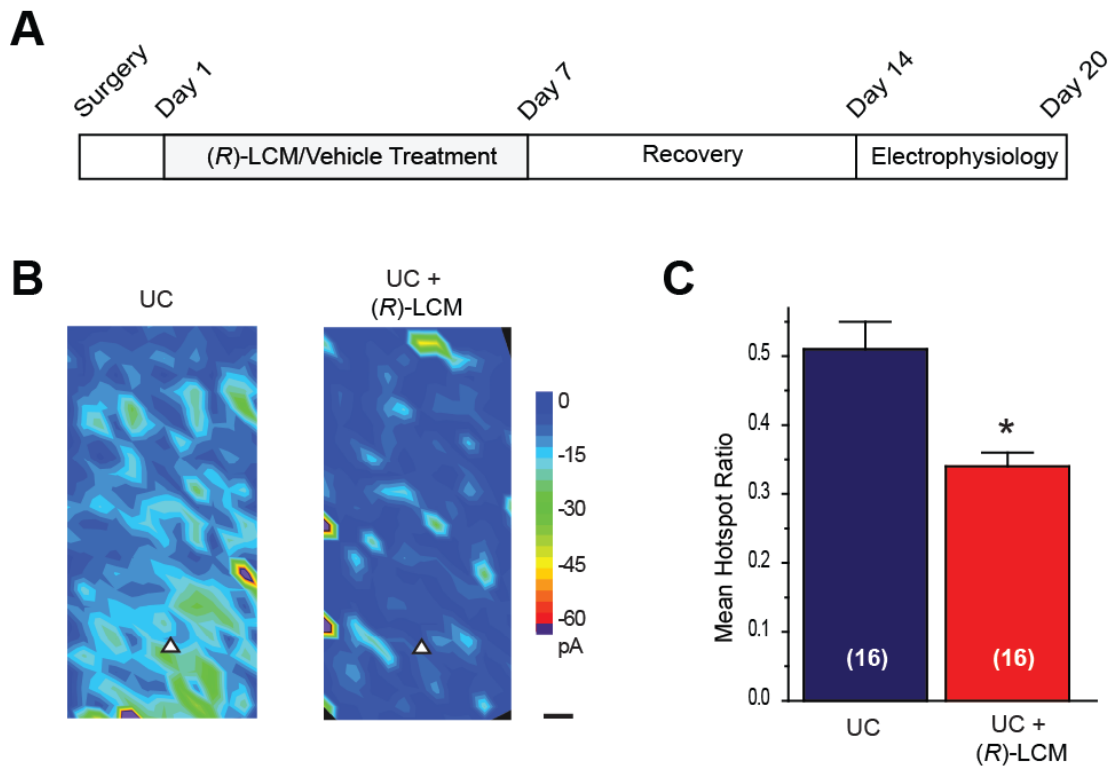
Figure 1.3. (*R*)-LCM treatment reduces excitatory connectivity following neocortical isolation. (**A**) Timeline of experimental design. Undercut surgery is represented as day 0. (*R*)-LCM or vehicle treatment began 1 day following surgery and continued for 7 days. Animals were allowed to recover from treatment until neocortical slices were obtained, 14-20 days after surgery. (**B**) Average uncaging evoked EPSC maps of layer V pyramidal neuron in the undercut (UC) and UC + (*R*)-LCM groups. Arrowhead: soma; color scale: composite amplitude of evoked EPSCs (pA); black scale bar: 50 μm. (**C**) Uncaging activated hotspots in average map of (*R*)-LCM treated-animals were significantly less than that of the injured control group. (* < 0.05, Student's t-test) (values represent mean ± SEM) (n = 16). From *Wilson et al., Prevention of posttraumatic axon sprouting by blocking CRMP2-mediated neurite outgrowth and tubulin polymerization. Neuroscience. 2012. (Wilson et al., 2012)*

neuronal injury that was correlated by a delay in the expression of pro-inflammatory mediator genes and reduced microglial activation (Wang et al., 2013). *(R)*-LCM-treated mice demonstrated improved function in both the rotorod and Morris water maze paradigms. Interestingly, the emergence of mossy fiber projections into the inner molecular layer was not altered by *(R)*-LCM treatment. However, mossy fiber sprouting is viewed as a progressive process and is typically measured in much later stages following injury. Unfortunately, the extent of mossy fiber sprouting was not examined at later time points.

Recently, Licko and colleagues sought to expand previous reports on the anti-epileptogenic potential of *(R)*-LCM (Licko et al., 2013). To avoid any possible interference with the induction of sustained SE, *(R)*-LCM treatment began following its cessation and was continued for 23 days. On the molecular level, many hallmarks associated with SE were altered by *(R)*-LCM treatment. Chronic *(R)*-LCM treatment prevented both neurogenesis of granule neurons as well as cell loss within the piriform cortex and CA1 region of the hippocampus, yet did not impede the aberrant migration of neurons into the hilus. Unfortunately, the extent of mossy fiber sprouting was not determined in this report. However, *(R)*-LCM treatment was associated with a decrease in the number of SE-induced persistent basal dendrites present in the hilar region. Despite the impact on molecular changes induced by SE and contrary to previous reports, *(R)*-LCM treatment did not successfully prevent the development of spontaneous recurring seizures. Additionally, latency to first seizure and the frequency of spontaneous seizures were not attenuated by chronic *(R)*-LCM treatment. While the treatment paradigm was somewhat unorthodox, combining oral administration and continuous

infusion via osmotic minipump, it is unlikely that this would account for the lack of efficacy in preventing the development of spontaneous seizures. In light of all the aforementioned work in vivo, it is difficult to determine whether *(R)*-LCM is anti-epileptogenic in nature.

<u>1.6. Thesis aims</u>

As the molecular mechanisms contributing to mossy fiber sprouting in acquired epilepsies are relatively unknown, in this thesis I will investigate the potential role of CRMP2 in this phenomena. In order to do so, a tool must be developed for selectively targeting CRMP2 activity. It is my hypothesis that the inactivation of GSK3β following the precipitating injury underlies an increase in CRMP2 activity which contributes to increased plasticity and circuit reorganization (i.e. mossy fiber sprouting). To test this hypothesis I employed the following aims:

1. In order to identify a method for preferentially targeting CRMP2-mediated neurite outgrowth, I propose to determine if CRMP2 function is directly impacted by interaction with (*R*)-LCM.

2. To avoid the impact of (*R*)-LCM on voltage-gated sodium channels, I propose to identify a derivative of (*R*)-LCM that selectively targets CRMP2.

3. As GSK3β is inactivated following TLE-related insults I propose to determine if CRMP2-mediated neurite outgrowth is regulated by changes in GSK3β activity.

4. As injury results in inactivation of GSK3β, I propose to determine if CRMP2 phosphorylation is altered following TBI.

5. As many epileptogenic processes are attributed to activity-driven phenomena, I propose to determine if CRMP2 phosphorylation is regulated by neuronal activity.

6. As CRMP2 activity appears to be increased throughout the latent period following injury, I propose to determine if targeting CRMP2 *in vivo* prevents mossy fiber sprouting followingTBI.

CHAPTER 2. MATERIALS AND METHODS

2.1. Lacosamide compounds and recombinant proteins

(*R*)- and (*S*)-LCM, as well as, several other derivatives for *in vitro* studies were generously provided by the laboratory of Harold Kohn, Ph.D. at the University of North Carolina, Chapel Hill. Additionally, (*S*)-LCM for *in vivo* studies was provided by the laboratory of Ki Duk Park, Ph.D. at the Korea Institute of Science and Technology. Recombinant CRMP2 and CRMP2$_{5ALA}$ proteins were previously purified by a former member of the Khanna laboratory, Joel Brittain, Ph.D. Briefly, a CRMP2-GST construct containing 5 amino acids in predicted LCM-binding regions of CRMP2 mutated to alanine (CRMP25ALAGST; Glu-360, Ser-363, Lys-418, Ile-420, and Pro-443) was generated by subcloning the mutation containing portion of CRMP25ALA into wild-type CRMP2-GST (using restriction enzymes RsrII and BglII). Both wild-type and mutant recombinant proteins were purified as previously described (Brittain et al., 2009, Wang et al., 2010a).

2.2. NT-647 labeling of CRMP2 proteins

Recombinant CRMP2 and CRMP2$_{5ALA}$ proteins underwent primary amine labeling using the Monolith^{TM} NT.115 RED-NHS protein labeling kit (NanoTemper) per the manufacturer's instructions. Protein concentration was adjusted to 2-20 μM using the provided labeling buffer. The concentration of dye was adjusted to 2-3 fold the concentration of the protein. Protein and dye were mixed in a 1:1 ratio (200 μl final) and incubated 30 m in the dark at room temperature (RT). Supplied gravity-flow columns were washed and equilibrated with the provided buffers. Labeling mixture was loaded onto the column and eluted using a HEPES buffer. The purity of the sample was determined by measuring the ratio of protein to dye via spectroscopy. Protein absorption

was measured at 280 nm and compared to dye absorption at 650 nm. Labeling resulted in a 1:1 ratio of protein to dye. Calibration curves were completed using the Monolith NT.115 instrument (NanoTemper) and compared to free dye to determine the optimum concentration of labeled-protein to be used.

2.3. Microscale Thermophoresis (MST) binding analyses

MST, the directed movement of molecules in optically generated microscopic temperature gradients, permits an immobilization-free fluorescence methodology for the analysis of interaction of biomolecules (Wienken et al., 2010, van den Bogaart et al., 2012). This thermophoretic movement is determined by the entropy of the hydration shell around molecules. The microscopic temperature gradient is generated by an infrared laser. In a typical MST experiment, the concentration of the labeled molecule is kept constant while the concentration of the unlabeled interaction partner is varied. A constant concentration of NT647-labeled CRMP2 or CRMP2$_{5ALA}$ (final labeled protein concentration of 500 nM) was incubated for 10 min at room temperature in the dark with ascending concentrations of (R)- or (S)-LCM in MST buffer (Table 2.1). Immediately afterward, 3–5 µl of the samples were loaded into standard glass capillaries (Monolith NT Capillaries, NanoTemper), and the thermophoresis analysis was performed on a NanoTemper Monolith NT.115 instrument (40% LED, 40% IR laser power). The MST curves were fitted with a Hill method using GraphPad Prism 5 software to obtain K_d values for binding between CRMP2 and LCM compounds.

2.4. Primary cortical neuron cultures

Rat cortical neuron cultures were prepared from cortices dissected from embryonic day 19 (E19) rats as described (Goslin and Banker, 1989), with some

Table 2.1. Buffers	
Buffer	**Contents**
Depolarizing Tyrode's	32 mM NaCl, 90 mM KCl, 2 mM $CaCl_2$, 2 mM $MgCl_2$, 25 mM HEPES pH 7.5, 30 mM Glucose
External Sodium Recording Solution	100 mM NaCl, 10 mM tetraethylammonium chloride (TEA-Cl), 1 mM $CaCl_2$, 1 mM $CdCl_2$., 1 mM $MgCl_2$, 10 mM D-glucose, 4 mM 4-AP, 0.1 mM $NiCl_2$, 10 mM HEPES (pH 7.3, 310-315 mOsm/L)
G-PEM Buffer	80 mM PIPES, pH 6.9, 1 mM EGTA, 2 mM $MgCl_2$, 5% Glycerol
Glucose-Free BSS	116 mM NaCl, 5.4 mM KCl, 0.8 mM $MgSO_4$, 1.0 mM NaH_2PO_4, 26.2 mM $NaHCO_3$, 0.8 mM $CaCl_2$, 20 mM sucrose
Internal Sodium Recording Solution	110 mM CsCl, 5 mM $MgSO_4$, 10 mM EGTA, 4 mM ATP Na, and 25 mM HEPES (pH 7.2, 290-310 mOsmo/L)
MST Buffer	20 mM Tris, 150 mM NaCl, 0.01 mM EDTA with 0.01% Polyoxyethylene Sorbitan Monolaurate (Tween-20)
Non-Depolarizing Tyrode's	119 mM NaCl, 2.5 mM KCl, 2 mM CaCl2, 2 mM MgCl2, 25 mM HEPES pH 7.5, 30 mM Glucose
Phopshate Buffer	8.1 mM Na_2HPO_4, 1.9 mM NaH_2PO_4
Sodium Sulfide Perfusate	150 mM NaS_2, 8.1 mM Na_2HPO_4, 1.9 mM NaH_2PO_4
TBST	25 mM Tris-Cl, pH 8.0, 125 mM NaCl, 0.1% to 2% Polyoxyethylene Sorbitan Monolaurate (Tween-20)
TIMM Solution	132 mM Citric Acid, 79.5 mM Sodium Citrate, 153.6 mM Hydroquinone, 5 mM $AgNO_3$, 30% Gum Arabic

modifications. Briefly, cortices were dissected out of E19 rats, and cells were dissociated enzymatically and mechanically (trituration through Pasteur pipette) in a Papain solution (12 U/ml; Worthington) containing Leibovitz's L-15 medium (Invitrogen), 0.42 mg/ml cysteine (Sigma), 250 U/ml DNase 1 (type IV; Sigma), 25 mM NaHCO3, penicillin (50U/ml)/streptomycin (50 μg/ml), 1 mM sodium pyruvate, and 1 mg/ml glucose (Invitrogen). After dissociation, the cells were gently washed by sequential centrifugation in Neurobasal medium containing either 2 mg/ml or 20 mg/ml BSA and Pen/Strep, glucose, pyruvate, and DNase1 (as above) and then plated on poly-D-lysine-coated coverslips or 96-well plates at ~400 cells per mm^2. Growth media (1 ml/well or 100 μl/well for 12- and 96-well plates, respecitvely) consisted of Neurobasal medium continaing 2% NuSerum, 2% NS21 (Chen et al., 2008), supplemented with penicillin/streptomycin (100 U/ml; 50 μg/ml), 0.1 mM L-Glutamine and 0.4 mML-glutamax (Invitrogen). 5-fluoro-2′-deoxyuridine (1.5 μg/mL) (Sigma) was added 48 h after plating to reduce the number of nonneuronal cells. After 4 d in culture and 2× each week thereon, half of the growth medium was replaced with medium without 5-fluoro-2'-deoxyuridine. Cultures were mixed yet consisted predominantly of excitatory neurons (Figure 2.1).

Cortical neurons were chosen for the *in vitro* experiments despite the apparent disconnect between their origin and that of dentate granule cells for several reasons. Much of the same phenomena presented herein have been previously observed through the use of cultured hippocampal neurons in our laboratory (data not shown). However, for techniques requiring large amounts of cells such as analysis of neurite outgrowth via IamgeXpress or immunoblot assay the use of hippocampal cultures is not ideal due to the

relatively low yield of each preparation. Additionally, as sprouting in response to injury as well as seizure activity has also been observed within the cortex (Salin et al., 1995), I feel that the use of cortical neurons in these experiments does not present a significant problem.

2.5. Transfection of cortical neuron cultures

Neurons were transfected with various cDNA's via Lipofectamine 2000 (Invitrogen) per the manufacturer's instructions. Briefly, transfection reagent and cDNA's were separately incubated in a serum-free media base (Neurobasal) (Invitrogen) for 5 min. Mixtures were combined and incubated for 25 min. The combined reagent mixture was added to cells in a drop-wise manner. Cultures were returned to normal culture conditions (37°C, 5% CO_2) for 3-4 h, at which point transfection reagents were fed off with normal media

.2.6. Immunocytochemistry

Cortical neuron cultures were washed with sterile PBS, fixed with 4% paraformaldehyde for 20 min at RT, and permeabilized with 0.2% TritonX-100 for 10 min at RT. Neurons were then pre-incubated in 10% bovine serum albumin (in PBS) for 1 h at RT to block nonspecific binding. Primary antibodies (diluted in BSA) (Table 2.2) were applied for 2 h at RT. Neurons were washed with PBS and fluorescently-conjugated secondary antibodies (Alexa-fluor 488 or Alexa-fluor 650) (diluted 1:500 in PBS) were applied to the cells for 30 min in RT. Following another PBS wash, coverslips were mounted onto microscope slides with Prolong Antifade Gold mounting media + DAPI (Molecular Probe). Neurons were imaged on Nikon Eclipse 90i microscope.
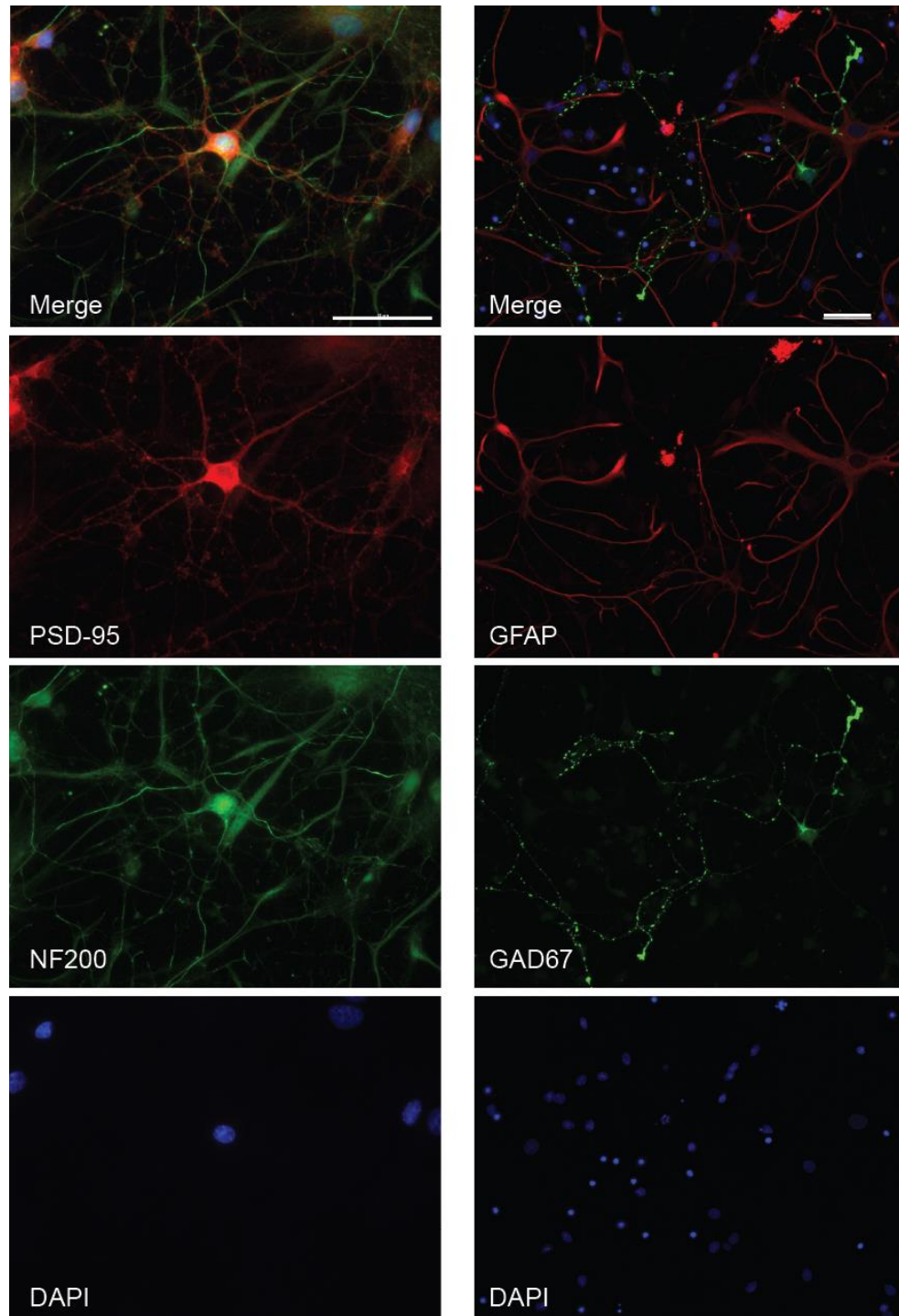
Figure 2.1. Composition of neuronal cultures. Cortical neurons (7 DIV) immunostained for PSD-95 to reveal excitatory neurons, NF-200 to reveal neurons, GFAP to reveal astrocytes, and GAD67 to reveal inhibitory neurons. Scale bar: 50 µm.

2.7. Sholl analysis

Neurite outgrowth of cortical neurons, transfected with enhanced green fluorescent protein (EGFP), CRMP2-EGFP, CRMP2 siRNA + EGFP, or CRMP2$_{5ALA}$-EGFP was assessed as previously described (Wang et al., 2010a). Cortical neurons were transfected at 9 DIV and maintained for an additional 48 h before fixation and imaging. Any treatment ((R)-LCM or VGSC inhibitors) occurred at 24 h post-transfection and lasted 18-24 h. Sholl analysis was performed with ImageJ software using an automated Sholl analysis plug-in, in which the soma boundary is approximated by an ellipsoid, and neurite intersections are assessed at radial distances (20 µm increments) from the soma. Transfection of EGFP into neurons allowed optical identification and unequivocal determination of their arborizations. No attempt was made to distinguish between axons and dendrites in the Sholl analysis. However, using immunocytochemistry with a dendritic marker, MAP2, dendrites could be selectively identified (Figure 2.2). Images were acquired with a Nikon Eclipse 90i microscope by an experimenter blinded to transfection/drug conditions. Images were acquired across 3 separate culture wells.

2.8. siRNA knockdown of CRMP2

Validated small interfering RNAs (siRNAs) against the rat CRMP2 (5′-ACTCCTTCCTCGTGTACAT-3′) sequence (Nishimura et al., 2003) and controls (scrambled sequence with approximately the same percentage of GC but no sequence homology) were used for CRMP2 knockdown (Invitrogen) in cortical neurons as described (Brittain et al., 2009, Chi et al., 2009, Brittain et al., 2011a, Brittain et al., 2011b). Cortical neurons were transfected with either control or CRMP2 siRNA, as well as EGFP to allow visualization. Following transfections, neurons were maintained an
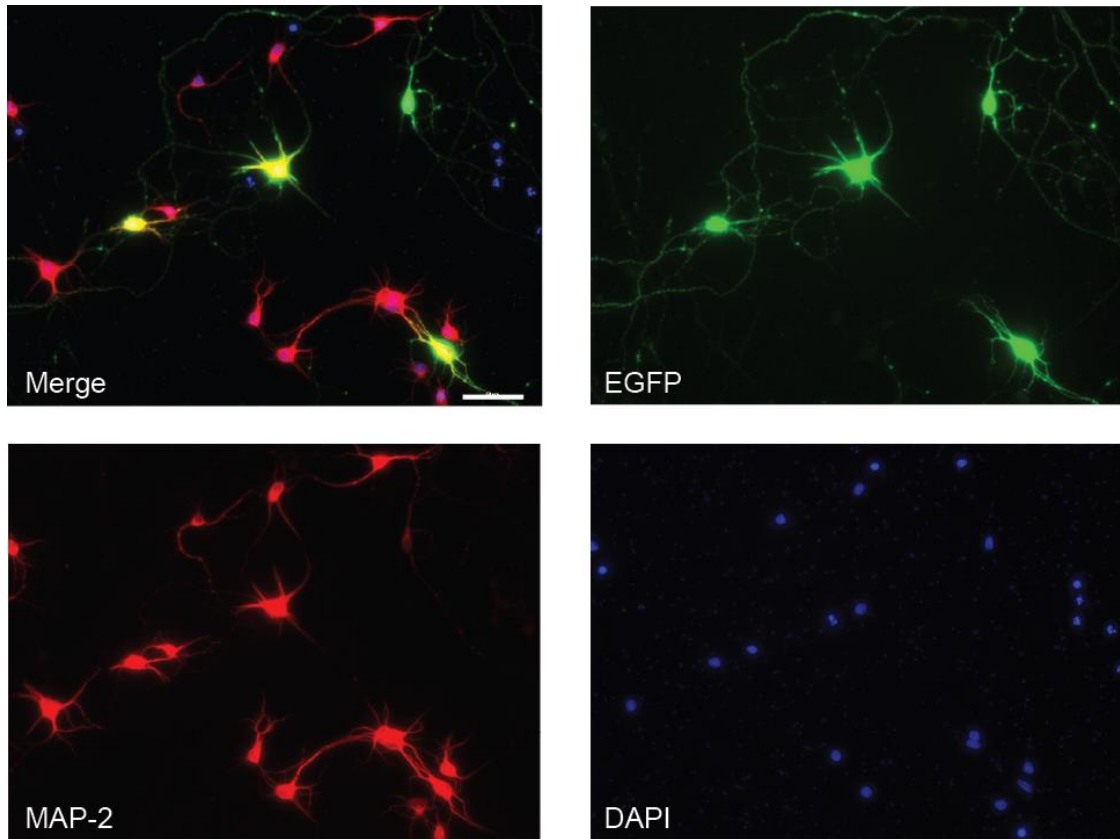
Figure 2.2. Distinction of cortical neuron axons and dendrites. Cortical neurons transfected with EGFP at 5 DIV and immunostained for MAP-2 at 7 DIV to identify dendrites. Scale bar: 50 μm.

additional 48 h prior to imaging. As neuronal transfection rates are relatively low (10-15%), it is difficult to observe siRNA knockdown via western blot analysis. Therefore, a neuronal progenitor cell line was used to verify siRNA knockdown of CRMP2.

Cathecholamine A Differentiated (CAD) cells were grown in Ham's F12/EMEM medium (Gibco) supplemented with 8% fetal bovine serum (Sigma) and 1% penicillin/streptomycin at 37°C and 5% CO_2. CAD cells were transfected with CRMP2 or control siRNA (250 nM) and maintained for an additional 48 h, at which time extent of knockdown was assessed via immunoblot analysis. As reported previously (Chi et al., 2009), we observed a loss of CRMP2 immunoreactivity following knockdown of CRMP2 compared to control siRNA (Figure 2.3). Knockdown of CRMP2 with this siRNA has also previously been verified in cultured neurons via immunocytochemistry (Brustovetsky et al., 2014).
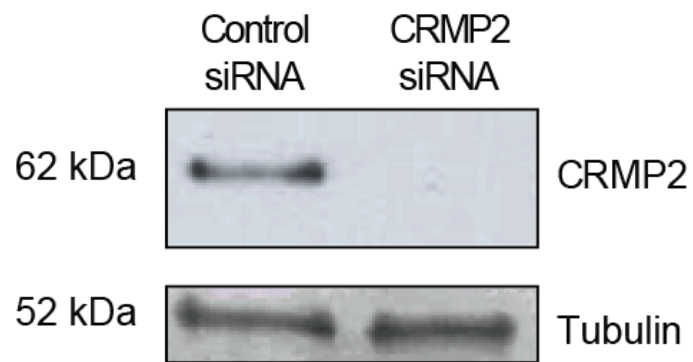
Figure 2.3. siRNA knockdown of CRMP2. Levels of CRMP2 and tubulin in CAD cells following 48 h incubation in control- or CRMP2-siRNA (250 nM).

2.9. Co-Immunoprecipitations

Lysates were generated from post-natal day 1 (PN1) rat brains using lysis buffer composed of RIPA #1 buffer (see table X) and protease inhibitors. Lysates were incubated in either DMSO ($< 0.01\%$) or (R)-LCM (3, 30, or 300 μM) for 30 minutes, at which point they were incubated overnight in primary antibody against CRMP2 (Table 2.2). The antibody-captured complexes were recovered with fresh protein A agarose beads (30 μl, 50% slurry in RIPA #1) by incubation with lysate-antibody mixture for 2 h at 4°C. Beads were then washed three times with lysis buffer and processed for immunoblot assay.

2.10. Immunoblot assay

Protein samples were boiled in Laemmli sample buffer for 5 min and fractionated on 4-15% separating SDS polyacrylamide gels. Apparent molecular weights were determined using broad range standards (Fisher). Following electrophoresis, proteins were transferred to PVDF membranes (Invitrogen) for immunoblotting. Membranes were occasionally stained with ponceau (BioRad) to monitor transfer efficiency. Following transfer, membranes were blocked for 1 h in 5% skim milk powder + 0.05% BSA in TBST (Table 2.1) at RT. Primary antibody incubations (see Table 2.2 for antibody information) were either 2 h at RT or overnight at 4°C. Membranes were extensively washed in TBST and incubated in secondary antibody (goat anti-rabbit, goat anti-mouse, or donkey anti-sheep IgG horseradish peroxidase (HRP)) (G Biosciences) or (goat anti-rabbit, goat anti-mouse IgG dylight 650 or 800 conjugated) (Pierce) (1:15,000). Membranes incubated with HRP-conjugated secondary antibodies were washed extensively in TBST prior to probing with Enhanced Chemiluminescence Western

blotting substrate (Fisher) before exposure to photographic film. Blots were exposed for a range of durations to ensure the generation of a print in which the film is not saturated. Membranes incubated with dylight-conjugated secondary antibodies were washed extensively in TBST prior to imaging with the LI-COR Odyssey imaging system. Both images obtained from film and LI-COR were digitized and quantified using Un-Scan-It gel V6.1 scanning software (Silk Scientific Inc, Orem), limiting our analysis to the linear range.

2.11. Turbidimetric assay for tubulin polymerization

Polymerization of tubulin was performed as described previously (Chae et al., 2009) with modifications. This assay is based on the principle that light is scattered by microtubules to an extent that is proportional to the concentration of microtubule polymer (Shelanski et al., 1973, Lee and Timasheff, 1977). Polymerization was performed in 0.1 M G-PEM buffer (Table 2.1), 1 mM Na-GTP (Sigma), and 2 mg/ml tubulin (Cytoskeleton, Inc). CRMP2 proteins (0.2 µM) as well as 3 µM (*R*)-LCM or 0.01% DMSO were added to the samples and pipetted onto a 96-well plate at 37°C. Turbidity changes were assessed at 340 nm using a Viktor V3 spectrophotometer (Perkin Elmer, Indianapolis, IN), which had previously been pre-warmed to 37°C. Absorbances were measure over time and compared to background samples which contained only buffer + GTP.

2.12. Synaptic bouton size

Synaptic bouton size was determined as previously described (Brittain et al., 2009). Briefly, cultured cortical neurons (6 DIV) were exposed to (*R*)-LCM (100 µM) or DMSO ($< 0.01\%$) for 24 h. Presynaptic terminals were loaded with the fluorescent styryl

Table 2.2. Antibodies Used						
Protein	**Dilution**	**Source**	**Epitope**	**Applications**	**Company**	**Cat #**
CDK5	1:500	Rabbit	Whole Protein	WB, ICC	Cell Signaling	2506S
CRMP2	1:1000	Rabbit	476-493	WB, IP	Sigma	C2933
CRMP2 (pSer522)	1:500	Rabbit	Phospho-peptide	WB, ICC	ECM Biosciences	CP2191
CRMP2 (pThr509/514)	1:500	Sheep	504-517	WB	Kinasource	PB-043
GSK3β	1:500	Rabbit	Whole Protein	WB	Millipore	PK1111
GSK3β (pSer9)	1:500	Rabbit	Phospho-peptide	WB	Millipore	07-835
GFAP	1:500	Mouse	411-422	ICC	NeuroMab	N206A/8
MAP-2	1:500	Mouse	Whole Protein	ICC	AbCam	Ab2832
NF200	1:350	Rabbit	Whole Protein	ICC	Sigma	N4142
P35	1:500	Rabbit	C-terminal peptide	WB	Cell Signaling	C64B10
PSD-95	1:500	Mouse	77-299	ICC	Neuromab	K28/43
Tubulin (βIII)	1:2000	Mouse	373-378	WB, ICC	Promega	G7121
WB: western blot, IP: Immunoprecipitation, ICC: Immunocytochemistry						

dye   N-(3-triethylammoniumpropyl)-4-(6-(4-(diethylamino)phenyl)   hexatrienyl)

pyridinium dibrodmide (FM4-64; 15 µM) by incubation in a depolarizing tyrode's

solution (Table 2.1) for 1 min. Cells were then washed with Ca2+-free solution with

advasep-7 (200 µM; Biotinium, Inc.) to quench dye not taken up by endocytosis. Nerve

terminals were identified under a confocal microscope (Nikon Livescan SFC inverted

microscope) using an oil-immersion CFI Plan APO VC x60 objective lens (Nikon).

Fluorescence of the FM4-64 dye was excited at 543 nm and terminals capable of dye

uptake were considered functional release sites. Bouton size was determined by outlining

the fluorescent puncta in regions of interest (ROI) using NIS Elements software (Nikon).

The area of each ROI was then determined.

2.13. Glutamate release

Glutamate release from cultured cortical neurons was determined as previously

described (Wang et al., 2010b). Cultured cortical neurons (6 DIV) were exposed to (R)-

LCM (3, 30, 100 µM) or DMSO ($< 0.01\%$) for 24 h. Cells were washed three times with

a non-depolarizing Tyrodes buffer (Table 2.1). Following the third wash, 150 µl of each

sample was collected and boiled for 5 min. Release was then stimulated by incubating

cells in a depolarizing Tyrode's buffer (Table 2.1), at which point 150 µl was collected

and boiled. A second basal measurement was obtained by re-incubating in the non-

depolarizing buffer. The remaining content was determined by incubating cells in the

non-depolarizing buffer with 2% Triton X-100 (Sigma) to release intracellular glutamate.

Total content was determined to be the sum of the basal, stimulated, second basal, and

remaining samples. Glutamate content in each sample was determined using the Amplex

Red glutamic acid/glutamate oxidase assay kit (Invitrogen), where L-glutamic acid is

oxidized by glutamate oxidase to produce α-ketoglutarate, NH_2, and H_2O_2. The reaction between the Amplex Red reagent and H_2O_2 is catalyzed by horseradish peroxidase to generate the fluorescent product resorufin. Fluorescence was measured in a Victor2 V multilabel plate reader (PerkinElmer) via excitation at 530 nm and emission at 590 nm and compared to a standard curve.

2.14. ImageXpress neurite outgrowth

Primary cortical neurons plated on 96-well culture plates were transfected via lipofectamine 2000 (Invitrogen) with EGFP, control siRNA +EGFP, or CRMP2-siRNA + EGFP at 4 DIV 48 h before imaging with ImageXpress Micro (Molecular Devices). Immediately prior to imaging, media was exchanged with sterile phosphate buffered saline (PBS). The overexpression of EGFP allowed for visualization of a small percentage of neurons while maintaining optimal cell densities required for survival. EGFP fluorescence was imaged at 4x magnification. To enable laser-based autofocus, laser offset was determined via z-stack. Optimum exposure time was determined to prevent saturation.

Analysis of neurite outgrowth was completed using a neurite outgrowth analysis protocol within the MetaXpress software (Molecular Devices). Cell soma and processes are detected by defining separate size and fluorescence intensity threshold parameters. Maximun width and minimum area parameters for determining somas were set to 50 μm and 300 μm^2, respectively. For identifying processes, maximum width and minimum length parameters were set to 8 μm and 3 μm, respectively. Cells were excluded if they were determined not to be neurons based on morphology, if processes extended beyond the image field, or if no processes were longer than 50 μm. The following parameters are

recorded and summarized into a final "total outgrowth" parameter: number of processes, number of branches, mean process length, and maximum process length.

2.15. Whole-cell patch-clamp recordings

Whole-cell voltage recordings were performed at RT on primary cultured cortical neurons (7 DIV) using an EPC 10 Amplifier (HEKA Electronics). Electrodes were pulled from thin-walled borosilicate glass capillaries (Warner Instruments) with a P-97 electrode puller (Sutter Instrument) such that the final electrode resistances were 2-3 MΩ when filled with internal solutions. Composition of internal and external recording solutions can be found in Table 2.1. Whole-cell capacitance and series resistance (70-80%) were compensated with the amplifier. Cells were considered only when the seal resistance was more than 1 GΩ and the series resistance was less than 10 MΩ. Linear leak currents were digitally subtracted by P/4.

2.16. Oxygen-glucose deprivation (OGD)

Cortical neurons cultured in 96-well plates were exposed to OGD as previously described (Lei et al., 2006). To allow visualization, cortical neurons were transfected with EGFP at 8 DIV and maintained for 48 h. At 10 DIV, cultures were washed with sterile PBS and imaged using the ImageXpress system to obtain a "pre-OGD" image. Immediately following imaging, cells were returned to normal media conditions. Cultures were then placed in an anaerobic chamber (ThermoForma) containing 5% CO_2, 10% H_2, 85% N_2. The culture medium was replaced with deoxygenated, glucose-free BSS (Table 2.1). The chamber was humidified and maintained at 37°C, and cells were exposed to the OGD condition for 2 h. OGD was terminated by returning the cultures to the normal medium and standard incubator. In some experiments, (*S*)-LCM (200 μM)

was applied after OGD. Twenty-four hours after OGD, cultures were washed into sterile PBS and imaged on the ImageXpress system to obtain a "post-OGD" image.

2.17. Traumatic brain injury (TBI)

All procedures involving animals were approved by the Institutional Animal Care and Use Committee of Indiana University School of Medicine and were carried out according to NIH guidelines and regulations. Animals were doubly-housed and maintained in a 12 h light/12 h dark cycle environment with access to foor and water *ad libitum*. Adult male Sprague Dawley rats (275-300 g) were subjected to controlled cortical impact (CCI) injury. Rats were anesthetized with a ketamine/xylazine mixture (80 mg/kg and 5 mg/kg, respectively) and placed in a stereotaxic frame prior to TBI. Using sterile procedures, the skin was retracted, and a ~ 4 mm craniotomy was performed approximately 3 mm lateral to midline and 3 mm posterior to the bregma suture. The skullcap was removed without disruption of the dura. The impacting tip (3 mm) was angled on a medial-lateral plane so that it was perpendicular to the exposed cortical surface. The deformation impact depth was set a 1.5 mm, and the piston velocity was controlled at 3.0 m/s. Following impact, the exposed tissue was covered with bone wax (Henry Schein) and the midline incision was sutured with 5.0 monofilament (Ethicon). Following surgery, animals received a bolus of sterile saline and post-operative analgesic Buprenorphine (0.5 mg/kg). During all surgical procedures and recovery, the core body temperature of the animals were maintained at 36-37°C. Sham animals received the same craniotomy and post-operative care.

2.18. Tissue processing for immunoblot

At 24 h or 4 wk post-TBI, animals were sacrificed and transcardially perfused with 0.1 M phophate buffer (Table 2.1). For perfusion, an incision is made in the left ventricle to allow insertion of a needle attached to a peristaltic pump through the ventricle and into the ascending aorta. The needle was clamped into position and a second incision was made in the right atrium for drainage. Following perfusion, brains were extracted and hippocampi ipsilateral and contralateral to the injury site were dissected, frozen in liquid nitrogen, and stored at -80°C. Prior to immunoblot assay, tissue was thawed and homogenized using a sonicator.

2.19. Activity dependent neurite outgrowth

To elicit activity-dependent neurite outgrowth, cultured cortical neurons were exposed to 25 mM KCl (Tan et al., 2013) or vehicle (< 0.01% sterile saline) beginning at 2 DIV. At 4 DIV, neurons were transfected with EGFP to allow visualization. As the transfection process results in a complete replacement of media, when feeding off transfection 25 mM KCl or vehicle was again included in the media. For determining the involvement of CRMP2, cultures also received 200 μM (*S*)-LCM or 200 μM (*S*)-LCM + 25 mM KCl at the previously mentioned time points. Outgrowth was assessed 48 h post-transfection (6 DIV).

2.20. I*n vivo* administration of (*S*)-LCM

To provide continuous infusion, (*S*)-LCM was delivered via an implanted osmotic mini-pump (Alzet). To compensate for animal growth over the 4-week treatment period, the animals were weighed prior to surgery and the amount of (*S*)-LCM was adjusted to account for the expected weight gain and an infusion rate of 2.5 μl/h to allow for

administration of an average of 5 mg/kg per day of (*S*)-LCM or < 0.01% DMSO for vehicle. Immediately following CCI surgery, sterile mini-pumps were subcutaneously implanted. An incision was made on the back, between the shoulder blades. A small pocket was created by carefully separating skin from muscle near the incision site. The mini-pump was placed into the pocket and the incision was closed with 5.0 monofilament.

2.21. Tissue processing for TIMM staining

At 4 w following TBI, animals were sacrificed and transcardially perfused (as previously described) with a sodium sulfide perfusate solution (Table 2.1), followed by 4% paraformaldehyde. Following perfusion, brains were extracted and placed in 4% paraformaldehyde for 24 h at 4°C. Brains were then transferred to 0.1 M phosphate buffer + 30% sucrose for 48 h at 4°C. Tissue was embedded into Optimal Cutting Temperature (OCT) compound (Tissue-Tek) on dry ice. Coronal slices (35 µm thickness) were made on a cryostat (Leica). Slices were mounted onto gelatin-coated microscope slides and stored at -20°C.

2.22. TIMM staining

Tissue sections were allowed to thawed and processed for TIMM staining with the RAPID TIMM Stain Kit (FD Neurotechnologies). Tissue sections were washed in 0.1 M phosphate buffer 3 times, 3 min each and transferred to the TIMM solution (Table 2.1), where they were rocked gently in the dark for 45-60 min at 30°C. Sections were then rinsed in ddH$_2$O for 3 min in the dark, followed by gently washing them in running water for 30 min to remove excess stain. Sections were dehydrated in 50%, 75%, and 95% ethanol for 3 minutes each. Sections were incubated in absolute ethanol 3 times, 3

min each and then cleared in xylene (Fisher) 3 times, 3 min each. Coverslips were added using a resinous mounting medium (Aquamount) (Fisher).

Once slides had dried, stained sections were imaged on a light microscope (Nikon) at 4x and 10x magnification. Images focused on the dentate gyrus of the hippocampus. TIMM staining was quantified using a previously established scoring system (Figure 2.4) Briefly, images were given a score between 0 and 5, with 0 accounting for a complete lack of TIMM granules within the supragranular zone and 5 describing sections with a dense, laminar band of TIMM granules within the inner molecular layer.
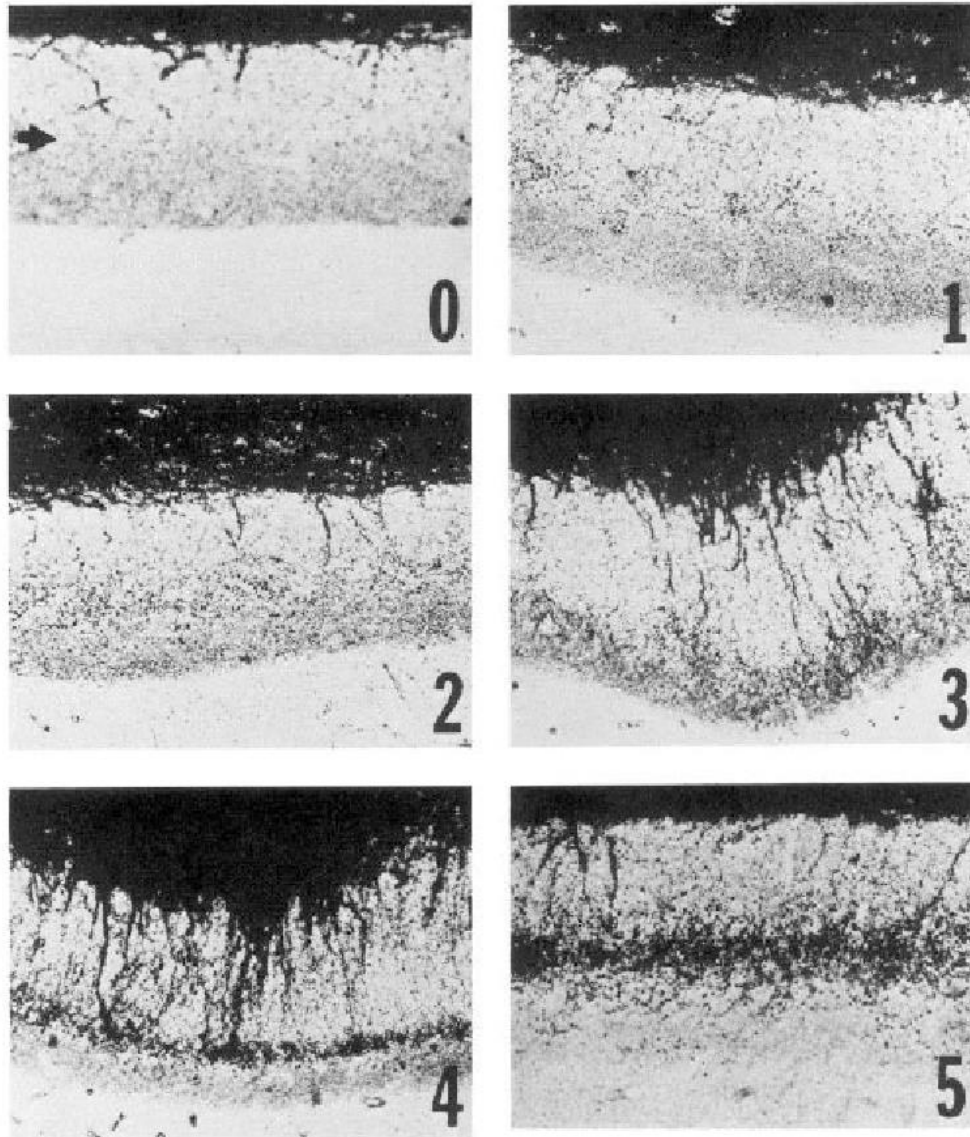
Figure 2.4. Scoring scale for evaluation of TIMM staining. *Figure 2 from Cavazos, Golarai, and Sutula. Mossy fiber synaptic reorganization induced by kindling: time course of development, progression, and permanence. Journal of Neuroscience. 1991* (Cavazos et al., 1991). Distribution of TIMM granules in the supragranular region (black arrow) was rated on a scale of 0-5 based on the following criteria: 0, no reactivity in the supragranular region; 1, sparse granules in the supragranular region in a patchy distribution; 2, more numerous granules in the supragranular region in a continuous distribution; 3, prominent granules in the supragranular region in a continuous pattern; 4, prominent granules in the supragranular region that form a dense laminar band; 5, confluent dense laminar band of granules within the supragranular region that extends into the inner molecular layer.

CHAPTER 3. DEVELOPMENT OF A NOVEL TOOL TO TARGET CRMP2 FUNCTION

3.1 Introduction

3.1 Introduction

The antiepileptic drug lacosamide (*(R)*-LCM) has been heralded as having a "dual mode of action" due to its proposed ability to bind CRMP2 in addition to the voltage-gated sodium channel (VGSC) (Beyreuther et al., 2007). However, opposing reports suggest that the action of *(R)*-LCM on CRMP2 is indirect (Wolff et al., 2012). Therefore, the ability of *(R)*-LCM to directly interact with CRMP2 and impact its function remained controversial. If *(R)*-LCM were able to selectively target CRMP2-mediated neurite outgrowth, it would be an extremely valuable tool in understanding the contribution of CRMP2 in the network reorganization commonly observed in TLE.

3.2 Binding of *(R)*-LCM to wildtype but not mutant CRMP2

Using the novel technique of microscale thermophoresis (MST), potential binding between *(R)*-LCM and CRMP2 was investigated. MST employs the movement of proteins induced by microscopic temperature gradients to measure interactions between ligands and target proteins. Thermophoretic movement away from the field of interest is indicated by a drop of fluorescence (Figure 3.1A). Binding of other proteins, peptides, or small molecules alters the hydration shell, resulting in a change in thermophoretic movement (Wienken et al., 2010). Primary-amine labeled CRMP2 was incubated with varying concentrations of *(R)*-LCM (0.009-150 μM and 0.03-1000 μM, respectively). Standard capillaries (Monolith NT Capillaries, NanoTemper) were filled with ~5 μl of sample mixture and thermophoresis analysis was performed on a NanoTemper Monolith NT.115 instrument. MST curves were fitted using GraphPad Prism software to obtain relative Kd values. Thermophoresis of labeled CRMP2 was altered by increasing
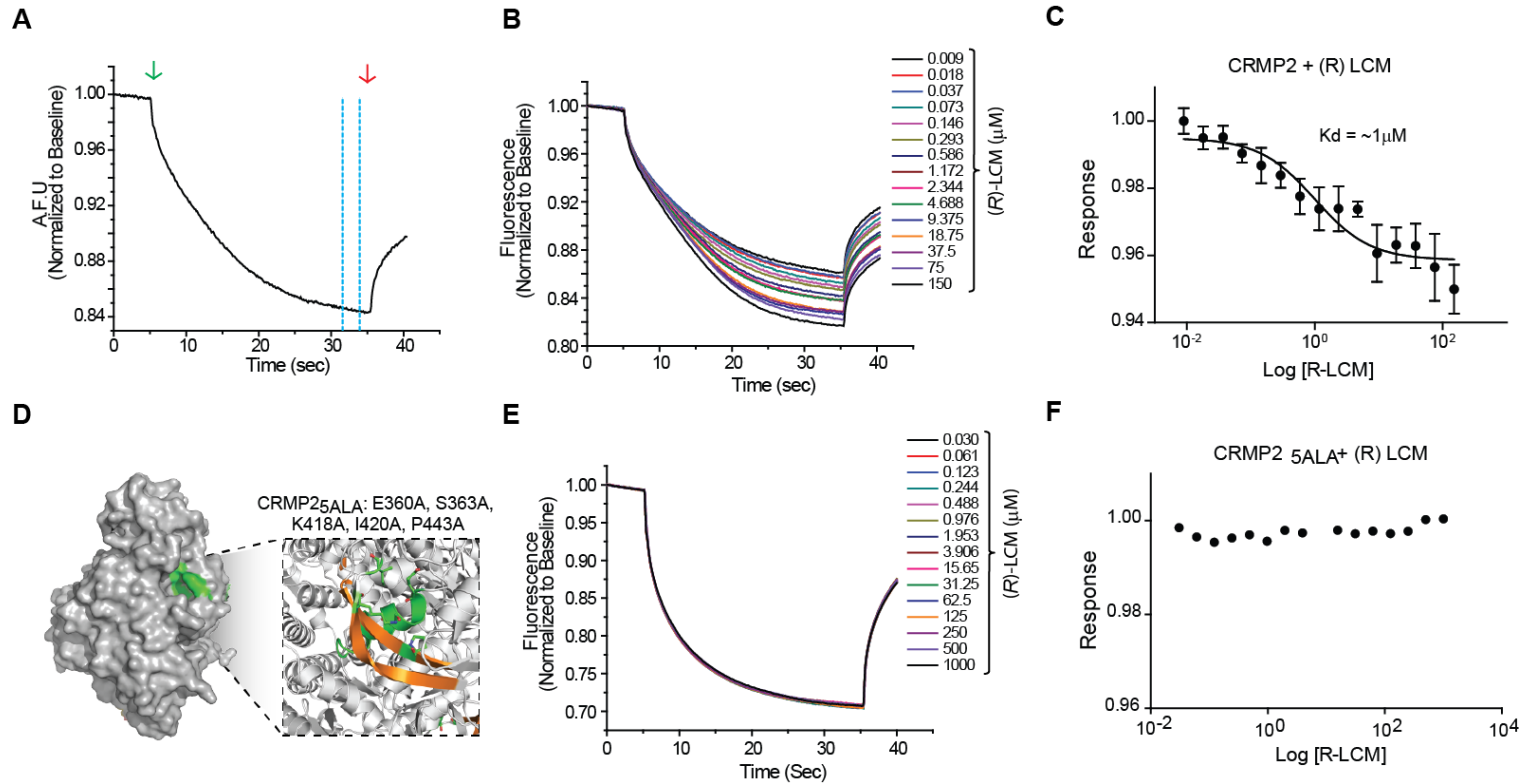
Figure 3.1. Binding of (*R*)-LCM to wildtype but not mutant CRMP2 in solution. **(A)** Representative microscale thermophoresis (MST) curve. A standard capillary containing NT647-labeled protein is locally heated by an IR laser (green arrow). Labeled protein diffuses away from the heated spot, causing a local depletion and drop in fluorescence. Fluorescence returns following cessation of the IR laser (*red arrow*). Dashed blue lines indicate the point at which the degree of thermodiffusion is measured. **(B, E)**. MST time traces of wildtype CRMP2 and (*R*)-LCM (0.009-150 μM) (B) and CRMP2$_{5ALA}$ and (*R*)-LCM (0.030-1000 μM). Thermodiffusion of CRMP2 but not CRMP2$_{5ALA}$ was altered by increasing concentrations of (*R*)-LCM. **(C, F)** Logarithmic dose-response curve used to determine the dissociation constant of (*R*)-LCM to fluorescently labeled CRMP2 (C) or CRMP2$_{5ALA}$ (F). Values represent mean ± SEM from 3 separate trials. **(D)** CRMP2 surface representation highlighting the location of the (*R*)-LCM binding pocket (green). The box represents an enlarged view of the binding pocket highlighting the helices and beta-strands (gold) involved in coordinating (*R*)-LCM binding. The mutated residues comprising CRMP2$_{5ALA}$ are indicated in single amino acid letter code.

concentrations of *(R)*-LCM, indicating an interaction with an apparent Kd value of approximately 1μM (Figure 3.1B-C). In previous work using molecular modeling, cavities in the CRMP2 structure were identified that could coordinate LCM binding (Wang et al., 2010a). A quintuplicate CRMP2 mutant (CRMP2$_{5ALA}$), harboring alanine mutations within the highest affinity LCM-binding pocket of CRMP2 (Figure 3.1D) was created using site-directed mutagenesis (Wang et al., 2010a). These mutations did not alter the protein's ability to mediate neurite dynamics, as the level of neurite complexity in the CRMP2$_{5ALA}$ mutant overexpressing neurons was not different from wildtype CRMP2-overexpressing neurons. Unlike wildtype CRMP2, thermophoresis of labeled CRMP2$_{5ALA}$ was not affected by *(R)*-LCM, even at concentrations as high as 1mM (Figure 3.1E-F). The lack of association with CRMP2$_{5ALA}$ suggests both that the ability of *(R)*-LCM to alter thermophoresis of wildtype CRMP2 is not due to non-specific binding and that the interaction between *(R)*-LCM and CRMP2 is coordinated by the binding pockets previously identified via *in silico* docking.

3.3 *(R)* LCM impairs neurite outgrowth, independent of actions on VGSC

While *(R)*-LCM may preferentially bind CRMP2, it is not known if it can alter its function. As CRMP2 is a positive regulator of neurite outgrowth, I tested the effect of 300 μM *(R)*-LCM on neurite complexity in CRMP2-overexpressing cortical neurons. While this concentration is well above the required concentration for modulation of sodium channel function, it was chosen as a starting point as *(R)*-LCM's interaction with CRMP2 remains poorly classified. In order to assess the degree of neurite growth and branching I employed Sholl analysis on cortical neuron cultures overexpressing EGFP or CRMP2-EGFP. This technique measures the number of neurites crossing concentric

circles (denoted as intersections or branch points) at various radial distances from the cell soma (Sholl, 1953). This consecutive-circles (cumulative intersection) analysis specifies dendritic geometry, ramification richness, and dendritic branching patterns. Cortical cultures were transfected with EGFP or CRMP2-EGFP at 9 DIV and analyzed 2 days following transfection. Consistent with its canonical role, overexpression of CRMP2-EGFP led to a significant increase in neurite complexity compared to EGFP overexpression (Figure 3.2). In order to determine the effect of *(R)*-LCM on this phenomenon, 300 μM *(R)*-LCM was applied overnight to CRMP2-EGFP overexpressing cells 24 h following transfection. Application of 300 μM *(R)*-LCM completely blocked the CRMP2-induced increase in neurite complexity (Figure 3.2A-B). To address the possibility that the observed reductions in neurite complexity were due to the effects of *(R)*-LCM on voltage-gated Na+ channels, we repeated the morphological experiments in the presence of classical VGSC channel blockers which do not target CRMP2 including carbamazepine (300 μM), lidocaine (200 μM), or tetrodotoxin (100 nM). No significant changes in neurite complexity were observed following these treatments (Figure 3.2C), suggesting the mechanism for the reduction in the neurite outgrowth is independent of *(R)*-LCM's effect on voltage-gated sodium channels.

3.4. Concentration-response of *(R)* LCM on neurite outgrowth

To further characterize the effect of *(R)*-LCM on CRMP2-mediated neurite outgrowth, concentration-response curves were completed in CRMP2-EGFP and EGFP over-expressing neurons. At 24 h following transfection, varying doses of *(R)*-LCM were administered overnight and the effect on neurite branching/outgrowth was analyzed (Figure 3.3A). IC_{50} values for inhibition of neurite complexity were obtained by
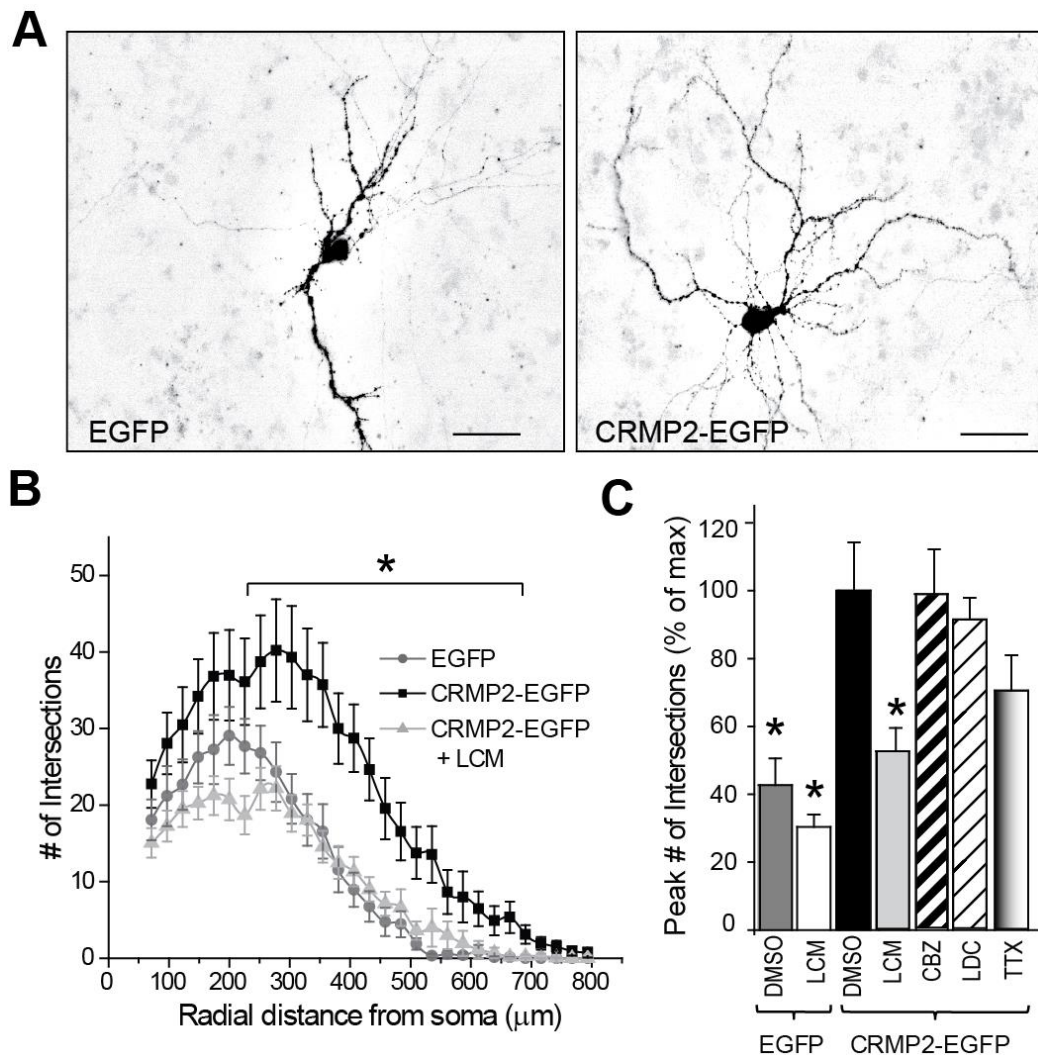
Figure 3.2. **CRMP2-mediated neurite outgrowth is blocked by (*R*)-LCM.** **(A)** Representative inverted black and white images of cortical neurons 48 h after transfection with EGFP or CRMP2–EGFP. Scale bar = 50 µm. **(B)** Neurite complexity was calculated by Sholl analysis of cultured cortical neurons transfected at 9 DIV (and grown for 48 h). Peak numbers of intersections were observed at 275 µm from the soma. Significant increase in neuritic complexity was seen in CRMP2-EGFP neurons (*, $p < 0.05$ vs. EGFP at each distance between 250–700 µm; Student's t- test). Overnight application of 300 µM (*R*)-LCM in CRMP2-EGFP overexpressing neurons returned neuritic complexity to levels comparable to EGFP-overexpressing neurons. At least 17 neurons were analyzed, in a blinded manner for each condition. **(C)** Summary of the average peak neurite complexity for EGFP and CRMP2-EGFP transfected neurons treated with vehicle (0.01% DMSO), 300 µM (*R*)-LCM, 300 µM carbamezapine (CBZ), 200 µM lidocaine (LDC) or 100 nM tetrodotoxin (TTX). To allow direct comparison, peak # of intersections are represented as a percentage of CRMP2-EGFP + DMSO. (values represent mean ± SEM) (n= 15-25 for each condition) (*, $p < 0.05$ versus CRMP2-DMSO; one-way ANOVA, Bonferroni *post-hoc* analysis.)
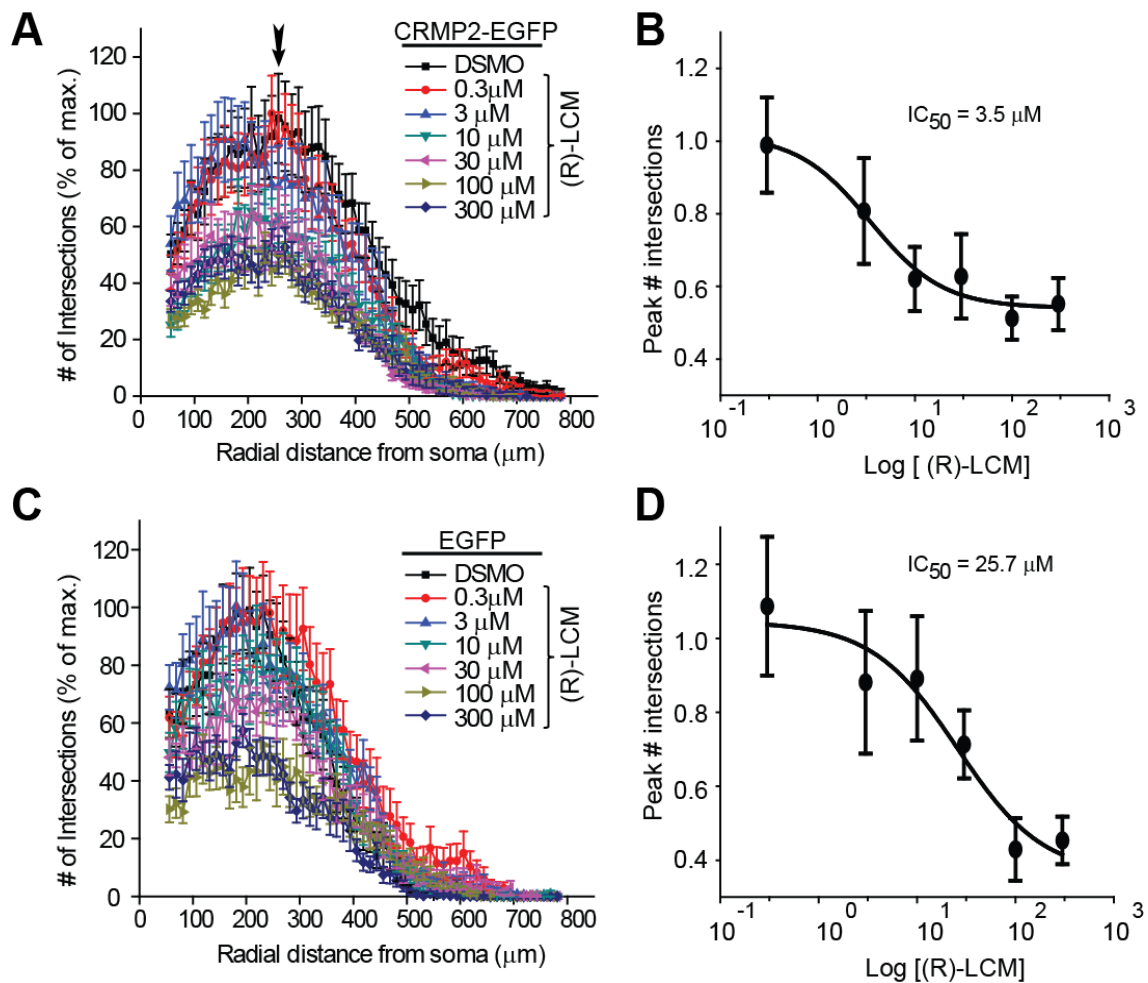
Figure 3.3. (*R*)-LCM causes a dose-dependent reduction in neurite outgrowth. Sholl analysis of cortical neurons overexpressing CRMP2-EGFP (**A**) or EGFP (**C**) and treated for 24 hr with 0.3 μM to 300 μM (*R*)-LCM or 0.1% DMSO (control). To allow direct comparison of the effect of (*R*)-LCM between CRMP2-EGFP and EGFP expressing cells, number of intersections was normalized to the maximum number of intersections in each experiment. Arrow in **A** denotes the peak number of intersections, which occurred at ~275 μm radial distance from the soma. Logarithmic dose-response plots of mean peak # of intersections for CRMP2-EGFP (**B**) and EGFP (**D**) transfected neurons. Average peak # of intersections, obtained from the Sholl analyses, values were normalized to the average peak # of intersections in the vehicle (DMSO)-treated condition. The IC50 for inhibition of neurite complexity by (*R*)-LCM was determined by fitting the curve to a Sigmoidal dose response function (values represent mean ± SEM) (n= 15–25 cells for each condition from at least 3 separate culture

71

comparing the number of intersections at ~275 µm from the soma, as this was the relative distance at which the number of intersections peaked. For neurons overexpressing CRMP2-EGFP, the IC_{50} of neurite inhibition was observed at 3.5 ± 1.7 µM *(R)*-LCM (Figure 3.3B). In contrast, in cells overexpressing EGFP, the calculated IC_{50} was 25.7 ± 1.9 µM LCM (Figure 3.3C-D). While kinetic models predict that over-expression should not alter potency, the output measured in these experiments (neurite outgrowth/branching) is not a binary reaction. It is assumed that in our calculations, only a proportion of branching is CRMP2-mediated under naïve conditions. However, in CRMP2-overexpressing cells, a larger proportion of branching is attributable to CRMP2 and can, therefore, be targeted by *(R)*-LCM. It is unlikely that differences in IC_{50} values reflect separate actions of LCM.

3.5. Loss or mutation of CRMP2 impairs the effect of *(R)*-LCM on neurite outgrowth

To verify that the ability of *(R)*-LCM to reduce neurite outgrowth is attributed to its interaction with CRMP2, experiments were repeated in neurons overexpressing CRMP2$_{5ALA}$. Despite the enhanced neurite complexity seen following overexpression of CRMP2$_{5ALA}$ (Figure 3.4A-B), the IC_{50} value for inhibition of neurite complexity by *(R)*-LCM was calculated to be 25.7 ± 1.8 µM, almost exactly that of EGFP-overexpressing neurons (Figure 3.4C-D), suggesting that *(R)*-LCM is only targeting endogenous CRMP2 in this system. The inability of *(R)*-LCM to target CRMP2$_{5ALA}$- mediated enhancement of outgrowth demonstrates that the effect is specific to *(R)*-LCM's interaction with CRMP2. To further verify the specificity of *(R)*-LCM's effect on neurite outgrowth, we repeated the aforementioned experiments following knockdown of endogenous CRMP2. Sholl analysis was performed 48 h post-transfection with CRMP2 siRNA + EGFP. As
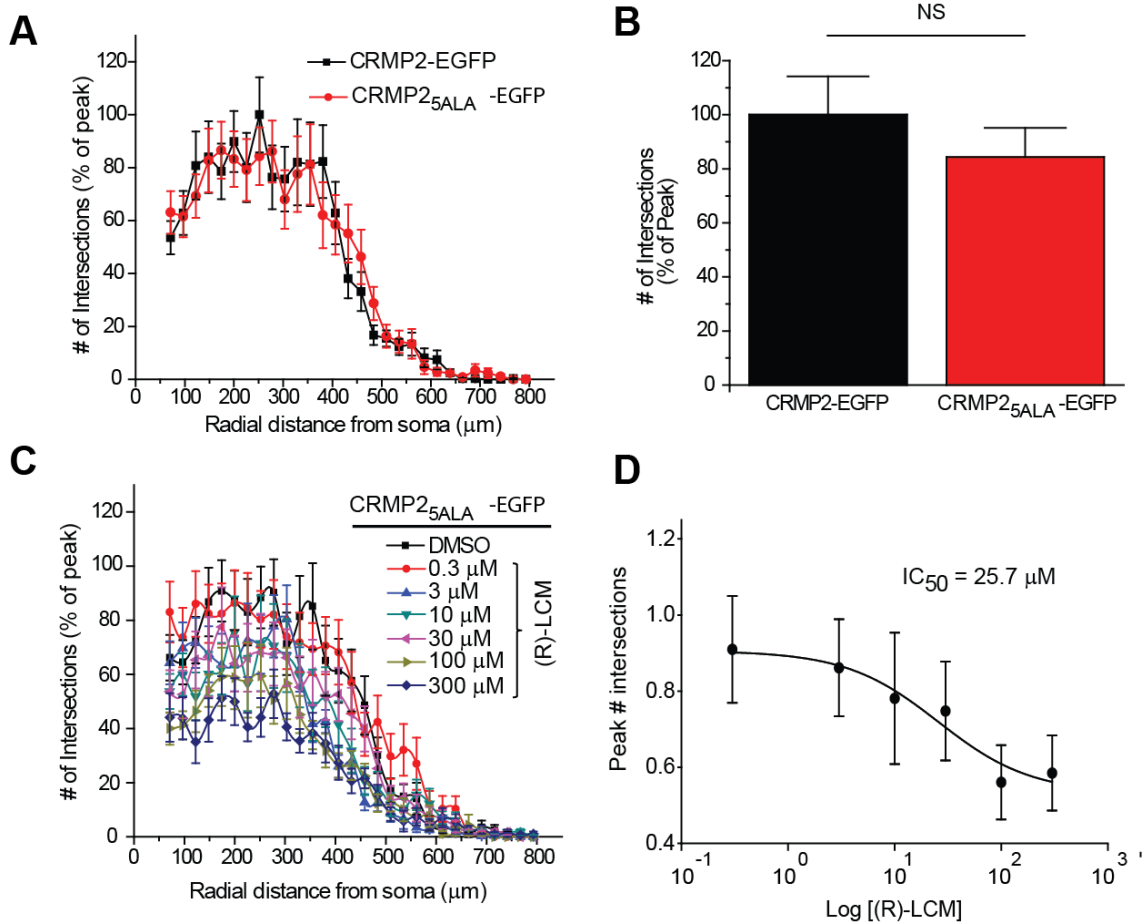
Figure 3.4. Inhibition of neurite outgrowth by (*R*)-LCM following mutation of putative (*R*)-LCM binding sites within CRMP2. **(A,B)** Sholl analyses of neurons expressing CRMP2 or CRMP2$_{5ALA}$. Mutation of the LCM coordinating residues does not impair the ability of this mutant protein to promote neurite complexity. **(C)** Sholl analyses of neurons expressing CRMP2$_{5ALA}$ and incubated in varying concentrations of (*R*)-LCM as indicated. **(D)** Logarithmic concentration-response plot of mean peak # of intersections for CRMP2$_{5ALA}$ expressing neurons. The IC$_{50}$ for inhibition of neurite complexity by (*R*)-LCM was determined by fitting the curve to a Sigmoidal dose response function (values represent mean ± SEM) (n=15-25 cells per condition from at least 3 separate culture wells).

expected, the loss of CRMP2 expression reduced overall neurite outgrowth. Overnight application of 300μM *(R)*-LCM did not lead to a further reduction in neurite complexity (Figure 3.5).

3.6. *(R)* LCM impairs CRMP2-enhanced tubulin polymerization

The ability to bind and promote tubulin polymerization is necessary for CRMP2's role in neurite outgrowth and branching (Charrier et al., 2003). To investigate the mechanism behind the effect of *(R)*-LCM on CRMP2-mediated neurite dynamics, the amount of tubulin binding to CRMP2 was determined in the presence and absence of *(R)*-LCM. Co-immunoprecipitations were performed with a polyclonal CRMP2 antibody from postnatal day 1 rat brain lysates following 30 min incubations in either DMSO or *(R)*-LCM. Co-immunoprecipitation of tubulin with CRMP2 was not altered by incubation of 3, 30, or 300 μM *(R)*-LCM (Figure 3.6A-B).

Distinct from its ability to bind tubulin, CRMP2 has been shown to accelerate tubulin polymerization by enhancing the GTPase activity of tubulin (Chae et al., 2009). To determine if this process was altered in the presence of *(R)*-LCM, microtubule polymerization was measured via a turbidimetric assay. Purified tubulin and recombinant CRMP2 or CRMP2$_{5ALA}$ were combined in a glycerol-PEM buffer in the presence of DMSO or 3 μM *(R)*-LCM. Increases in tubulin polymerization were determined by measuring absorbance at 340 nm every 30 seconds. To compare overall changes in tubulin polymerization, the area under the curve was calculated for each condition, using the first 5 measurements from the naïve condition (tubulin alone) as a baseline. Consistent with previous reports, addition of CRMP2 enhanced tubulin polymerization (Chae et al., 2009). Importantly, CRMP2$_{5ALA}$ also led to a similar enhancement. Co-
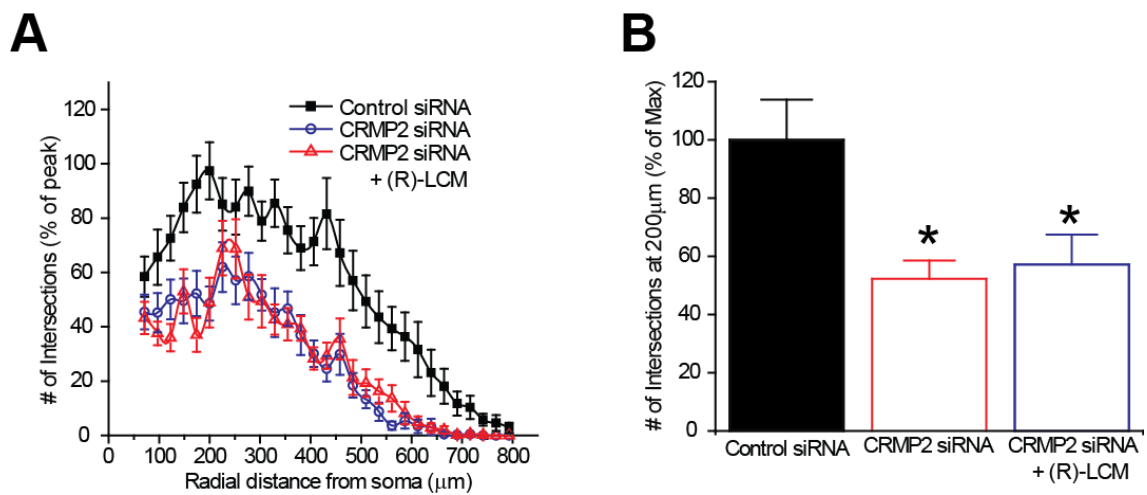
Figure 3.5. siRNA knockdown of CRMP2 reduces neurite outgrowth. **(A)** Sholl analysis of neurons transfected with control or CRMP2 siRNA $\pm$ 300 μM (R)-LCM. **(B)** To allow direct comparisons, the number of intersections were compared at ~200 μm from the soma, as this was that point at which intersections peaked, and expressed as a percentage of max. The siRNA knockdown of CRMP2 decreased neurite outgrowth compared to control siRNA. Overnight incubation of 300 μM (R)-LCM did not cause a further decrease in complexity. (values represent mean $\pm$ SEM) (*, $p < 0.05$; One-Way ANOVA, Bonferroni *post-hoc* analysis).
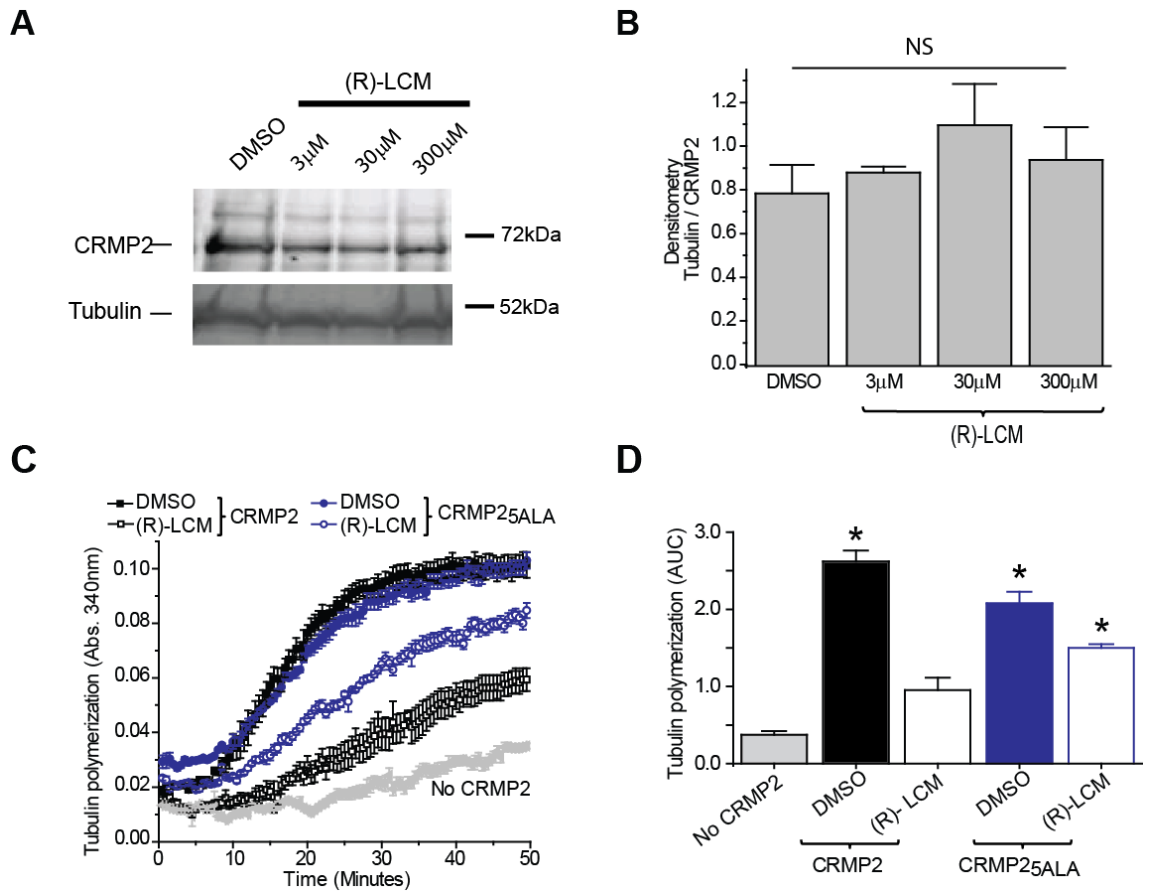
Figure 3.6. (*R*)-LCM reduces CRMP2-enhanced tubulin polymerization. (A) Co-immunoprecipitation of tubulin with CRMP2 in the presence of 3, 30 or 300 μM (*R*)-LCM compared to 0.1% DMSO (control). (B) (*R*)-LCM treatment did not affect the amount of tubulin co-immunoprecipitated with CRMP2 as determined by densitometric analysis (data represents arbitrary densitometric units, n = 4). (C) Effects of CRMP2 and CRMP2$_{5ALA}$ recombinant proteins on microtubule assembly were measured by light scattering and absorbance at 340 nm. Similar levels of tubulin polymerization were facilitated by CRMP2 and CRMP2$_{5ALA}$ proteins. Inclusion of (*R*)-LCM (3 μM) with the CRMP2 protein caused a greater reduction in tubulin polymerization compared to similar treatment of the CRMP2$_{5ALA}$ protein. Also shown is the basal tubulin self-polymerization in the absence of any CRMP2 (no CRMP2). Background absorbance was subtracted from each experiment. (D) Average area under the curve (AUC) values calculated from the tubulin polymerization curves shown in **C**. Addition of 3 μM (*R*)-LCM led to a significant reduction in the tubulin polymerization AUC for wildtype CRMP2 (*, p < 0.05; One-Way ANOVA, Bonferroni *post-hoc* analysis). There was no statistical difference in the tubulin polymerization AUC for CRMP2$_{5ALA}$ in the absence or presence of (*R*)-LCM (p > 0.05, One-Way ANOVA, Bonferroni *post-hoc* analysis) (values represent mean ± SEM) (n = 3-4).

application of 3 µM *(R)*-LCM prevented CRMP2- mediated enhancement of polymerization (Figure 3.6C-D). *(R)*-LCM failed to prevent CRMP2$_{5ALA}$-mediated enhancement of polymerization as the trending effect of (R)-LCM did not reach significance. In the absence of CRMP2 protein, tubulin polymerization was not altered by as much as 300 µM *(R)*-LCM (1.3 ± 0.5) versus naïve (0.4 ± 0.1; n=3, p> 0.05, Student's t-test). These results show that the effect of (R)-LCM is specific to CRMP2-mediated enhancement of tubulin polymerization.

3.7. *(R)* LCM does not alter synaptic bouton size or release of glutamate

As it has previously been demonstrated that increased CRMP2 expression leads to an associated increase in synaptic bouton size (Brittain et al., 2009), the impact of (R)-LCM on this parameter was investigated. Styryl (FM) dyes enable the detection of presynaptic vesicle recycling and release (Ryu et al., 2008, Brittain et al., 2011a). Functional presynaptic terminals were loaded with FM4-64 (15 µM) by stimulating with 90 mM KCl, followed by unloading in a Ca^{2+}-free solution. The area of FM4-64 labeled presynaptic terminals in cortical neurons was determined following overnight incubation of 100 µM *(R)*-LCM, compared to .01% DMSO. Exposure to this level of *(R)*-LCM, sufficient enough to result in maximum reduction of CRMP2-mediated neurite outgrowth, did not alter bouton size (Figure 3.7A-B). As CRMP2 is also a positive regulator of voltage-gated calcium channel function and subsequent neurotransmitter release, the effect of *(R)*-LCM on glutamate release was also investigated. Importantly, overnight exposure to *(R)*-LCM did not affect glutamate release from cortical neurons stimulated with high K^+ (90 mM) compared to 0.01% DMSO (Figure 3.7C-D). These
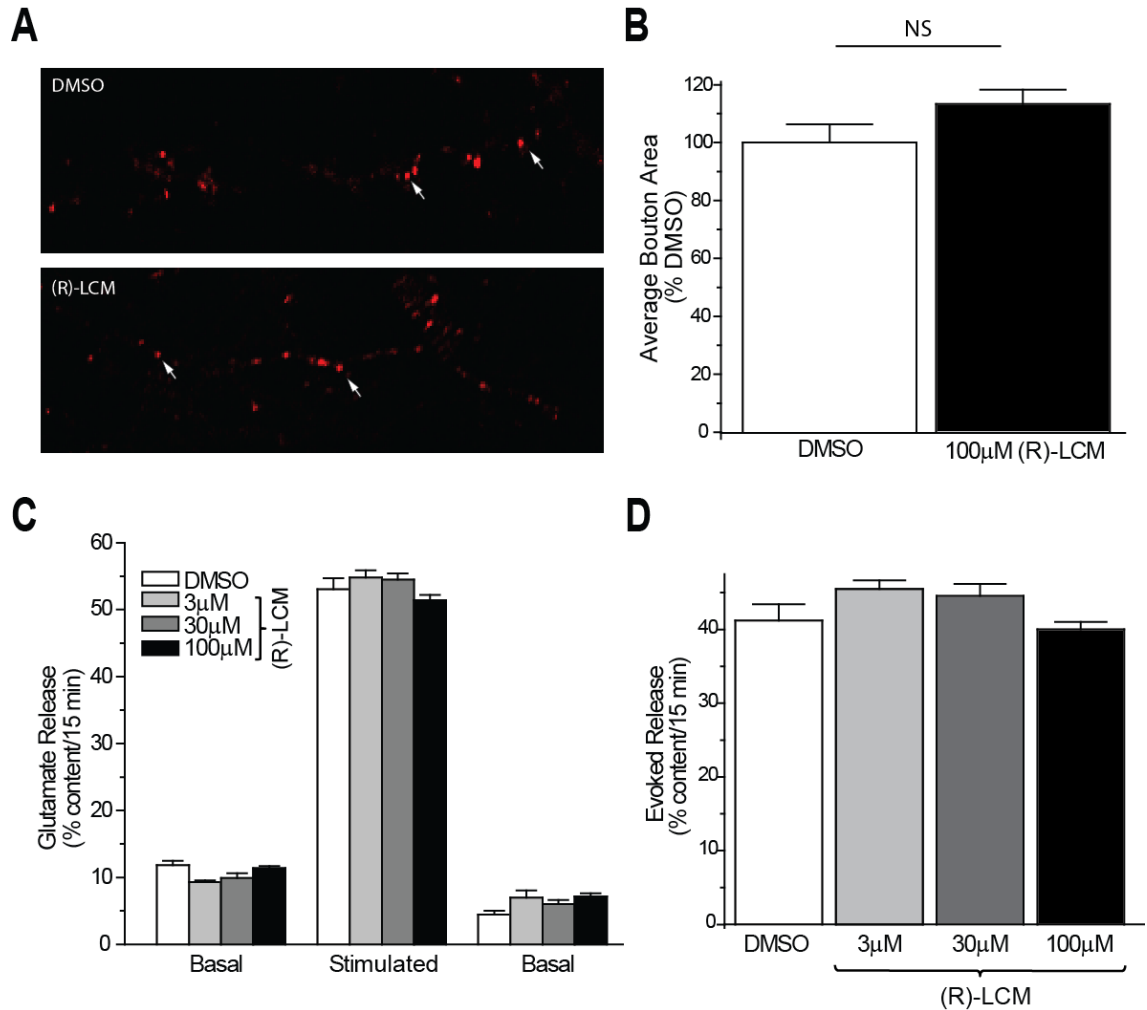
Figure 3.7. (*R*)-LCM does not alter synaptic bouton size or glutamate release. (A) FM4-64 loading of synaptic boutons in cortical neurons. Arrows denote representative boutons. **(B)** Overnight treatment with 100 μM (*R*)-LCM did not affect bouton area. ($p > 0.05$, Student's *t*-test). **(C)** Glutamate release from cortical neurons following overnight treatment with 3 μM, 30 μM, and 100 μM LCM compared to 0.1% DMSO (control). Data are represented as percent of total glutamate content.**(D)** Evoked glutamate release following (*R*)-LCM treatment did not differ from control condition, where evoked release represents: (Stimulated-Basal) as a percent of total glutamate content. ($p > 0.05$, one-way ANOVA, Bonferroni *post-hoc* analysis) (values represent mean ± SEM).

78

results provide further evidence that *(R)*-LCM is preferentially targeting the ability of CRMP2 to mediate neurite outgrowth.

3.8. *(S)* LCM retains the ability to bind CRMP2

While *(R)*-LCM demonstrates potential in targeting CRMP2-mediated neurite outgrowth, its use a tool to determine the role of CRMP2 in mossy fiber sprouting is hindered by its action on the VGSC. Interestingly, as the *(S)* isomer of lacosamide (formerly SPM 6953) requires much higher concentrations to halt seizure activity *in vivo*, LCM is considered stereoselective (Andurkar et al., 1999, LeTiran et al., 2001). It was unknown, however, if the *(S)* isomer retains the ability to impair neurite outgrowth via a direct interaction with CRMP2. MST was used to determine if *(S)*-LCM could interact with recombinant CRMP2. NT647-labeled CRMP2 protein was incubated with varying concentrations of *(S)*-LCM (0.006-100 µM) and apparent Kd values were obtained by fitting curves using the Hill method. MST experiments revealed that *(S)*-LCM bound to CRMP2 with an apparent Kd of 1.5 ± 0.01 µM (Figure 3.8A-B). As it was previously demonstrated that mutation of 5 key residues within the CRMP2 protein resulted in the loss of *(R)* LCM binding, experiments were repeated in the presence of CRMP2$_{5ALA}$ (Figure 3.8C). MST experiments revealed that *(S)*-LCM also did not interact with NT647-labeled CRMP2$_{5ALA}$ (Figure 3.8D), suggesting that the same binding pocket is necessary for coordinating both *(R)*- and *(S)*-LCM binding.

3.9. 200 µM *(S)* LCM phenocopies siRNA knockdown of CRMP2

Although *(S)*-LCM was shown to interact with CRMP2, it is imperative to determine the effect of this interaction on CRMP2 function. Ideally, the effect of *(S)*-LCM on neurite outgrowth should mimic that of siRNA knockdown of CRMP2 sans the
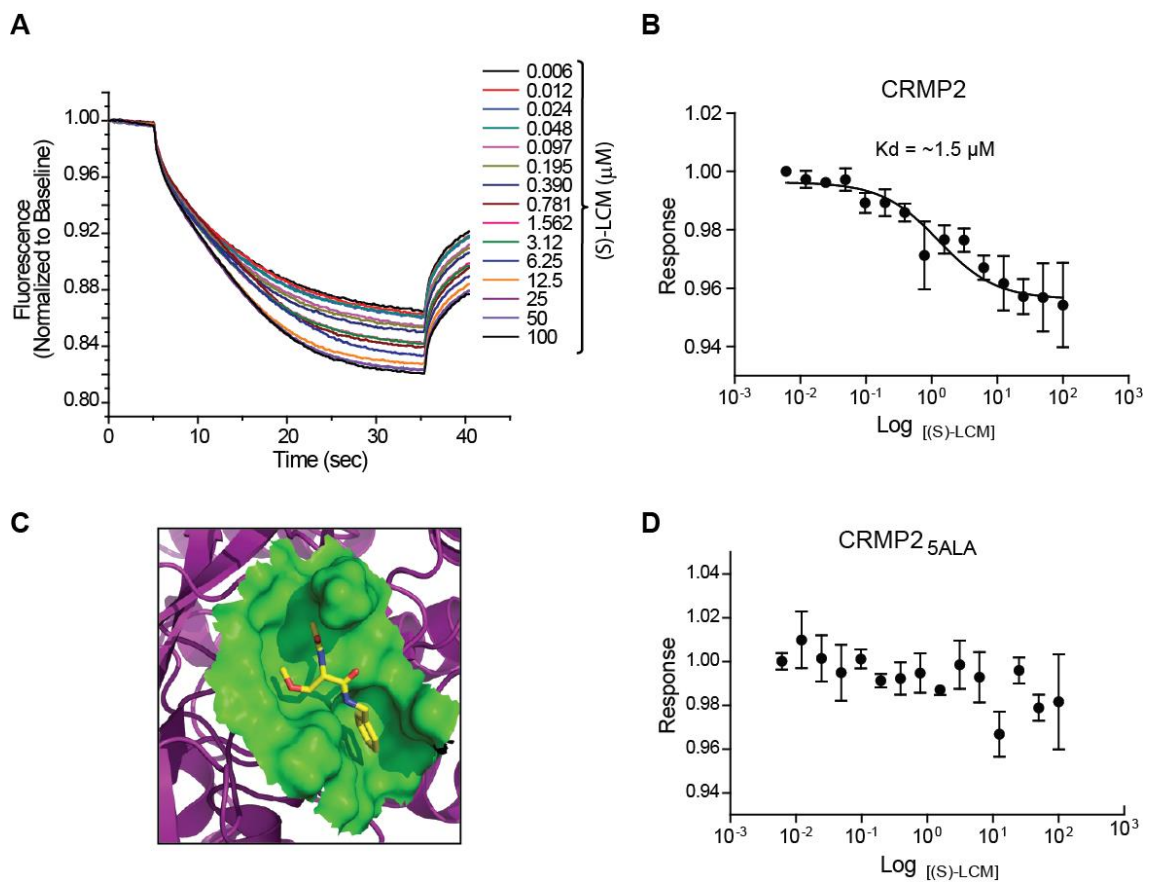
Figure 3.8. (*S*)-LCM retains the ability to bind CRMP2. (A) MST time traces of wildtype CRMP2 and (*S*)-LCM (0.006-100 µM). **(B)** Logarithmic dose-response data used to determine dissociation constant between CRMP2 and (*S*)-LCM (values represent mean ± SEM from 3 separate trials). **(C)** Surface representation depicting (*S*)-LCM docked in the previously identified binding pocket on CRMP2 (green). **(D)** Logarithmic dose-response of MST data for CRMP2$_{5ALA}$ and (*S*)-LCM MST. (values represent mean ± SEM from 3 separate trials).
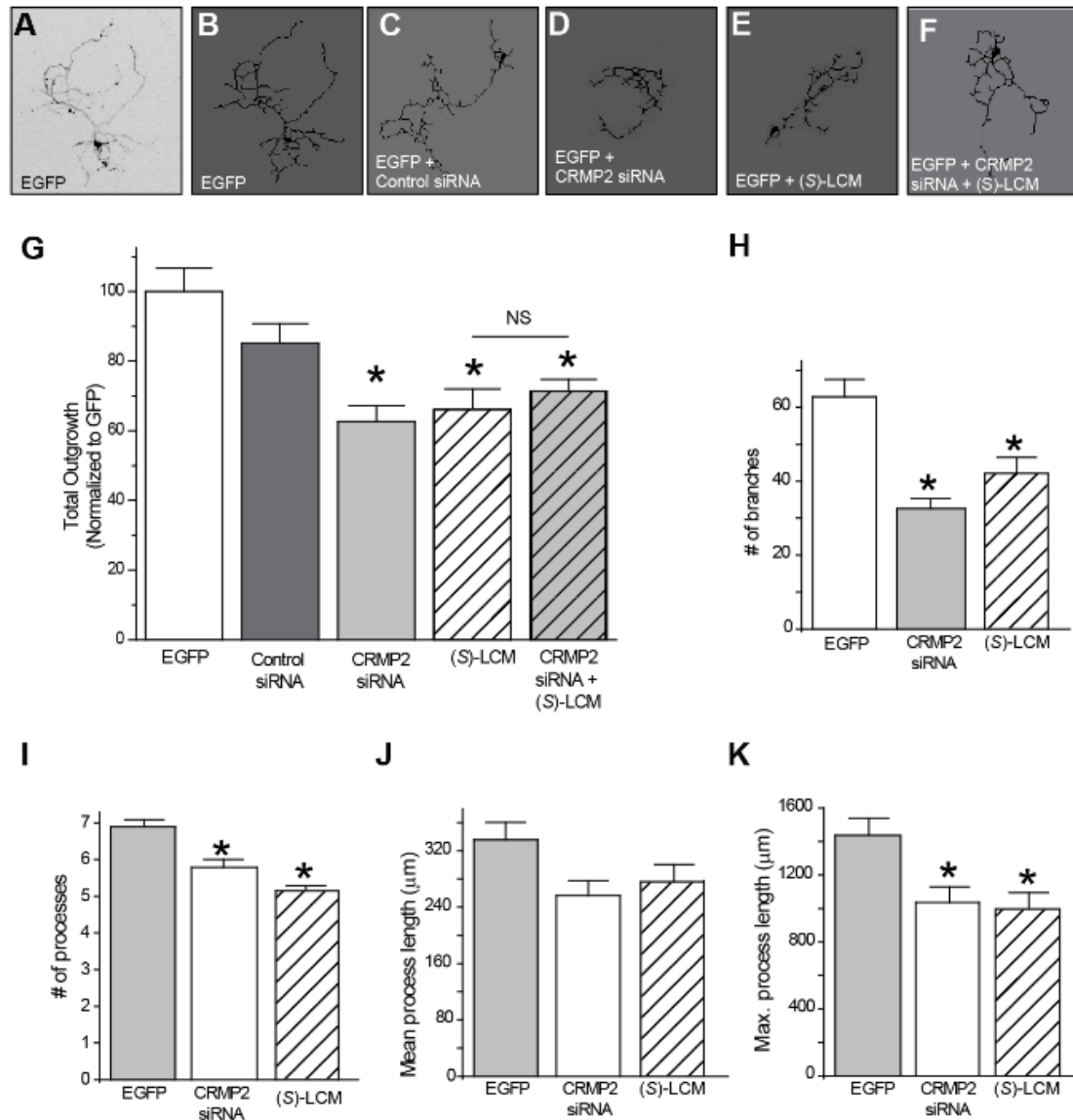
Figure 3.9. (*S*)-LCM inhibits neurite outgrowth similar to that of CRMP2 siRNA. **(A)** Inverted black and white representative image of a cortical neuron 48 hr following EGFP-transfected neuron. **(B-F)** Representative tracings of neurons transfected with EGFP ± control siRNA, CRMP2 siRNA, 200 μM (*S*)-LCM, or CRMP2 siRNA + (*S*)-LCM. **(G)** Total outgrowth of neurons transfected with EGFP, control siRNA, or CRMPsiRNA combined with 24 hr (*S*)-LCM treatment (200 μM). CRMP2 siRNA and (*S*)-LCM reduced outgrowth to a similar level. Combination of CRMP2 and (*S*)-LCM did not produce a further reduction. **(H-K)** Comparison of the effects of CRMP2 siRNA and (*S*)-LCM on # of branches, # of processes, mean process length, and maximum process length. (*, $p < 0.05$ vs EGFP, one-way ANOVA, Tukey's *post-hoc* analysis) (values represent mean ± SEM) (n = 86-320 cells, 8 separate culture wells).

off-target effects on other CRMP2-dependent signaling pathways. Therefore, outgrowth was measured from EGFP-transfected primary cortical neurons (Figure 3.9A-E) using the ImageXpress Micro and MetaXpress software systems (Molecular Devices). This analysis combines the following measurements: number of primary neurites, number of branches, mean process length, and maximum process length to determine a summary of total outgrowth per cell. Consistent with previous reports (Wilson et al., 2012), siRNA knockdown of CRMP2 led to a ~ 37% decrease in total outgrowth (62.6 ± 4.5) compared to control (100 ± 6.6) (Figure 3.9G). Importantly, neurite outgrowth was not altered by conrol siRNA (85.1 ± 5.6) ($p > 0.05$). The effect of CRMP2siRNA was mimicked by overnight application of 200 µM *(S)*-LCM, which decreased total outgrowth by ~34% compared to control (66.2 ± 4.5) ($p < 0.05$). Importantly, *(S)*-LCM was not able to provide a further reduction following CRMP2 knockdown [(71.3 ± 3.3) vs (62.6 ± 4.5)] ($p > 0.05$) (Figure 3.9G). Total outgrowth is a representative summary of the following parameters: number of branches, number of processes, mean process length, and maximum process length (Figure 3.9H-K), all of which, aside from mean process length, were reduced by both *(S)*-LCM and CRMP2 siRNA.

3.10. *(S)*-LCM does not impact VGSC slow inactivation

To ensure that *(S)*-LCM is unable to alter VGSC function at the concentration used to impair outgrowth, whole cell recordings were used to measure levels of slow inactivation. Neurons were held at −100 mV, conditioned to potentials ranging from −10 mV to +20 mV (in +10 mV increments) for 5 s, and then fast-inactivated channels were allowed to recover for 150 ms at a hyperpolarized pulse to −120 mV, and the fraction of channels available was tested by a single depolarizing pulse, to 0 mV, for 15 ms (Figure
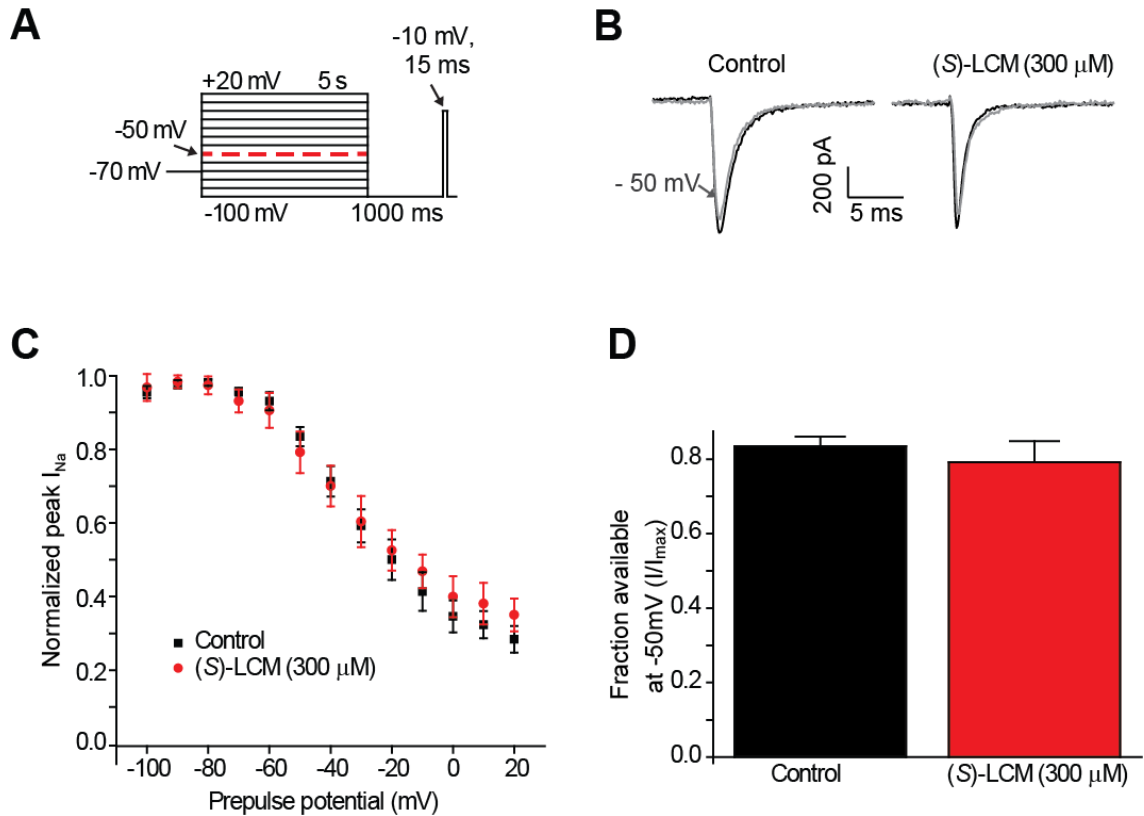
Figure 3.10. (S- LCM does not alter slow inactivation of voltage-gated sodium channels.
(A) Voltage protocol for slow inactivation. Currents were evoked by 5 s prepulses between -100 mV and +20 mV and then fast-inactivated channels were allowed to recover for 1 s at a hyperpolarized pulse to -100 mV. The fraction of channels available was determined by a 15 ms test pulse at -10 mV. **(B)** Representative peak Na+ currents, in response to a step to -10 mV following a prepulse at -100 mV (black trace) and -50 mV (grey trace) in neurons in the absence (left) or presence (right) of 300 μM (*S*)-LCM. **(C)** Summary of steady-state slow inactivation curves for cortical neurons ± 300 μM (*S*)-LCM. **(D)** For comparison, the fraction of current available following a -50 mV prepulse is depicted. (*S*)-LCM did not alter sodium channel steady-state slow inactivation in cortical neurons. ($p > 0.05$) (Student's t-test) (values represent mean ± SEM).

3.10A). Addition of 300 μM *(S)*-LCM did not alter the onset or extent of slow inactivation (Figure 3.10B-D). Therefore, the ability of *(S)*-LCM to impair neurite outgrowth is likely due to its interaction with CRMP2 and is independent of VGSC function. As the effect of *(S)*-LCM on neurite outgrowth phenocopies that of siRNA knockdown of CRMP2, it is thus positioned as a valuable tool for isolating this select function of CRMP2 in a given process.

3.11. Lacosamide derivative screen

Through a collaboration with the laboratory from which *(R)*-LCM was originally developed (Harold Kohn, Ph.D., University of North Carolina, Chapel Hill), several derivatives of *(R)*-LCM were available with varying effects on sodium channel function. In attempt to identify more compounds that were able to impact CRMP2-mediated neurite outgrowth without altering VGSC function, LCM derivatives that had previously exhibited poor efficacy in targeting VGSC slow-inactivation were examined for their ability to reduce neurite outgrowth (Table 3.1). While both *(R)*-and *(S)*-LCM reduced neurite outgrowth compared to DMSO, neither of the 2 identified derivatives were effective. Therefore, *(S)*-LCM is the most likely candidate for preferentiallyly targeting CRMP2 function.

3.12. Discussion

Despite the controversy surrounding the relationship between LCM and CRMP2, these results provide further support for a direct interaction. It was demonstrated that LCM has a functional impact on CRMP2, reducing neurite outgrowth by impairing the ability of CRMP2 to enhance tubulin polymerization. Intriguingly, *(R)*-LCM was able to impact CRMP2 function at concentrations below those required for effective

enhancement of sodium channel slow inactivation (Errington et al., 2008, Sheets et al., 2008). While *(R)*-LCM prevented the increase in neurite outgrowth following overexpression of CRMP2, its efficacy in EGFP-expressing neurons suggests it was also able to alter the function of

endogenous CRMP2. Differences in the potency of *(R)*-LCM in CRMP2-EGFP or EGFP-overexpressing neurons likely reflect the ability of (R)-LCM to target a larger percentage of the output measure (neurite outgrowth) under conditions of CRMP2 overexpression. As the level of CRMP2 expression is increased, so will the proportion of outgrowth attributable to CRMP2 function. That these morphological reductions were observed at concentrations of LCM lower than those reported as the clinical therapeutic plasma concentrations (40–80 μM) (Greenaway et al., 2010), further supports our hypothesis that *(R)*-LCM's mode of action involves CRMP2 in addition to its action on VGSCs.

The mechanism by which *(R)*-LCM impairs neurite outgrowth was demonstrated to be impairment of CRMP2's ability to enhance tubulin polymerization. The region on CRMP2 responsible for enhancing the GTPase activity of tubulin lies within residues 480–509 (Chae et al., 2009). As the binding pocket for *(R)*-LCM is in proximity to this domain (i.e. prime binding pocket residues: E360, S363, K418, I420, and P443) (Wang et al., 2010a), it is possible that the binding of *(R)*-LCM may decrease CRMP2-enhanced microtubule assembly by altering the accessibility of the GTPase accelerating domain of CRMP2 to its effectors. Despite these promising findings, the use of *(R)*-LCM as a tool to investigate CRMP2-mediated neurite outgrowth as it relates to pathological conditions is limited. As neuronal activity is an important element in many pathological processes,

	Table 3.1 Lacosamide Derivatives			
Compound	**Structure**	**Slow Inactivation IC$_{50}$ (µM)**	**Total Outgrowth (% of Vehicle)**
(*R*)-LCM		85	81.6 ± 3.7*
(*S*)-LCM		>1000	66.2 ± 5.9*
Derivative 1		>2400	95.8 ± 4.3
Derivative 2		>1000	98.0 ± 4.5

Slow inactivation IC$_{50}$ values were obtained from previous reports (Wang et al., 2010c, Wang et al., 2011). Total outgrowth represents outgrowth following a 24 h incubation in 300 µM of each compound. For ease of comparison values were normalized to vehicle. (*, $p < 0.05$ vs vehicle) (Student's t-test) (values represent mean ± SEM) (n = 263-394 cells from 8 separate culture wells).

especially epileptogenesis, the impact of *(R)*-LCM on VGSC function may be a confounding factor. Therefore, the identification of a lacosamide derivative, which retains the ability to act on CRMP2, but not the VGSC, was imperative. Our findings indicate that the presumed "inactive analog" *(S)*-LCM is able to interact with CRMP2 and impact its function similar to that of *(R)*-LCM but without affecting VGSC function. As neurite outgrowth is merely one facet of CRMP2 function, *(S)*-LCM can be used in place of genetic knockdown strategies to selectively study this process.

CHAPTER 4. DECREASED GSK3β PHOSPHORYLATION OF CRMP2 MAY DRIVE MORPHOLOGICAL CHANGES DURING THE EARLY PHASE FOLLOWING TBI

4.1. Introduction

        In regards to its outgrowth-promoting function, the activity of CRMP2 is

regulated by phosphorylation state. In the unphosphorylated form CRMP2 is considered

active and thereby growth-promoting; however, upon phosphorylation by a variety of

kinases, most notably GSK3β and CDK5, CRMP2 is rendered inactive (Arimura et al.,

2000, Brown et al., 2004, Cole et al., 2004, Arimura et al., 2005, Uchida et al., 2005,

Yoshimura et al., 2005, Cole et al., 2006, Hou et al., 2009, Uchida et al., 2009).

Tonically active under naïve conditions, GSK3β is inactivated following insults

commonly associated with TLE such as TBI (Shapira et al., 2007, Dash et al., 2011, Zhao

et al., 2012), hypoxia-ischemia (Sasaki et al., 2001, Endo et al., 2006, Xiong et al., 2012),

and status epilepticus (SE) (Lee et al., 2012). This inactivation of GSK3β may lead to an

overall decrease in the level of phosphorylated (inactive) CRMP2, thereby promoting

neurite outgrowth.

4.2. GSK3β phosphorylation of CRMP2 under naïve conditions

        In order for inactivation of GSK3β to impact CRMP2 function, a proportion of

CRMP2 must be phosphorylated by GSK3β under normal conditions. To determine the

extent of GSK3β phosphorylation of CRMP2, primary cultured cortical neurons

following exposure to the GSK3β inhibitor Lithium Chloride (LiCl) (10 mM) or the

protein phosphatase inhibitor okadaic acid (200 nM) for 18-24 h (Figure 4.1A). Western

blot analysis was performed with an antibody specific to phosphorylation at GSK3β

phosphorylation sites on the CRMP2 protein (i.e. Thr509 and Thr514). Importantly,

CRMP2 appears to be phosphorylated by GSK3β under control conditions (Figure 4.1B-

C). Prevention of dephosphorylation by okadaic acid increased phosphorylation by ~2-
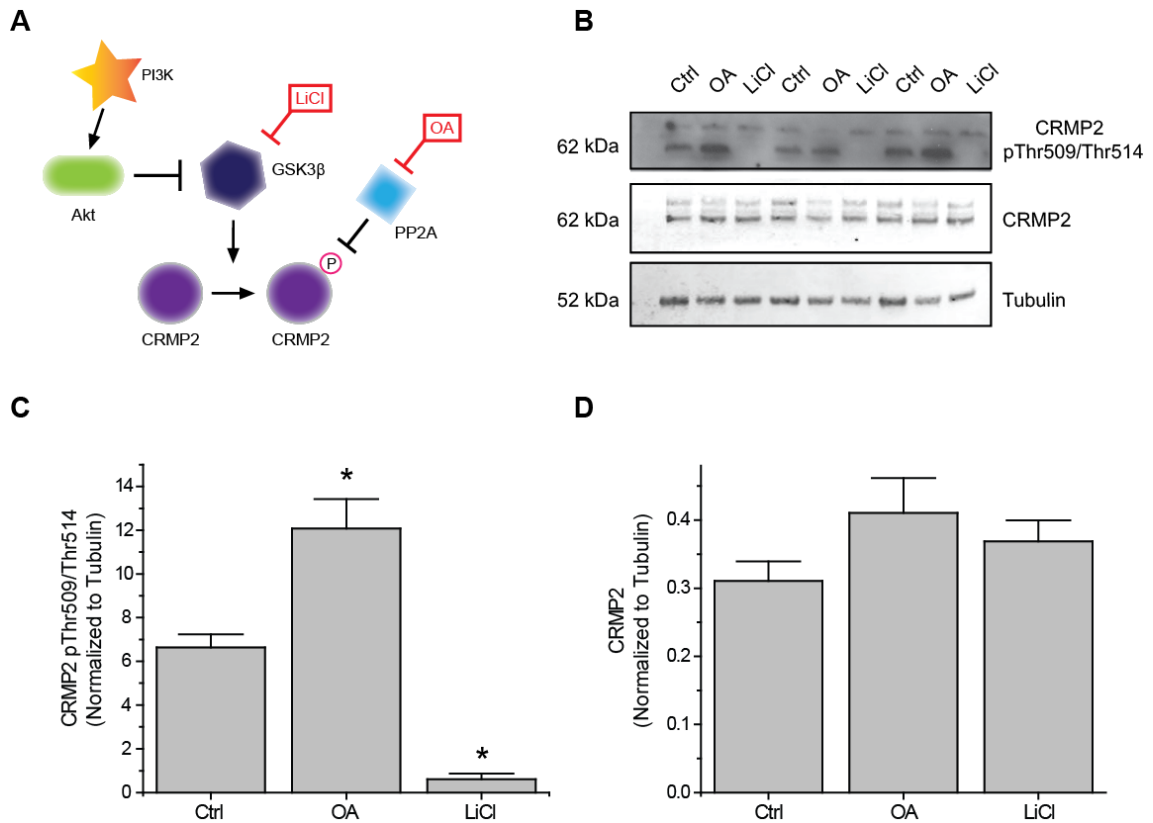
Figure 4.1. Phosphorylation of CRMP2 by GSKβ. (A) Signaling cascade involved in changes in phosphorylation of CRMP2 by GSK3β. Inactivation of GSK3β occurs following activation of Akt or exogenous exposures to lithium chloride (LiCl). Dephopshorylation of CRMP2 by PP2A is prevented by exposure to okadaic acid (OA). **(B)** Levels of GSK3β-phosphorylated CRMP2 and total CRMP2 following 24 hr treatment with LiCl (10 mM) or OA (200 nM). **(C-D)** Summary of western blot analysis of GSK3β-phosphorylated CRMP2 and total CRMP2 levels in cortical neurons ± LiCl or OA (*, $p < 0.05$ vs Ctrl, one-way ANOVA, Dunnet's *post-hoc* analysis) (values represent mean ± SEM) (n = 3).

fold (12.1 ±1.3) compared to control (6.6 ± 0.6), while lithium-mediated inhibition of GSK3β resulted in an ~90% loss of phosphorylation (0.6 ± 0.3) (p < 0.05) (Figure 4.1B-C). Levels of total CRMP2 protein remained unchanged (control: 0.31 ± 0.03; okadaic acid: 0.41 ± 0.05; and lithium chloride: 0.37 ± 0.03) (p > 0.05) (Figure 4.1D). This data suggests that a proportion of CRMP2 is phosphorylated by GSK3β under normal conditions and loss of GSK3β activity dramatically reduces the amount of phosphorylated CRMP2. GSK3β phosphorylation of CRMP2 appears to be dynamically regulated, as evidenced by active dephosphorylation under control conditions.

4.3   GSK3β inhibition increases neurite outgrowth via CRMP2

In regards to its ability to promote neurite outgrowth, phosphorylation by GSK3β effectively inactivates CRMP2. Therefore, inactivation of GSK3β should be growth promoting. EGFP-transfected cortical neurons were exposed to lithium chloride for 18-24hrs to determine the effect of GSK3β inhibition on neurite outgrowth (Figure 4.2A). Immediately following exposure, neurons were imaged using the ImageXpress Micro system and neurite outgrowth was determined via the MetaXpress software system. As expected, inhibition of GSK3β increased total outgrowth (154.5 ± 5.9) compared to controls (99.8 ± 4.0) (p < 0.05) (Figure 4.2B-D). To ensure that the increase in outgrowth was in fact due to changes in CRMP2 activity, the experiment was repeated in the presence of *(S)*-LCM (200 μM). As *(S)*-LCM alone decreases outgrowth, it was included in both lithium chloride and control conditions. In the presence of *(S)*-LCM, LiCl only increased total outgrowth by ~15% (15.3 ± 5.1) compared to ~54% (54.9 ± 5.9) in the absence of *(S)*-LCM (p < 0.05) (Figure). Importantly, the effect of *(S)*-LCM once

91

again mimicked that of CRMP2siRNA [(15.3 ± 5.1) vs (-8.0 ± 15.7)] (p > 0.05) (Figure 4.2E).

4.4. Increased neurite outgrowth following OGD is CRMP2-dependent

By depriving primary cultured neurons of both oxygen and glucose, one can simulate the disruption of the supply of oxygen and nutrients to the brain during a stroke (Goldberg and Choi, 1993). Similar to what is observed in whole-animal hypoxia-ischemia models, *in vitro* oxygen glycose deprivation (OGD) induces inactivation of GSK3β via the PI3K/Akt cascade (Chong and Maiese, 2007, Ueno et al., 2012). Interestingly, OGD is also associated with an increase in axonal/dendritic elongation and branching (Piccini and Malinow, 2001, Lei et al., 2006), that is reduced by preventing the inactivation of GSK3β (Ueno et al., 2012). To further verify the role of CRMP2 in neurite outgrowth mediated by GSK3β inhibition, EGFP transfected cortical neurons were exposed to OGD for 2 h followed by reperfusion with normal media containing either *(S)*-LCM (200 μM) or DMSO (< 0.01%). To better compare the effect of OGD on outgrowth in the different conditions, neurons were imaged immediately prior to OGD to obtain a "pre-OGD" image as well as 24 h following reperfusion to obtain a "post-OGD" image (Figure 4.3A). This method allowed comparison of the same neuronal population before and after insult. Total outgrowth measured 24 h following reperfusion was increased by ~100% (207.6 ± 38.5) compared to before OGD (100 ± 10.5) (p < 0.05) (Figure 4.3B-C). When *(S)*-LCM was applied during reperfusion, neurite outgrowth post-OGD (68.35 ± 18.8) did not differ from that measured pre-OGD (100 ± 10.5) (p > 0.05) (Figure 4.3B-C), suggesting that OGD-induced neurite outgrowth is mediated by CRMP2.
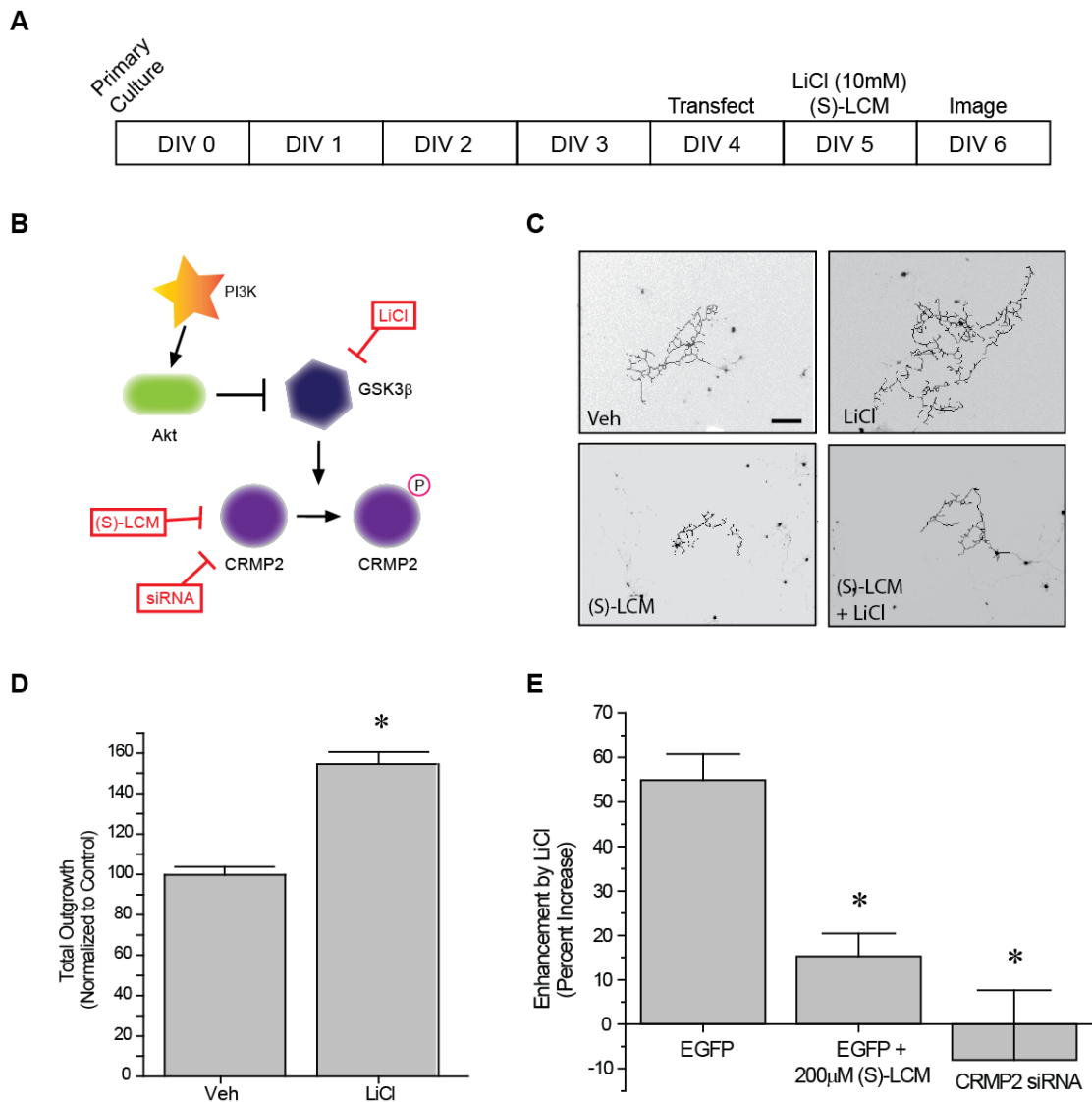
Figure 4.2. Inactivation of GSK3β enhances neurite outgrowth in a CRMP2-dependent manner. (**A**) Experimental timeline. Cortical neurons were transfected with EGFP or CRMP2siRNA + EGFP at 4 DIV and exposed to vehicle (< 0.01% DMSO), LiCl (10 mM), (*S*)-LCM (200 µM), or LiCl + (*S*)-LCM for 24 hr starting at 5 DIV and imaged at 6 DIV. (**B**) GSK3β signaling cascade. (**C**) Representative tracings of neurons transfected with EGFP and exposed to LiCl, (*S*)-LCM, or both. (Scale bar = 150 µm). (**D**) Total outgrowth of neurons exposed to LiCl for 24 hr (*, $p < 0.05$, student's *t*-test) (values represent mean ± SEM). (**E**) Enhancement of outgrowth by LiCl under conditions of (S)-LCM treatment or CRMP2 siRNA knockdown (*, $p < 0.05$ vs EGFP, one-way ANOVA, Dunnet's *post-hoc* analysis) (values represent mean ± SEM) (n = 92-150 cells from 8 separate culture wells).
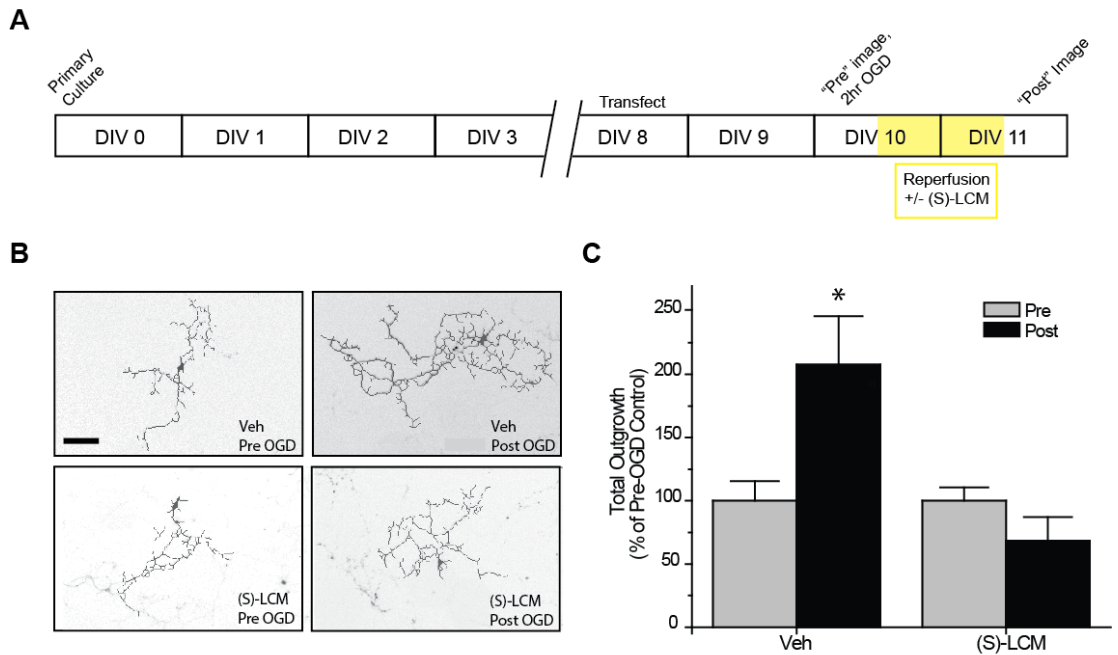
Figure 4.3. Increased neurite outgrowth following OGD is CRMP2-dependent. **(A)** Experimental timeline. Cortical neurons were transfected with EGFP at 8 DIV. At 10 DIV cells were imaged to produce a "pre"-OGD image and then immediately exposed to OGD conditions for 2 hr. Following a 24 hr period where cells were reperfused with normal media + vehicle (< 0.01% DMSO) or (*S*)-LCM (200 μM), cells were imaged to yield a "post"-OGD image. **(B)** Representative traces of EGFP-transfected neurons before (pre) and after (post) OGD ± (*S*)-LCM. (Scale bar = 150 μm). **(C)** Summary of neurite outgrowth before and after OGD ± (*S*)-LCM (*, $p < 0.05$ vs Pre-OGD, one-way ANOVA, Tukey's *post-hoc* analysis) (values represent mean ± SEM on a per well basis) (n = 4-6 wells).

4.5. Loss of CRMP2 phosphorylation following TBI

Evidence of increased Akt activation within the hippocampus as well as other regions has been observed following TBI (Zhang et al., 2006, Zhao et al., 2012). Corresponding to changes in Akt activity, levels of phosphorylated (inactive) GSK3β are also increased following TBI (Shapira et al., 2007, Dash et al., 2011, Zhao et al., 2012). To determine if changes in CRMP2 phosphorylation were the driving force behind the increased neurite outgrowth in the hippocampus in TLE-related insults, hippocampal tissue was collected at both early (24 h) and late (4 wk) phases following TBI. Consistent with previous reports, levels of phosphorylated (inactivated) GSK3β were increased in the early phase following TBI (1.31 ± 0.08) compared to sham controls (1.00 ± 0.05) ($p < 0.05$) (Figure 4.4A-B). Importantly, total expression of GSK3β remained unchanged [(1.00 ± 0.11) vs (0.81 ± 0.12)] ($p > 0.05$) (Figure 4.4A-B). The increase in GSK3β phosphorylation appeared to be transient, as levels did not differ at 4 wk following TBI (0.97 ± 0.12) compared to sham controls (1.00 ± 0.06) ($p > 0.05$) (Figure 4.4C-D).

Subsequent to the observed inactivation of GSK3β, levels of GSK3β-phosphorylated CRMP2 were reduced in the early phase following TBI (0.52 ± 0.07) compared to sham controls (1.00 ± 0.13) ($p < 0.05$) (Figure 4.5A-B). No change in total CRMP2 expression was observed [(1.10 ± 0.12) vs (1.00 ± 0.04)] ($p > 0.05$) (Figure 4.5A-B). Despite the observed transience of GSK3β inactivation, levels of GSK3β-phosphorylated CRMP2 remained reduced in the late phase following TBI (0.62 ± 0.08) compared to sham controls (1.00 ± 0.09) ($p < 0.05$) (Figure 4.5 C-D). These results suggest that there is an increased level of active (unphosphorylated) CRMP2 in both the
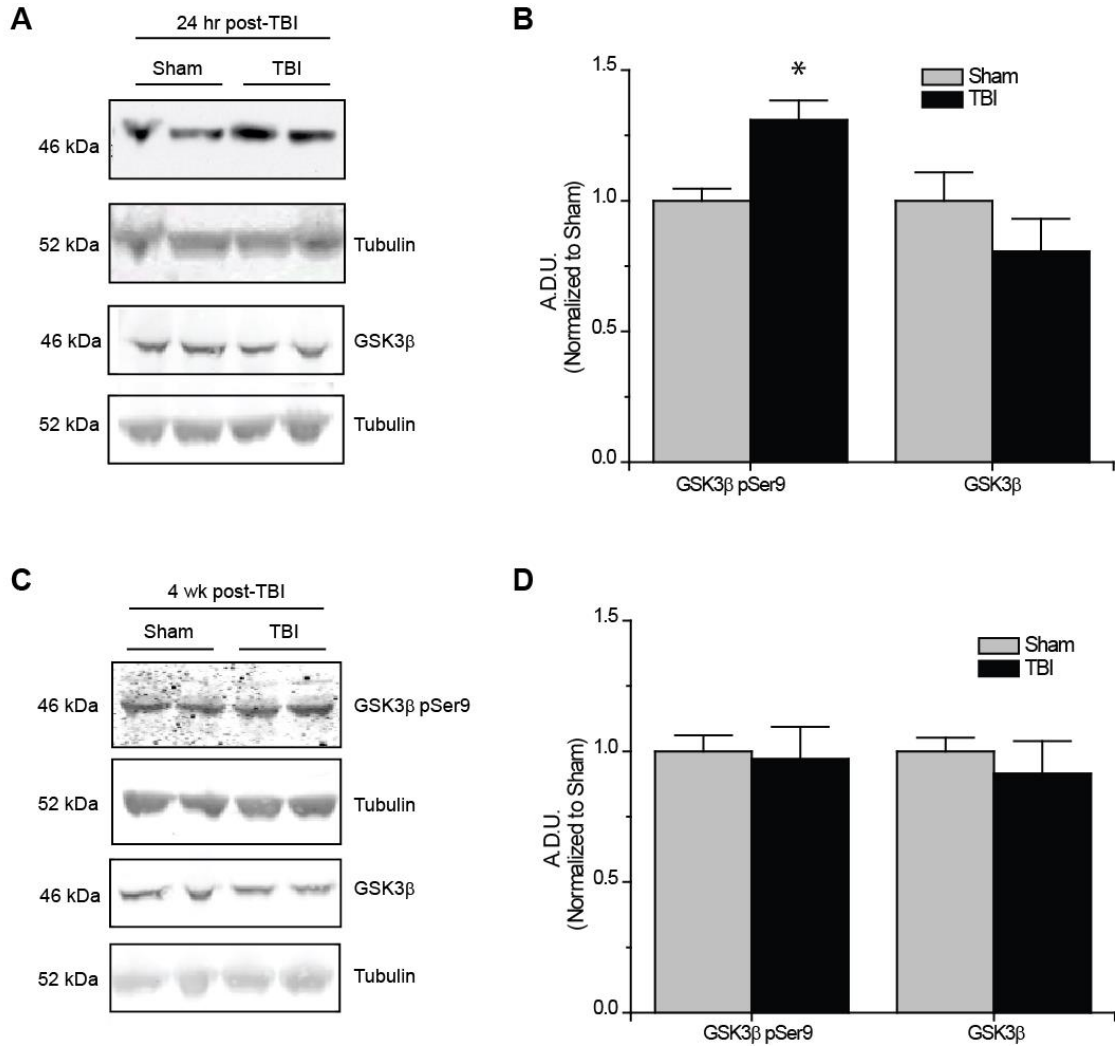
Figure 4.4. Changes in GSK3β phosphorylation following TBI. **(A)** Western blots of phosphorylated and total GSK3β from hippocampal tissue 24 hr following TBI. **(B)** Summary of GSK3β pSer9 and total GSK3β levels 24 hr following TBI. (Data is depicted as arbitrary densitometric units (A.D.U.)). **(C)** Western blots of phosphorylated and total GSK3β from hippocampal tissue 4 wk following TBI. **(D)** Summary of GSK3β pSer9 and total GSK3β levels 4 wk following TBI (*, $p < 0.05$ vs sham, Student's *t*-test) (values represent mean ± SEM) (n = 4-5).
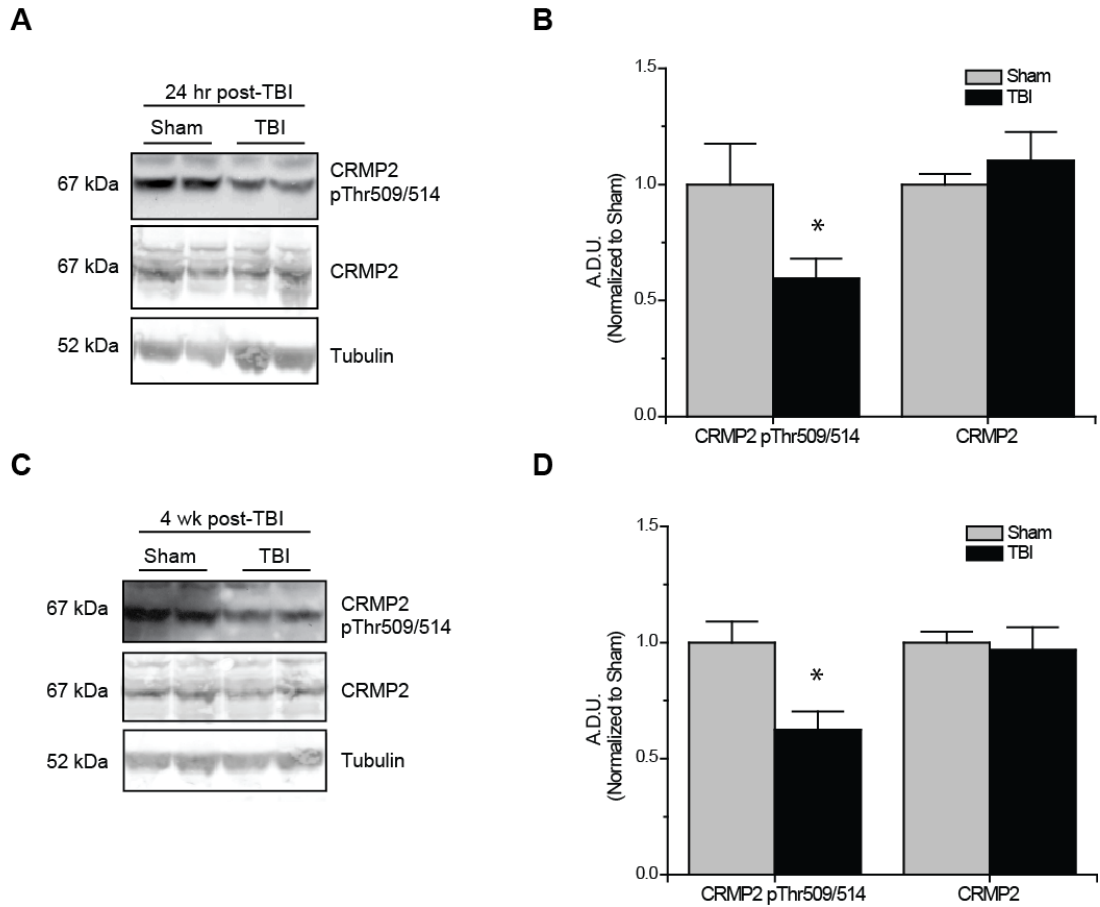
Figure 4.5. Changes in CRMP2 phosphorylation by GSK3β following TBI. **(A)** Western blots of GSK3β-phosphorylated and total CRMP2 from hippocampal tissue 24 hr following TBI. **(B)** Summary of CRMP2 pThr509/514 and total CRMP2 levels 24 hr following TBI (raw data represents protein of interest normalized to tubulin and further normalized to sham to allow for easy comparison) (data is represented as arbitrary densitometric units (A.D.U)). **(C)** Western blots of GSK3β-phosphorylated and total CRMP2 from hippocampal tissue 4 wk following TBI. **(D)** Summary of CRMP2 pThr509/514 and total CRMP2 levels 4 wk following TBI. Data was normalized to sham conditions for ease of comparison. (*, $p < 0.05$ vs sham, Student's *t*-test) (values represent mean ± SEM) (n = 4-5)

97

early and late phases following TBI. Interestingly, while the decrease in CRMP2 phosphorylation at 24 h post-TBI is directly correlated with an inactivation of GSK3β, the sustained decrease observed at 4 wk post-TBI appears to be independent of changes in GSK3β activity.

4.6. Discussion

In order for changes in GSK3β activity to impact CRMP2 function, a balance of GSK3β-phosphorylated and unphosphorylated CRMP2 must be present. Importantly, GSK3β phosphorylation of CRMP2 appears to be dynamically regulated in naïve neurons, as inhibition of GSK3β led to an almost complete loss of phosphorylation within 24 hours. Additionally, the increase in phosphorylation following okadaic acid exposure provides evidence for active dephosphorylation. Therefore, changes in GSK3β activity can directly impact CRMP2 function. Indeed, inhibition of GSK3β led to increases in neurite outgrowth in a CRMP2-dependent manner. As inactivation of GSK3β in these experiments resulted from an exogenous source (LiCl), it was important to demonstrate the involvement of CRMP2 in GSK3β-associated neurite outgrowth under pathological conditions. Outgrowth of cortical neurons following OGD, which is prevented by inhibition of PI3K, coincides with an increase in GSK3β phosphorylation by Akt (Ueno et al., 2012). Through the use of the novel tool *(S)*-LCM, it was determined that neurite outgrowth following OGD was, in fact, dependent on CRMP2.

Given that inactivation of GSK3β has previously been demonstrated following TBI, decreased phosphorylation of CRMP2 may account for the changes in neurite elongation and branching observed within the hippocampus. Our findings indicate that TBI leads to decreased GSK3β phosphorylation of CRMP2 at both 24 h and 4 wk post-

injury. As mossy fiber sprouting is considered a progressive process, the maintained loss of phosphorylation throughout later phases following injury is an important finding. In contrast to early phases following TBI, the loss of GSK3β phosphorylation at 4 wk post-injury is likely not attributed to a prolonged inactivation of GSK3β. In fact, previous reports suggest that levels of Akt-phosphorylated GSK3β return to baseline within 14 days (Dash et al., 2011). These findings suggest that while CRMP2 may play an integral role in promoting neurite outgrowth both immediately following injury as well as in later phases, the mechanisms underlying the increase in CRMP2 activity during these phases may differ.

CHAPTER 5. DECREASED CDK5 PHOSPHORYLATION OF CRMP2 MAY DRIVE MORPHOLOGICAL CHANGES DURING LATE PHASE FOLLOWING TBI

5.1. Introduction

It has been suggested that epileptogenesis during the latent period following TLE-related insults is mediated by kindling-like events (Sutula, 2004). These events are driven by subclinical episodes of network synchronization. As such, many of the involved-processes may be activity dependent. Previous reports have demonstrated that total activity blockade is able to prevent the development of hyperexcitability following neocortical injury (Graber and Prince, 1999). Neurite outgrowth in particular is highly responsive to changes in neuronal activity (Van Ooyen et al., 1995). Recently, CRMP2 was identified to be involved in activity-dependent neurite outgrowth of cerebellar granule cells (Tan et al., 2013). Unlike other central neurons, cerebellar granule cells require slightly depolarizing conditions for survival *in vitro*. Therefore, it is difficult to generalize this finding to other neuron populations within the central nervous system. As such, it is not known if CRMP2 is involved in outgrowth induced by depolarization in neurons where it is not necessary for survival.

5.2. Targeting CRMP2 prevents KCl-facilitated outgrowth

To determine the involvement of CRMP2 in activity-driven neurite outgrowth, cortical neurons overexpressing EGFP were exposed to 25 mM KCl and maintained for 96 h to ascertain the extent of activity dependent neurite outgrowth (Figure 5.1A). This concentration of KCl was chosen as it has previously been used to investigated the role of CRMP2 in activity-dependent neurite outgrowth of cerebellar granule neurons (Tan et al., 2013). As expected, chronic depolarization with 25 mM KCl led to a ~43% increase in total neurite outgrowth (143.1 ± 11.5) compared to control (100 ± 6.6) ($p < 0.05$) (Figure 5.1 B-C). Notably, blockade of CRMP2-mediated neurite outgrowth by *(S)*-LCM was
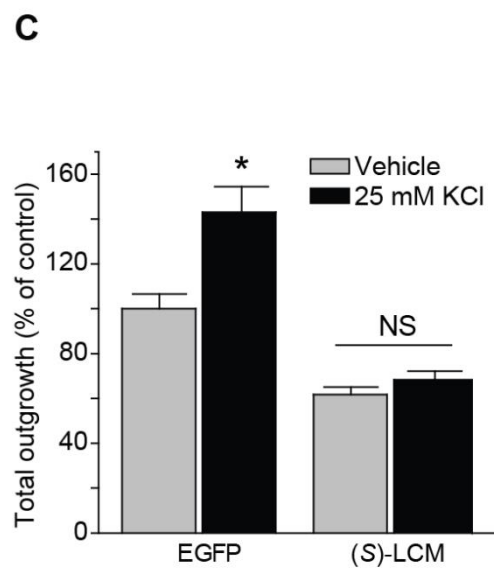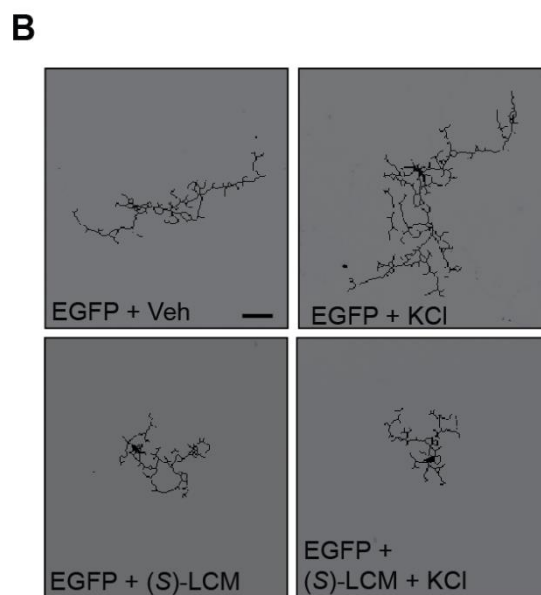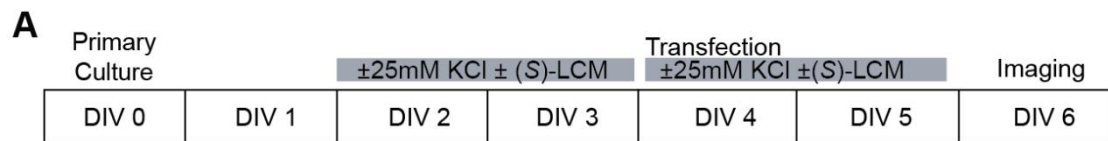
Figure 5.1. Targeting CRMP2 prevents KCl-facilitated increase in neurite outgrowth. (A) Timeline of experimental procedures. (B) Representative tracings of cortical neurons expressing EGFP and incubated for 96 h in vehicle (< 0.01% DMSO), 25 mM KCl, 200 μM (*S*)-LCM, or 25 mM KCl + 200 μM (*S*)¬-LCM. Scale bar = 150 μm. (C) Total outgrowth of cortical neurons exposed to 25 mM KCl in the presence or absence of 200 μM (*S*)-LCM (*, p < 0.05 vs vehicle, Student's *t*-test) (values represent mean ± SEM) (n = 127-205 cells from 8 separate culture wells).

sufficient to prevent activity dependent growth induced by KCl (68.4 ± 3.8 vs 61.7 ± 3.5) (p > 0.05) (Figure 5.1 B-C). As our earlier data demonstrated that *(S)*-LCM is not affecting VGSC function in these neurons, these data suggest that activity-dependent neurite outgrowth is dependent on CRMP2.

5.3. Activity reduces CRMP2 phosphorylation by GSK3β without affecting kinase activity

As phosphorylation by GSK3β regulates the ability of CRMP2 to enhance neurite outgrowth, western blot analysis was used to determine the level of GSK3β-phosphorylated CRMP2 following acute (30 min) and chronic exposure to KCl (96 h) (Figure 5.2A). Both acute and chronic treatments with 25 mM KCl reduced the level of GSK3β-phosphorylated CRMP2 (8.9 ± 1.5 and 10.0 ± 1.5, respectively) compared to control (22.1 ± 3.5) (p < 0.05), while total CRMP2 expression did not change (Figure 5.2B-D). Therefore, exposure to KCl leads to increased levels of active, unphosphorylated CRMP2.

To determine if the decrease in CRMP2 phosphorylation induced by KCl is due to decreased levels of GSK3β activity, the amount of Ser9-phosphorylated GSK3β was measured following KCl exposure (Figure 5.3A). Interestingly, phosphorylation of GSK3β was unaffected by acute or chronic KCl exposure [(16.4 ± 3.1 and 17.1 ± 4.3) vs (18.7 ± 3.6)] (p > 0.05) (Figure 5.3B-C). Additionally, total GSK3β expression remained unchanged (Figure 5.3D-E). Similar to what was observed in the late phase following TBI, these results suggest that the decrease in GSK3β-phosphorylated CRMP2 is not attributed to a change in GSK3β expression or activity.
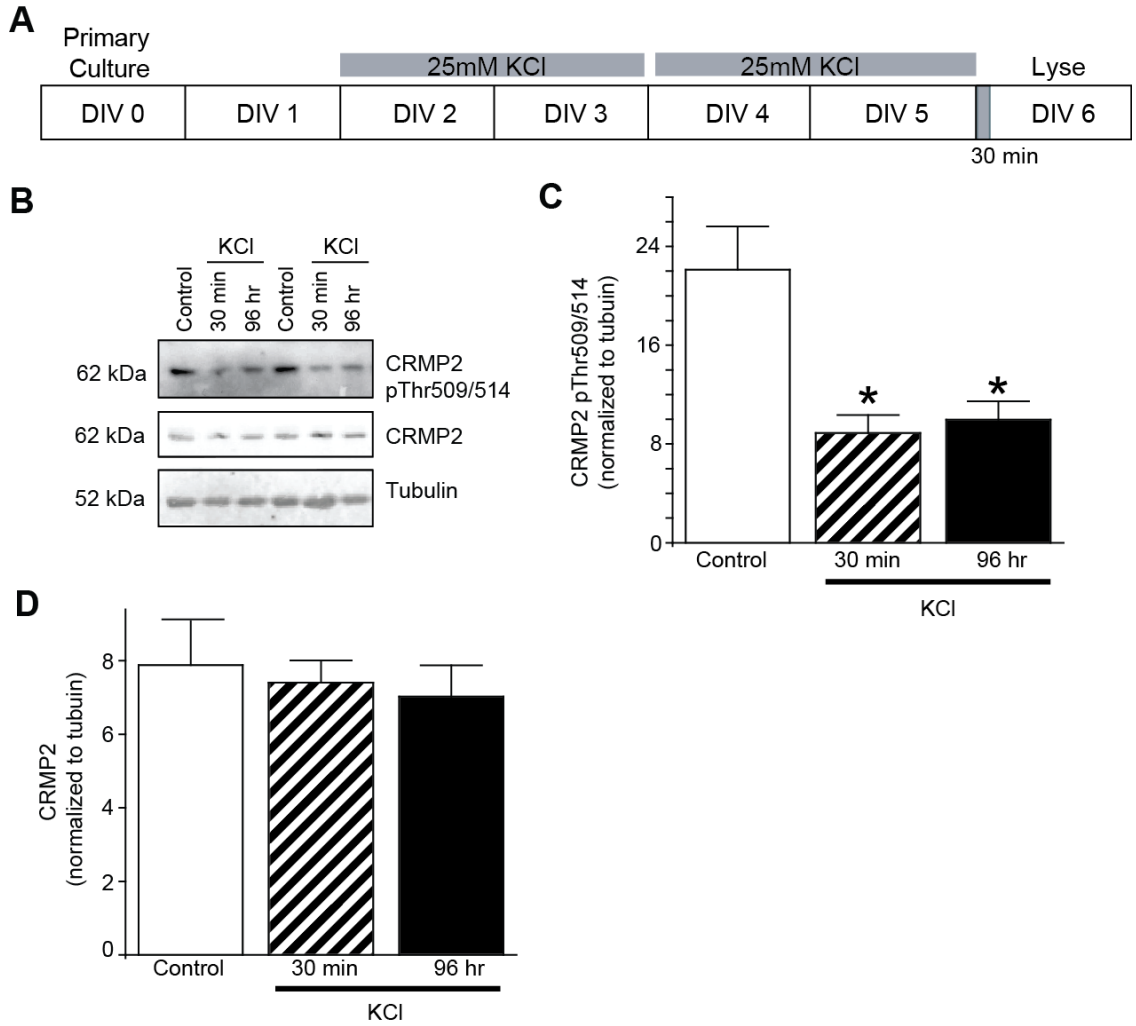
Figure 5.2. KCl-induced activity decreases GSK3β phosphorylation of CRMP2. (A) Timeline of experimental procedures. **(B)** Western blot of GSK3β-phosphorylated CRMP2 (CRMP2 pThr509/514) and total CRMP2 from naïve cortical neurons compared to those exposed to KCl for 30 min or 96 hr. **(C-D)** Summary of CRMP2 pThr509/514 and total CRMP2 following KCl exposure (*, $p < 0.05$ vs control) (One-way ANOVA, Tukey's *post-hoc* analysis) (values represent mean ± SEM) (n = 4).
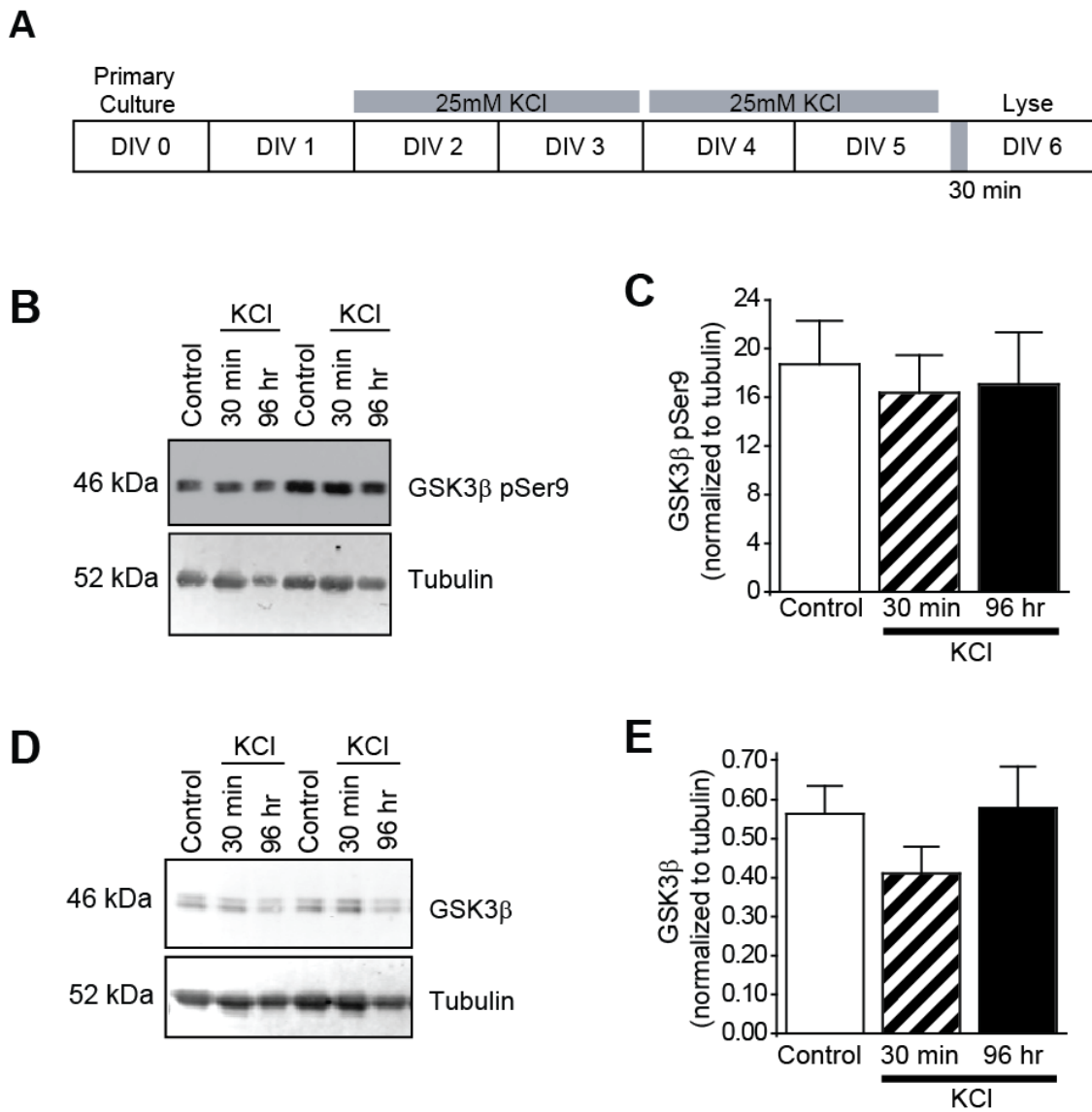
Figure 5.3. KCl-induced activity does not alter GSK3β activity or expression. **(A)** Timeline of experimental procedures. **(B)** Western blot of inactivated (Ser9 phosphorylated) GSK3β from naïve cortical neurons compared to those exposed to KCl for 30 min or 96 hr. **(C)** Summary of GSK3β pSer9 levels following KCl exposure. **(D)** Western blot of GSK3β levels from naïve cortical neurons compared to those exposed to KCl for 30 min or 96 hr. **(E)** Summary of GSK3β levels following KCl exposure. Expression of GSK3β pSer9 or total GSK3β did not change following 30 min or 96 hr KCl treatment. (One-way ANOVA, Tukey's *post-hoc* analysis) (values represent mean ± SEM) (n = 4).

5.4. Activity reduces CDK5 priming of CRMP2

As previously mentioned, CRMP2 phosphorylation by GSK3β first requires phosphorylation by CDK5 at a downstream site (Ser522), which "primes" the protein for subsequent GSK3β phosphorylation (Figure 5.4B). Therefore, western blot analysis of CDK5-phosphorylated CRMP2 (pSer522) was used to determine if the KCl-induced decrease in GSKβ phosphorylation is due to a reduction in CDK5 priming. Both acute and chronic exposure to KCl decreased the level of CDK5-phosphorylated CRMP2 in a time dependent manner (11.7 ± 2.9 and 3.2 ± 1.7, respectively) compared to control (21.2 ± 1.5) ($p < 0.05$) (Figure 5.4C-D), suggesting that the activity-dependent decrease in GSK3β-phosphorylated CRMP2 can be attributed to decreased levels of CDK5-primed CRMP2.

As the CDK5 site on CRMP2 (Ser522) has been shown to be resistant to dephosphorylation (Cole et al., 2008), the involvement of protein phosphatases is unlikely. CDK5 activity is primarily determined by the level of its cofactor p35 (Lee et al., 1996, Zhu et al., 2005, Hisanaga and Endo, 2010). Further western analysis demonstrated that the loss of phosphorylation by CDK5 was not due to changes in expression of CDK5 or p35. Levels of p35 remained consistent following KCl exposure (0.011 ± 0.001) compared to controls (0.011 ± 0.001) ($p > 0.05$) (Figure 5.5). Similarly, levels of CDK5 protein were nearly identical in control neurons (0.0156 ± 0.0012) and those exposed to KCl (0.0156 ± 0.0004) ($p > 0.05$) (Figure 5.5). Therefore, at this point, the mechanism underlying the change in CDK5-phosphorylated CRMP2 is unknown. Mechanisms by which CDK5 is regulated following neuronal activity are not well understood.

Figure 5.4. KCl-induced activity decreases CDK5 phosphorylation of CRMP2. **(A)** Timeline of experimental procedures. **(B)** Diagram of GSK3β and CDK5 phosphorylation sites within the CRMP2 sequence. **(C)** Western blot of CDK5-phosphorylated CRMP2 (CRMP2 pSer522) from naïve cortical neurons compared to those exposed to KCl for 30 min or 96 hr. **(D)** KCl exposure led to a time-dependent decrease in the level of CRMP2 pSer522. (*, $p < 0.05$ vs control) (#, $p < 0.05$ vs 30 min KCl treatment) (One-way ANOVA, Tukey's *post-hoc* analysis) (values represent mean ± SEM) (n = 4-5).

Figure 5.5. KCl-induced activity does not alter expression of CDK5 or p35. **(A)** Timeline of experimental procedures. **(B-C)** Western blots of p35 and CDK5 levels from naïve cortical neurons compared to those exposed to KCl for 96 hr. **(D-E)** Levels of p35 and CDK5 expression were not altered following KCl treatment. (Student's *t*-test) (values represent mean ± SEM) (n = 4-5).

5.5. "Primed" CRMP2 is decreased in the late, but not early phase following TBI

As decreased levels of GSK3β-phosphorylated CRMP2 were observed following activity that were secondary, not to changes in GSK3β expression or activity, but rather decreased CRMP2 priming by CDK5, it is possible that changes in GSK3β-phosphorylated CRMP2 observed in later phases following TBI may be attributed to a decrease in phosphorylation by CDK5. Therefore, levels of CDK5-phosphorylated CRMP2 were assayed from hippocampal tissue collected at early (24 h) and late (4 wk) time points following TBI. Notably, CDK5 phosphorylation of CRMP2 at 24hr following TBI did not differ from sham controls [(1.05 ± 0.07) vs ((1.00 ± 0.12)] (p > 0.05) (Figure 5.6). However, at 4 wk following injury, levels of CDK5-phopshorylated CRMP2 were decreased (0.69 ± 0.07) compared to sham controls (1.00 ± 0.03) (p < 0.05) (Figure 5.6). These results suggest that CRMP2 is differentially regulated during early and late phases following injury. While a loss of GSK3β activity accounts for decreases in CRMP2 phosphorylation immediately following injury, the same phenotype during later phases is attributed to a loss of priming by CDK5.

5.6   Effects of targeting CRMP2 *in vivo* on mossy fiber sprouting

As changes in CRMP2 phosphorylation, and presumably activity, are observed within the hippocampus at both early and late time points following TBI, CRMP2 may be involved in both the induction and maintenance of mossy fiber sprouting following injury. To determine the importance of CRMP2 in this phenomenon, osmotic minipumps containing *(S)*-LCM (140 mg/kg) were implanted (subcutaneously) immediately following TBI surgery in adult male rats. This method allowed for continuous delivery of approximately 5 mg/kg (~ 0.21 mg/kg per hour) *(S)*-LCM per day over the course of 4
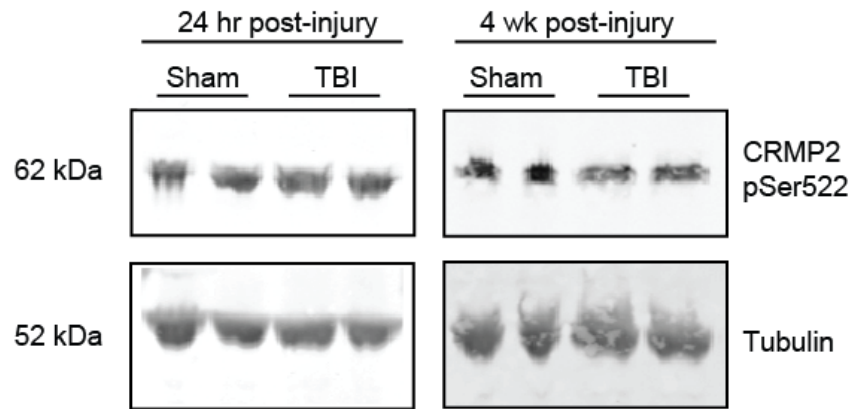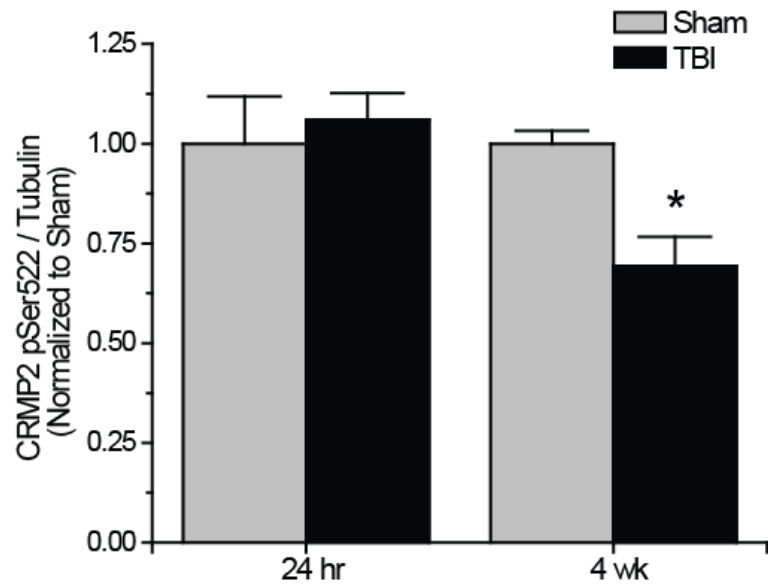
Figure 5.6. Changes in CRMP2 phopshorylation by CDK5 following TBI. **(A)** Western blots of CDK5-phosphorylared CRMP2 from hippocampal tissue 24 hr and 4 wk following TBI. **(B)** Summary of CRMP2 pSer522 levels at both 24 hr and 4 wk following TBI. For ease of comparison, data was normalized to the sham conditions. Levels of CRMP2 pSer522 were decreased at 4 wk, but not 24 hr following TBI. (*, p < 0.05, student's *t*-test) (values represent mean ± SEM) (n = 4-5).

weeks (Figure 5.7A). At the cessation of treatment, bilateral hippocampal tissue was obtained and processed for TIMM staining, to reveal the extent of mossy fiber sprouting within the inner molecular layer. Both low and higher magnification images were obtained using a light microscope (Nikon 90i) and scored by three observers blinded to the conditions, based on the scale originally established by Cavazos and colleagues (Cavazos et al., 1991). Briefly, the scoring system ranks TIMM staining on a scale of 0-5, with 0 being the absence of TIMM granules within the supragranular region and 5 indicating the existence of a dense band of TIMM granules within supragranular region, extending into the inner molecular layer. To avoid issues of variance among animals, scores were compared from contralateral and ipsilateral hippocampi from the same animal to yield the difference in TIMM scoring (Ipsilateral – Contralateral).

As expected, TBI led to increased TIMM differences (1.40 ± 0.25) compared to sham controls (0.25 ± 0.25) ($p < 0.05$) (Figure 5.7B-D). Importantly, differences in TIMM scores did not differ between sham (0.25 ± 0.25) and naïve animals (0.00 ± 0.32) ($p > 0.05$). Intriguingly, *(S)*-LCM treatment prevented the TBI-induced increase in TIMM differences (0.40 ± 0.25) compared to animals receiving TBI alone (1.40 ± 0.25) ($p < 0.05$) (Figure). However, the changes in TIMM scores following TBI did not differ between animals receiving *(S)*-LCM (0.40 ± 0.25) and vehicle (~0.01%DMSO) (1.00 ± 0.00) ($p > 0.05$) (Figure 5.7C-D). Therefore it cannot definitively be concluded that CRMP2 is necessary for mossy fiber sprouting following TBI.

5.7. Discussion

The multitude of contradicting reports concerning mechanisms underlying activity-dependent outgrowth may hint at the sheer complexity of this phenomenon. It is
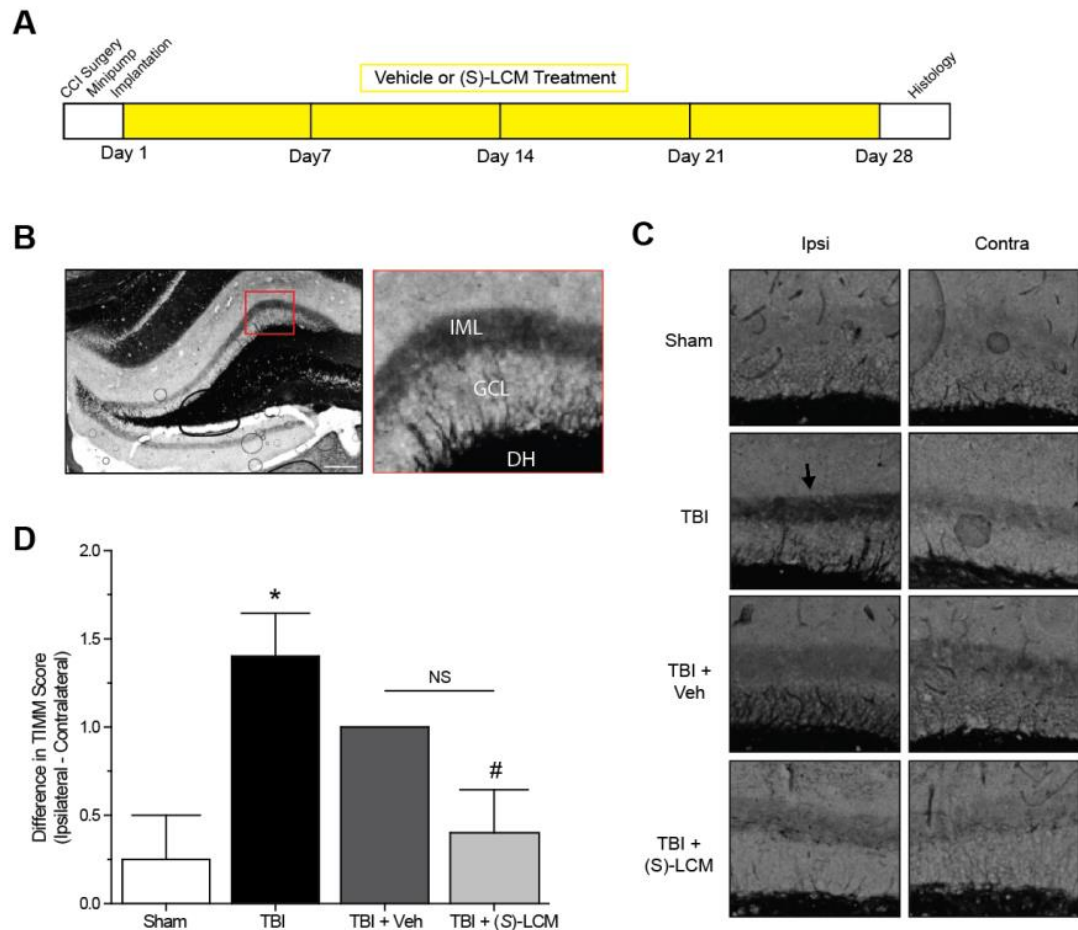
Figure 5.7. Effects of targeting CRMP2 *in vivo* on mossy fiber sprouting. **(A)** Timeline of experimental design. Animals received either controlled cortical impact or sham (craniotomy) surgery. Immediately following surgery, animals were implanted with osmotic mini-pumps containing either vehicle or (*S*)-LCM to be continuously infused at < 0.01% DMSO and ~5 mg/kg per day. Following 4 wk of treatment, tissue samples were prepared for histology. **(B)** (Left) Representative low-magnification image of a TIMM-stained coronal section. (Right) High magnification of highlighted region depicting the dentate hilus (DH), granule cells layer (GCL), and inner molecular layer (IML). **(C)** Representative 10x-magnification images of ipsilateral and contralateral TIMM-stained hippocampi. TBI led to a dense laminar band of TIMM reactivity within the supragranular zone extending to the inner molecular layer (*black arrow*). **(D)** Summary of TIMM scores from animals exposed to sham or TBI surgery ± vehicle or (*S*)-LCM. To minimize the impact of variance among animals, data is represented as the difference in TIMM score between ipsilateral and contralateral hippocampi from the same animal. (*S*)-LCM treatment prevented the TBI-induced increase in mossy fiber sprouting, however did not differ from vehicle. (*, $p < 0.05$ vs sham) (#, $p < 0.05$ vs TBI) (one-way ANOVA, Tukey's *post-hoc* analysis) (values represent mean ± SEM) (n = 4-5).

112

likely that specific mechanisms may depend largely on a variety of factors including, but not limited to, cell type, developmental stage, type of stimulation, and axonal/dendritic distinction. However, our findings, along with those of Tan and colleagues (Tan et al., 2013), represent two separate reports of the involvement of CRMP2 in activity-driven neurite outgrowth in two distinct cell populations. Specifically, KCl-driven activity led to changes in CRMP2 activity through regulation of its phosphorylation state. Interestingly, decreased levels of GSK3β-phosphorylated CRMP2 were observed following activity that were secondary, not to changes in GSK3β expression or activity, but rather decreased CRMP2 priming by CDK5.

The mechanism underlying the change in CDK5-phosphorylated CRMP2 remains unknown. As the CDK5 site on CRMP2 (Ser522) has been shown to be resistant to dephosphorylation (Cole et al., 2008), the involvement of protein phosphatases is unlikely. Unfortunately, mechanisms by which the activity of CDK5 is regulated following neuronal activity are not well understood. High levels of activity have been demonstrated to induce calpain cleavage of CDK5's cofactor p35, creating p25, which contributes to increased CDK5 activity (Patrick et al., 1999, Kerokoski et al., 2004). However, as these events typically culminate in apoptosis-related cell death it is likely that such high levels of activity were excitotoxic in nature and the events following cannot be generalized to all neuronal activity. Alternatively, activation of ionotropic glutamate receptors has been shown to induce auto-phosphorylation of the co-factor p35, thereby labeling it for proteosomal degradation and culminating in decreased CDK5 activity (Wei et al., 2005). This finding suggests that activity-dependent changes in CDK5 activity may be attributed to changes in p35. However, as levels of p35

113

expression remained constant in our investigation, it is unlikely that the decrease in CDK5-phopshorylated CRMP2 is due to p35 degradation. Similarly, work by Schuman and Murase suggests that neuronal activity driven by KCl depolarization leads to a decrease in CDK5 activity that is cofactor independent (Schuman and Murase, 2003). This work has since been corroborated in a report that demonstrated activity-dependent decreases in CDK5 activity that were p35 independent (Nguyen et al., 2007). Interestingly, protein kinase C (PKC) has been shown to decrease CDK5 phosphorylation of substrates without affecting kinase activity or cofactor expression (Sahin et al., 2008). Given the varying avenues that allow for regulation of CDK5, it is possible that the method by which CDK5 is regulated by activity may depend on a variety of factors, similar to that of activity-dependent neurite outgrowth.

Mossy fiber sprouting in TLE can likely be divided into 2 distinct phases: the induction phase, during which sprouting and outgrowth are attributed directly to the precipitating insult such as TBI, hypoxia-ischemia, or status epilepticus, and the maintenance phase (Sutula, 2004, Pitkänen and Lukasiuk, 2009). The latter phase involves processes secondary to the original insult such as hyperexcitability and network synchronization. Consistent with theories implying that the progression of mossy fiber sprouting is mediated by activity-dependent mechanisms, our results revealed that the decrease in GSK3β-phosphorylated CRMP2 during later phases following injury was in fact attributed to a decrease in priming by CDK5. In combination with changes in GSK3β activity that were observed during the early phase, phosphorylation of CRMP2 appears to be differentially regulated through both induction (early) and maintenance (late) phases following traumatic brain injury. As such, targeting CRMP2-mediated

114

neurite outgrowth throughout these stages may be sufficient to attenuate the progression of mossy fiber sprouting. Indeed, the extent of mossy fiber sprouting in animals that had received continuous administration of *(S)*-LCM following TBI was markedly decreased compared to untreated animals. However, the trending effect of vehicle administration is a confounding factor that prevents a definitive conclusion from being drawn. The lack of significant separation between *(S)*-LCM- and vehicle-treated groups may be a result of the nature of administration, despite the previous success observed with infusion of *(R)*-LCM in a separate study (Licko et al., 2013). While continuous subcutaneous infusion was considered to be preferable over daily intraperitoneal injections, it is possible that inflammation at the implantation site may have been a factor. The reduction in mossy fiber sprouting in *(S)*-LCM-treated animals suggests, at the very least, that CRMP2 may be one factor involved in initiation and progression of mossy fiber sprouting. However, that the reduction in mossy fiber sprouting over vehicle-treated animals does not reach significance is indicative that more work is needed in order to definitively claim that increases in CRMP2 activity account for aberrant mossy fiber sprouting following TBI.

CHAPTER 6. DISCUSSION

Despite previous controversy concerning the proposed interaction between CRMP2 and (R)-LCM, MST data demonstrated that (R)-LCM binds to CRMP2 in solution. Importantly, no association was detected between (R)-LCM and a CRMP2 mutant in which the five key residues previously identified to coordinate (R)-LCM binding had been mutated to alanines (CRMP2$_{5ALA}$). Functional analyses revealed that (R)-LCM reduces neurite outgrowth in a CRMP2-dependent manner. Notably, (R)-LCM was observed to directly impair the ability of CRMP2 to enhance tubulin polymerization. As (R)-LCM also enhances slow-inactivation of the VGSC, its use in studying CRMP2 function within a complex system is limited. However, the "inactive enantiomer" (S)-LCM was discovered to retain its ability to bind CRMP2 despite no longer being able to impact VGSC function. As no association could be detected between (S)-LCM and CRMP2$_{5ALA}$, it is assumed that the same binding pocket is responsible for coordinating both enantiomers on the CRMP2 protein. Given that (S)-LCM mimics the effect of CRMP2 knockdown on neurite outgrowth, it serves as an acceptable tool for the study of a specific role (i.e., promotion of neurite outgrowth) of this multi-functional protein. As many other CRMP2 functions such as regulation of voltage-gated calcium channels, neurotransmitter release, synaptic bouton size, and binding of tubulin were not affected by (R)-LCM, the assumption is made that these functions are also not altered by (S)-LCM. However, as this was not explicitly tested in my thesis work, it remains an assumption.

6.2. Overview of Chapter 4

Under naïve conditions, CRMP2 was observed to exist in a balance of phosphorylated (inactive) and unphosphorylated (active) forms, allowing for dynamic regulation of its activity. As a proportion of CRMP2 appears to be tonically phosphorylated by GSK3β, LiCl-induced inhibition of GSK3β resulted in a decrease in CRMP2 phosphorylation, thereby increasing the proportion of active (unphosphorylated) CRMP2 within the cell. This increase in CRMP2 activity was translated into increased neurite outgrowth that was determined to be CRMP2-dependent. Some neuronal insults (e.g., OGD) can lead to increased neurite outgrowth via inactivation of GSK3β. Through the use of (*S*)-LCM, increased neurite outgrowth following OGD was also determined to be CRMP2-dependent. As phosphorylation (inactivation) of GSK3β has been observed following TBI (Shapira et al., 2007, Dash et al., 2011, Zhao et al., 2012), I hypothesized that changes in CRMP2 activity could account for the mossy fiber sprouting induced by TBI. Interestingly, levels of active (unphosphorylated) CRMP2 were increased in both the early and late phases following TBI. The loss of GSK3β-phosphorylated CRMP2 during the early phase is attributed to an observed increase in phosphorylation (inactivation) of GSK3β. Consistent with previous reports (Dash et al., 2011, Zhao et al., 2012), levels of phosphorylated GSK3β had returned to baseline by 4 wk post-injury. Therefore, the sustained loss of GSK3β-phosphorylated CRMP2 during the late phase is likely independent of changes in kinase activity.

6.3. Overview of Chapter 5

Neurite outgrowth, both under normal conditions as well as in response to injury, has previously been associated with activity-driven phenomena (Van Ooyen et al., 1995,

Overman and Carmichael, 2014). As mossy fiber sprouting is also thought to involve activity-dependent processes (Sutula, 2004), I hypothesized that CRMP2 activity may be regulated by neuronal activity. Indeed, neurite outgrowth induced by chronic KCl exposure was observed to be CRMP2-dependent. The increase in outgrowth can be attributed to a dramatic decrease in GSK3β-phosphorylated CRMP2. Similar to what is observed in the late phase following TBI, the decrease in GSK3β-phosphorylated CRMP2 was observed to be independent of kinase activity. For some substrates of GSK3β (including CRMP2), phosphorylation of a nearby serine is required in order to be recognized and phosphorylated by GSK3β (DePaoli-Roach, 1984, Fiol et al., 1988). In the case of CRMP2, it must be first be phosphorylated by the serine/threonine kinase CDK5 (Yoshimura et al., 2005, Cole et al., 2006). Therefore, it was hypothesized that the activity-driven change in GSK3β phosphorylation of CRMP2 reflected a decrease in phosphorylation by CDK5, rather than a loss of GSK3β activity. Indeed, exposure to KCl resulted in a time-dependent decrease in the level of CDK5-phosphorylated CRMP2. As this could not be explained by changes in the expression of CDK5 or its co-factor p35, the mechanism responsible for activity-driven changes in CDK5-phosporylated CRMP2 remain unknown. While changes in phosphatase activity may be involved in changes in GSK3β-phosphorylated CRMP2, the CDK5 site has proven to be extremely resistant to dephosphorylation (Cole et al., 2008).

As TBI can lead to progressive hyperexcitability (Yang et al., 2010a), it was hypothesized that the activity-driven decrease in CRMP2 priming by CDK5 might account for the prolonged loss of GSK3β-phosphorylated CRMP2 following TBI. While there was no change in CDK5-phosphorylated CRMP2 in the early phase following

injury, levels were decreased during the late phase. Therefore, phosphorylation of CRMP2 is differentially regulated throughout both phases following injury. As a loss of phosphorylation would result in an overall increase in the amount of active CRMP2 within the hippocampus, it was hypothesized that increased CRMP2 activity may play an important role in mossy fiber sprouting following injury. To test this hypothesis, one must be able to preferentiallyly target the neurite outgrowth-promoting function of CRMP2, especially since CRMP2 has been shown to be involved in other TBI-related phenomena (Brittain et al., 2012). As I had demonstrated that (*S*)-LCM can serve as a tool for the study of CRMP2-mediated neurite outgrowth in complex systems, it was administered to TBI-injured animals throughout the 4 wk following the injury. While the TBI-induced increase in mossy fiber sprouting was effectively prevented in (*S*)-LCM-treated animals, the extent of sprouting did not differ from vehicle treated animals. Many factors may have contributed to the lack of significance observed over the vehicle-treated group including dose, route of administration (subcutaneous), and complications with minipump implantation. Further work is needed to verify if CRMP2 activity is *necessary* for mossy fiber sprouting.

6.4. Conclusion

It was initially presumed that molecular cues supporting mossy fiber sprouting were triggered solely by the precipitating injury and would decline over time, thereby providing a "critical period" for the prevention of mossy fiber sprouting (Lew and Buckmaster, 2011). However, use of the mTOR inhibitor Rapamycin has demonstrated that if administered for 2 months, which dramatically reduces sprouting, mossy fiber sprouting will return within 2-4 months (Buckmaster et al., 2009, Lew and Buckmaster,

2011). These findings suggest that the signals underlying mossy fiber sprouting persist for months following injury. A distinction is often made concerning the pathological events following traumatic insults, such as TBI. Alterations initiated by the injury itself are often referred to as primary damage, while secondary damage refers to pathological processes such as neurodegeneration, gliosis, or angiogenesis which are more indirectly related to the precipitating injury (Hayes et al., 1998, Reilly, 2001, Faden, 2002, Thompson et al., 2005, Pitkanen et al., 2006, Pitkänen et al., 2009). It may be necessary to make the same distinction of epileptogenesis.

Two separate theories exist concerning the development of epilepsy following injury: (1) the mechanisms underlying epileptogenesis are initiated by the precipitating injury yet are slow and progressive in nature (Mathern et al., 1996, Mathern et al., 2002). (2) Events directly caused by the initial injury are self-limiting, yet lead to a sequence of slowly-evolving phenomena which render the system vulnerable to the development of epilepsy (Sutula, 2004). The first theory suggests that epileptogenesis is a direct result of primary damage, while the second theory suggests that it is secondary damage that is responsible. The body of work presented here suggests that primary and secondary damages may not be mutually exclusive and that both may contribute to epileptogenic processes, such as circuit reorganization. It has been demonstrated that early events following injury, such as decreased phosphorylation of CRMP2 by GSK3β, can be attributed to injury-induced mechanisms (i.e., activation of pro-survival pathways such as PI3K). However, these events are transient in nature. The sustained loss of CRMP2 phosphorylation is likely due to progressive changes in neuronal function which are secondary to the precipitating injury, such as activity-driven changes in CDK5 function.

Although the exact role of CRMP2 in mossy fiber sprouting has not yet been determined, it is possible that the loss of GSK3β phosphorylation immediately following injury contributes to the induction of mossy fiber sprouting while the loss of priming by CDK5 in later phases contributes to the maintenance of mossy fiber sprouting. It is of great interest that these mechanistically distinct events culminate in a similar end-point: an increase in the amount of active CRMP2 (Figure 6.1).

At this point in time, however, a causal relationship has yet to be drawn between mossy fiber sprouting and epileptogenesis. The variety of pathologies and methods employed to induce spontaneous recurring seizures suggests that epileptogenesis and the progression of epilepsy symptoms are unlikely to be characterized in simple terms (Sutula, 2004). Prevailing theories suggest that mossy fiber sprouting likely in combination with other mitigating factors contributes to epileptogenesis. At the very least, mossy fiber sprouting is linked to the exacerbation of the progression of the disease as well as the manifestation of its symptoms (Zhang et al., 2002). The involvement of CRMP2 in such processes, however, remains unseen.
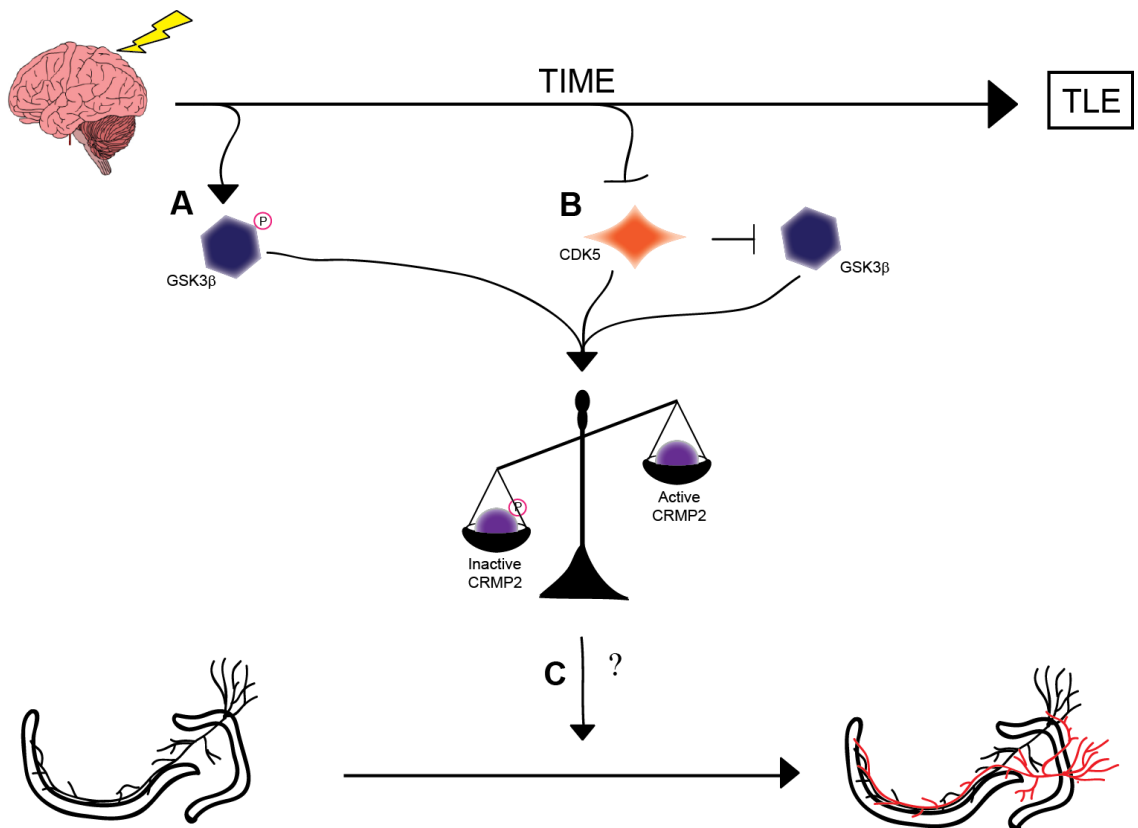
Figure 6.1. **Graphical summary of findings** **(A)** GSK3β is phosphorylated and thereby inactivated in the early phases following injury. This inactivation leads to decreased amounts of phosphorylated (inactive) CRMP2. **(B)** CDK5 phosphorylation of CRMP2 is decreased in the later phases following injury. This decrease in phosphorylation also indirectly reduces levels of GSK3β-phosphorylated CRMP2 through a loss of priming, resulting in an overall increase in the proportion of active CRMP2. **(C)** The sustained increase in unphosphorylated (active) CRMP2 in the hippocampus may underlie aberrant mossy fiber sprouting following injury.

CHAPTER 7. FUTURE STUDIES

As with any body of scientific investigation, there are questions that remain unanswered. If given the time and resources, I would explore the following areas:

7.1. What is the mechanism underlying the activity-driven decrease in CDK5 phosphorylation of CRMP2?

As previously discussed, the mechanisms by which CDK5 is regulated in response to neuronal activity are widely unknown. Contradicting studies report that activity-dependent changes in phosphorylation of CDK5 substrates is co-factor dependent/independent (Patrick et al., 1999, Schuman and Murase, 2003, Kerokoski et al., 2004, Wei et al., 2005, Nguyen et al., 2007). If given the opportunity, I would repeat the experiments mentioned in section 5.4 in which cortical neurons were exposed to KCl for 96 h. Lysates from these cells would then be used to perform *in vitro* kinase assays to determine if the CDK5 from neurons exposed to KCl is less active. Additionally, I would use immunoblot assays to determine the level of less-widely studied co-factor, p39. Finally, co-immunoprecipitations would be performed to determine if the association of CDK5 to p35 or p39 was affected by KCl. A decrease in co-factor binding may account for the decrease in substrate phosphorylation.

Once the mechanism for activity-driven regulation of CDK5 is determined, I would then determine if the same mechanisms were responsible for the loss of CDK5-phosphorylated CRMP2 following TBI. Unlike GSK3β, the involvement of CDK5 in injury-induced epileptogenesis has not been widely studied. Contrary to my findings, phosphorylation of CDK5 substrates was observed to be increased in a chemical kindling model (Tian et al., 2010). In this model the increase in phosphorylation was attributed to an increase in CDK5 mRNA and protein. In support of my hypothesis, CDK5 activity

was observed to be decreased during the late stages of electrical kindling (Tomizawa et al., 2000). In this report, however, decreased kinase activity was attributed to changes in expression of the co-factor, p35. What is of most interest to my studies is what was revealed by immunohistochemistry. The subcellular localization of CDK5 within the dentate gyrus was gradually altered throughout the kindling process. Prior to kindling, CDK5 immunoreactivity was mainly observed within the dendrites and axons of dentate granule cells. As kindling progressed however, CDK5 appeared to translocate to the soma as immunoreactivity in the processes decreased and somal expression increased. This finding raises a question as to the importance of recognizing phosphorylation changes within specific compartments (soma vs processes). For example, although overall levels of CDK5 expression remained constant, the loss of CDK5 from the axon and dendrites would greatly affect phosphorylation of substrates within these compartments. While CDK5-phopshorylated CRMP2 is observed within both the soma and processes (Figure 7.1), in which compartment phosphorylation occurs is at present unknown.

7.2. Is CRMP2 necessary and sufficient to induce mossy fiber sprouting?

The results gained from section 5.7 were unfortunately inconclusive. Therefore, if given the opportunity I would like to repeat these experiments with some modifications. I had originally planned to administer at least two different doses of (*S*)-LCM following TBI; however, I was limited by the amount of the compound that was available to me. It is my hypothesis that increasing the dose of (*S*)-LCM may provide clearer results. Despite past success using osmotic minipumps, it may also be necessary
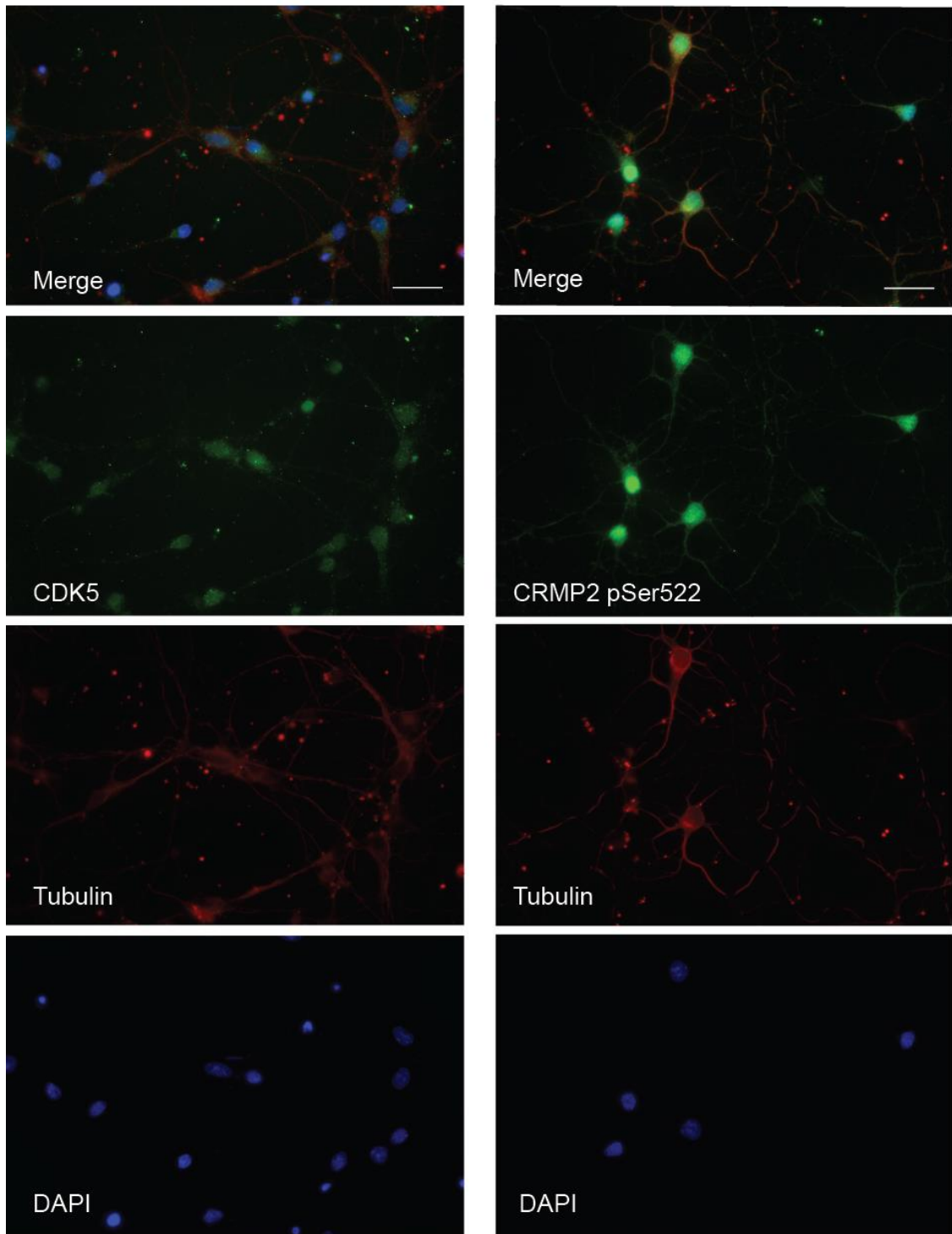
Figure 7.1. Subcellular distribution of CDK5-phopshorylated CRMP2. Cortical neurons (7 DIV) were immunostained for CDK5 or CRMP2 pSer522 along with tubulin to visualize the localization of each protein with the cell. Scale bar: 50 μm.

to alter the route of administration. The results from these experiments will answer to the necessity of CRMP2 in mossy fiber sprouting.

To determine if increased CRMP2 activity is sufficient to induce mossy fiber sprouting I would propose a transgenic approach. Dentate granule cells express high amounts of the zinc transporter-3 (ZnT-3) compared to cells in surrounding areas. Therefore, it may be possible to use an inducible Cre system behind the ZnT-3 promoter to selectively overexpress a phospho-null mutant CRMP2 (CRMP2 T509A/T514A) within the dentate granule cells. As this mutant cannot be phosphorylated by GSK3β, it should be constitutively active. It is my hypothesis that the overexpression of active CRMP2 within the dentate granule cells will be sufficient to induce mossy fiber sprouting.

7.3. What is the relationship between mossy fiber sprouting and epileptogenesis?

Whether a causal relationship exists between mossy fiber sprouting and epileptogenesis has long been under debate (Sutula, 2002). This is perpetuated by the lack of a method for specifically targeting mossy fiber spouting *in vivo*. Studies using rapamycin have published conflicting reports as to whether preventing mossy fiber sprouting impacts the development of spontaneous recurring seizures (Zeng et al., 2009, Huang et al., 2010, Buckmaster and Lew, 2011, Tang et al., 2012, Guo et al., 2013, Heng et al., 2013). Many factors may contribute to the lack of success in this area. Computer simulations have revealed that even a small amount of mossy fiber sprouting could potentially increase seizure susceptibility (Santhakumar et al., 2001, Dyhrfjeld-Johnsen et al., 2010). Therefore, it may be necessary to completely ablate mossy fiber sprouting before an effect on epileptogenesis can be observed. Additionally, as the target of

rapamycin, mTOR, is involved in numerous cellular processes, especially following injury, it is difficult to draw clear conclusions from its use in these studies.

Assuming that the experiments proposed in the section above were successful, I would employ continuous-video EEG monitoring of animals receiving (*S*)-LCM treatment following TBI, as well as other models of acquired epilepsy. If the relationship between mossy fiber sprouting and epileptogenesis is causal in nature, I would expect (*S*)-LCM treatment to decrease the frequency of spontaneous seizures, as well as increase the latency to the first seizure. For further verification, it would be interesting to determine if inducing mossy fiber sprouting *in vivo* leads to the development of spontaneous seizures. Using the aforementioned transgenic model, mossy fiber sprouting would be induced by overexpression of CRMP2 T509A/T514A within the dentate granule cells. Continuous video-EEG monitoring would determine if the animals demonstrated epileptiform activity.

At this point, it appears unlikely that mossy fiber sprouting is the only factor involved in epileptogenesis. However, it also seems unlikely that is does not contribute to the epileptogenic process. The most plausible explanation is that mossy fiber sprouting is one factor, which in combination with many others, may assist in the initiation and/or progression of epileptogenesis (Figure 7.2).
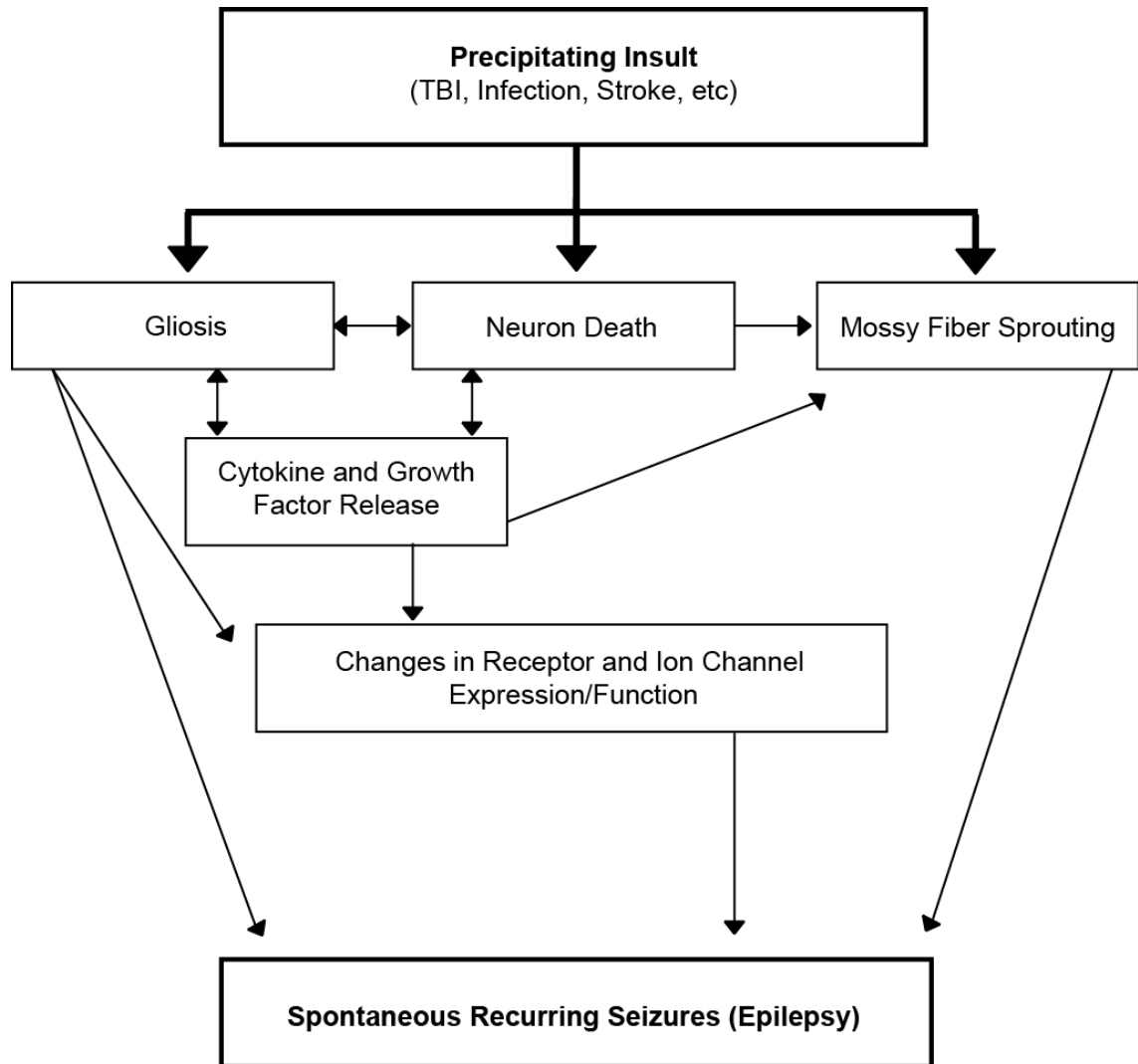
Figure 7.2. Schematic representation of the interplay between factors proposed to contribute to epileptogenesis. Adapted from *O'Dell et al., Understanding the basic mechanisms underlying seizures in mesial temporal lobe epilepsy and possible therapeutic targets: a review. Journal of Neuroscience Research. 2012.(O'Dell et al., 2012)*

REFERENCES

(IOM) IoM (2012) Epilepsy across the spectrum: promoting health and understanding. In: The National Academic Press Washington, DC.

Abe N, Borson SH, Gambello MJ, Wang F, Cavalli V (2010) Mammalian target of rapamycin (mTOR) activation increases axonal growth capacity of injured peripheral nerves. J Biol Chem 285:28034-28043.

Acsady L, Kamondi A, Sik A, Freund T, Buzsaki G (1998) GABAergic cells are the major postsynaptic targets of mossy fibers in the rat hippocampus. The Journal of neuroscience : the official journal of the Society for Neuroscience 18:3386-3403.

Akasu T, Muraoka N, Hasuo H (2002) Hyperexcitability of hippocampal CA1 neurons after fluid percussion injury of the rat cerebral cortex. Neuroscience letters 329:305-308.

Al-Hallaq RA, Conrads TP, Veenstra TD, Wenthold RJ (2007) NMDA di-heteromeric receptor populations and associated proteins in rat hippocampus. J Neurosci 27:8334-8343.

Alessi DR, Andjelkovic M, Caudwell B, Cron P, Morrice N, Cohen P, Hemmings BA (1996) Mechanism of activation of protein kinase B by insulin and IGF-1. Embo j 15:6541-6551.

Aloyz R, Fawcett JP, Kaplan DR, Murphy RA, Miller FD (1999) Activity-dependent activation of TrkB neurotrophin receptors in the adult CNS. Learning & memory (Cold Spring Harbor, NY) 6:216-231.

Andersen P, Bliss TV, Lomo T, Olsen LI, Skrede KK (1969) Lamellar organization of hippocampal excitatory pathways. Acta physiologica Scandinavica 76:4a-5a.

Andurkar SV, Stables JP, Kohn H (1999) The anticonvulsant activities of N-benzyl 3-methoxypropionamides. Bioorg Med Chem 7:2381-2389.

Annegers JF, Hauser WA, Coan SP, Rocca WA (1998) A population-based study of seizures after traumatic brain injuries. The New England journal of medicine 338:20-24.

Arimura N, Inagaki N, Chihara K, Menager C, Nakamura N, Amano M, Iwamatsu A, Goshima Y, Kaibuchi K (2000) Phosphorylation of collapsin response mediator protein-2 by Rho-kinase. Evidence for two separate signaling pathways for growth cone collapse. Journal of Biological Chemistry 275:23973-23980.

Arimura N, Kimura T, Nakamuta S, Taya S, Funahashi Y, Hattori A, Shimada A, Ménager C, Kawabata S, Fujii K, Iwamatsu A, Segal RA, Fukuda M, Kaibuchi K (2009) Anterograde Transport of TrkB in Axons Is Mediated by Direct Interaction with Slp1 and Rab27. Developmental Cell 16:675-686.

Arimura N, Menager C, Kawano Y, Yoshimura T, Kawabata S, Hattori A, Fukata Y, Amano M, Goshima Y, Inagaki M, Morone N, Usukura J, Kaibuchi K (2005) Phosphorylation by Rho kinase regulates CRMP-2 activity in growth cones. MolCell Biol 25:9973-9984.

Asikainen I, Kaste M, Sarna S (1999) Early and late posttraumatic seizures in traumatic brain injury rehabilitation patients: brain injury factors causing late seizures and influence of seizures on long-term outcome. Epilepsia 40:584-589.

Astle MV, Ooms LM, Cole AR, Binge LC, Dyson JM, Layton MJ, Petratos S, Sutherland C, Mitchell CA (2011) Identification of a proline-rich inositol polyphosphate 5-phosphatase (PIPP)*collapsin response mediator protein 2 (CRMP2) complex that regulates neurite elongation. J Biol Chem 286:23407-23418.

Aungst S, England PM, Thompson SM (2013) Critical role of trkB receptors in reactive axonal sprouting and hyperexcitability after axonal injury. Journal of neurophysiology 109:813-824.

Ayala GF, Dichter M, Gumnit RJ, Matsumoto H, Spencer WA (1973) Genesis of epileptic interictal spikes. New knowledge of cortical feedback systems suggests a neurophysiological explanation of brief paroxysms. Brain research 52:1-17.

Babb TL (1991) Bilateral pathological damage in temporal lobe epilepsy. The Canadian journal of neurological sciences Le journal canadien des sciences neurologiques 18:645-648.

Babb TL, Kupfer WR, Pretorius JK, Crandall PH, Levesque MF (1991) Synaptic reorganization by mossy fibers in human epileptic fascia dentata. Neuroscience 42:351-363.

Berling B, Wille H, Roll B, Mandelkow EM, Garner C, Mandelkow E (1994) Phosphorylation of microtubule-associated proteins MAP2a,b and MAP2c at Ser136 by proline-directed kinases in vivo and in vitro. European Journal of Cell Biology 64:120-130.

Bevilaqua LRM, Cammarota M, Paratcha G, De Stein ML, Izquierdo I, Medina Jorge H (1999) Experience-dependent increase in cAMP-responsive element binding protein in synaptic and nonsynaptic mitochondria of the rat hippocampus. European Journal of Neuroscience 11:3753-3756.

Beyreuther B, Stohr T, Freitag J (2009) Method for identifying crmp modulators. Google Patents.

Beyreuther BK, Freitag J, Heers C, Krebsfanger N, Scharfenecker U, Stohr T (2007) Lacosamide: a review of preclinical properties. CNSDrug Rev 13:21-42.

Bhave SV, Ghoda L, Hoffman PL (1999) Brain-derived neurotrophic factor mediates the anti-apoptotic effect of NMDA in cerebellar granule neurons: signal transduction

cascades and site of ethanol action. The Journal of neuroscience : the official journal of the Society for Neuroscience 19:3277-3286.

Binder DK, Routbort MJ, McNamara JO (1999a) Immunohistochemical evidence of seizure-induced activation of trk receptors in the mossy fiber pathway of adult rat hippocampus. The Journal of neuroscience : the official journal of the Society for Neuroscience 19:4616-4626.

Binder DK, Routbort MJ, Ryan TE, Yancopoulos GD, McNamara JO (1999b) Selective inhibition of kindling development by intraventricular administration of TrkB receptor body. The Journal of neuroscience : the official journal of the Society for Neuroscience 19:1424-1436.

Biton V (2012) Lacosamide for the treatment of partial-onset seizures. Expert Rev Neurother 12:645-655.

Blackstad TW, Kjaerheim A (1961) Special axo-dendritic synapses in the hippocampal cortex: electron and light microscopic studies on the layer of mossy fibers. The Journal of comparative neurology 117:133-159.

Boyle WJ, Smeal T, Defize LHK, Angel P, Woodgett JR, Karin M, Hunter T (1991) Activation of protein kinase C decreases phosphorylation of c-Jun at sites that negatively regulate its DNA-binding activity. Cell 64:573-584.

Brandt C, Heile A, Potschka H, Stoehr T, Löscher W (2006) Effects of the Novel Antiepileptic Drug Lacosamide on the Development of Amygdala Kindling in Rats. Epilepsia 47:1803-1809.

Brittain JM, Chen L, Wilson SM, Brustovetsky T, Gao X, Ashpole NM, Molosh AI, You H, Hudmon A, Shekhar A, White FA, Zamponi GW, Brustovetsky N, Chen J, Khanna R (2011a) Neuroprotection against traumatic brain injury by a peptide derived from the collapsin response mediator protein 2 (CRMP2). J Biol Chem 286:37778-37792.

Brittain JM, Duarte DB, Wilson SM, Zhu W, Ballard C, Johnson PL, Liu N, Xiong W, Ripsch MS, Wang Y, Fehrenbacher JC, Fitz SD, Khanna M, Park CK, Schmutzler BS, Cheon BM, Due MR, Brustovetsky T, Ashpole NM, Hudmon A, Meroueh SO, Hingtgen CM, Brustovetsky N, Ji RR, Hurley JH, Jin X, Shekhar A, Xu XM, Oxford GS, Vasko MR, White FA, Khanna R (2011b) Suppression of inflammatory and neuropathic pain by uncoupling CRMP-2 from the presynaptic Ca(2+) channel complex. Nature Medicine.

Brittain JM, Pan R, You H, Brustovetsky T, Brustovetsky N, Zamponi GW, Lee WH, Khanna R (2012) Disruption of NMDAR-CRMP-2 signaling protects against focal cerebral ischemic damage in the rat middle cerebral artery occlusion model. Channels (Austin) 6.

Brittain JM, Piekarz AD, Wang Y, Kondo T, Cummins TR, Khanna R (2009) An atypical role for collapsin response mediator protein 2 (CRMP-2) in neurotransmitter release via interaction with presynaptic voltage-gated calcium channels. Journal of Biological Chemistry 284:31375-31390.

Brown M, Jacobs T, Eickholt B, Ferrari G, Teo M, Monfries C, Qi RZ, Leung T, Lim L, Hall C (2004) Alpha2-chimaerin, cyclin-dependent Kinase 5/p35, and its target collapsin response mediator protein-2 are essential components in semaphorin 3A-induced growth-cone collapse. The Journal of neuroscience : the official journal of the Society for Neuroscience 24:8994-9004.

Brustovetsky T, Pellman JJ, Yang XF, Khanna R, Brustovetsky N (2014) Collapsin Response Mediator Protein 2 (CRMP2) Interacts with N-Methyl-D-aspartate (NMDA) Receptor and Na+/Ca2+ Exchanger and Regulates Their Functional Activity. J Biol Chem 289:7470-7482.

Buckmaster PS, Dudek FE (1999) In vivo intracellular analysis of granule cell axon reorganization in epileptic rats. Journal of neurophysiology 81:712-721.

Buckmaster PS, Ingram EA, Wen X (2009) Inhibition of the mammalian target of rapamycin signaling pathway suppresses dentate granule cell axon sprouting in a rodent model of temporal lobe epilepsy. The Journal of neuroscience : the official journal of the Society for Neuroscience 29:8259-8269.

Buckmaster PS, Lew FH (2011) Rapamycin suppresses mossy fiber sprouting but not seizure frequency in a mouse model of temporal lobe epilepsy. The Journal of neuroscience : the official journal of the Society for Neuroscience 31:2337-2347.

Buckmaster PS, Zhang GF, Yamawaki R (2002) Axon sprouting in a model of temporal lobe epilepsy creates a predominantly excitatory feedback circuit. The Journal of neuroscience : the official journal of the Society for Neuroscience 22:6650-6658.

Buhl EH, Otis TS, Mody I (1996) Zinc-induced collapse of augmented inhibition by GABA in a temporal lobe epilepsy model. Science 271:369-373.

Burneo JG, Tellez-Zenteno J, Wiebe S (2005) Understanding the burden of epilepsy in Latin America: a systematic review of its prevalence and incidence. Epilepsy research 66:63-74.

Byk T, Dobransky T, Cifuentes-Diaz C, Sobel A (1996) Identification and molecular characterization of Unc-33-like phosphoprotein (Ulip), a putative mammalian homolog of the axonal guidance-associated unc-33 gene product. The Journal of neuroscience : the official journal of the Society for Neuroscience 16:688-701.

Carpio A, Hauser WA (2009) Epilepsy in the developing world. Current neurology and neuroscience reports 9:319-326.

Cavazos JE, Golarai G, Sutula TP (1991) Mossy fiber synaptic reorganization induced by kindling: time course of development, progression, and permanence. The Journal of neuroscience : the official journal of the Society for Neuroscience 11:2795-2803.

Cavazos JE, Zhang P, Qazi R, Sutula TP (2003) Ultrastructural features of sprouted mossy fiber synapses in kindled and kainic acid-treated rats. The Journal of comparative neurology 458:272-292.

CDC CfDCaP (2012) Epilepsy in Adults and Access to Care - United States. 2010. MMWR 61:909-913.

Cernak I (2005) Animal models of head trauma. NeuroRx : the journal of the American Society for Experimental NeuroTherapeutics 2:410-422.

Chae YC, Lee S, Heo K, Ha SH, Jung Y, Kim JH, Ihara Y, Suh PG, Ryu SH (2009) Collapsin response mediator protein-2 regulates neurite formation by modulating tubulin GTPase activity. Cellular Signalling 21:1818-1826.

Charrier E, Reibel S, Rogemond V, Aguera M, Thomasset N, Honnorat J (2003) Collapsin response mediator proteins (CRMPs): involvement in nervous system development and adult neurodegenerative disorders. Molecular Neurobiology 28:51-64.

Chen Y, Stevens B, Chang J, Milbrandt J, Barres BA, Hell JW (2008) NS21: re-defined and modified supplement B27 for neuronal cultures. J Neurosci Methods 171:239-247.

Chi XX, Schmutzler BS, Brittain JM, Wang Y, Hingtgen CM, Nicol GD, Khanna R (2009) Regulation of N-type voltage-gated calcium channels (Cav2.2) and transmitter release by collapsin response mediator protein-2 (CRMP-2) in sensory neurons. Journal of Cell Science 122:4351-4362.

Choi D, Stables JP, Kohn H (1996) The anticonvulsant activities of functionalized N-benzyl 2-acetamidoacetamides. The importance of the 2-acetamido substituent. Bioorganic and Medicinal Chemistry 4:2105-2114.

Chong ZZ, Maiese K (2007) Erythropoietin involves the phosphatidylinositol 3-kinase pathway, 14-3-3 protein and FOXO3a nuclear trafficking to preserve endothelial cell integrity. British journal of pharmacology 150:839-850.

Claiborne BJ, Amaral DG, Cowan WM (1986) A light and electron microscopic analysis of the mossy fibers of the rat dentate gyrus. The Journal of comparative neurology 246:435-458.

Cohan CS, Kater SB (1986) Suppression of neurite elongation and growth cone motility by electrical activity. Science 232:1638-1640.

Cole AR, Causeret F, Yadirgi G, Hastie CJ, McLauchlan H, McManus EJ, Hernandez F, Eickholt BJ, Nikolic M, Sutherland C (2006) Distinct priming kinases contribute to differential regulation of collapsin response mediator proteins by glycogen synthase kinase-3 in vivo. J Biol Chem 281:16591-16598.

Cole AR, Knebel A, Morrice NA, Robertson LA, Irving AJ, Connolly CN, Sutherland C (2004) GSK-3 phosphorylation of the Alzheimer epitope within collapsin response mediator proteins regulates axon elongation in primary neurons. J Biol Chem 279:50176-50180.

Cole AR, Soutar MP, Rembutsu M, van AL, Hastie CJ, McLauchlan H, Peggie M, Balastik M, Lu KP, Sutherland C (2008) Relative resistance of Cdk5-phosphorylated CRMP2 to dephosphorylation. Journal of Biological Chemistry 283:18227-18237.

Colicos MA, Dixon CE, Dash PK (1996) Delayed, selective neuronal death following experimental cortical impact injury in rats: possible role in memory deficits. Brain research 739:111-119.

Connor JA (1986) Digital imaging of free calcium changes and of spatial gradients in growing processes in single, mammalian central nervous system cells. Proc Natl Acad Sci U S A 83:6179-6183.

Cortes S, Liao ZK, Watson D, Kohn H (1985) Effect of structural modification of the hydantoin ring on anticonvulsant activity. J Med Chem 28:601-606.

Coulter DA, Rafiq A, Shumate M, Gong QZ, DeLorenzo RJ, Lyeth BG (1996) Brain injury-induced enhanced limbic epileptogenesis: anatomical and physiological parallels to an animal model of temporal lobe epilepsy. Epilepsy research 26:81-91.

Croll SD, Suri C, Compton DL, Simmons MV, Yancopoulos GD, Lindsay RM, Wiegand SJ, Rudge JS, Scharfman HE (1999) Brain-derived neurotrophic factor transgenic mice exhibit passive avoidance deficits, increased seizure severity and in vitro hyperexcitability in the hippocampus and entorhinal cortex. Neuroscience 93:1491-1506.

Cronin J, Obenaus A, Houser CR, Dudek FE (1992) Electrophysiology of dentate granule cells after kainate-induced synaptic reorganization of the mossy fibers. Brain research 573:305-310.

Cross DA, Alessi DR, Cohen P, Andjelkovich M, Hemmings BA (1995) Inhibition of glycogen synthase kinase-3 by insulin mediated by protein kinase B. Nature 378:785-789.

D'Ambrosio R, Fairbanks JP, Fender JS, Born DE, Doyle DL, Miller JW (2004) Post-traumatic epilepsy following fluid percussion injury in the rat. Brain : a journal of neurology 127:304-314.

D'Ambrosio R, Fender JS, Fairbanks JP, Simon EA, Born DE, Doyle DL, Miller JW (2005) Progression from frontal-parietal to mesial-temporal epilepsy after fluid percussion injury in the rat. Brain : a journal of neurology 128:174-188.

Dash PK, Johnson D, Clark J, Orsi SA, Zhang M, Zhao J, Grill RJ, Moore AN, Pati S (2011) Involvement of the glycogen synthase kinase-3 signaling pathway in TBI pathology and neurocognitive outcome. PloS one 6:e24648.

Dasheiff RM, McNamara JO (1982) Electrolytic entorhinal lesions cause seizures. Brain research 231:444-450.

Davis GW, Schuster CM, Goodman CS (1996) Genetic Dissection of Structural and Functional Components of Synaptic Plasticity. III. CREB Is Necessary for Presynaptic Functional Plasticity. Neuron 17:669-679.

de Lanerolle NC, Kim JH, Robbins RJ, Spencer DD (1989) Hippocampal interneuron loss and plasticity in human temporal lobe epilepsy. Brain research 495:387-395.

de Lanerolle NC, Kim JH, Williamson A, Spencer SS, Zaveri HP, Eid T, Spencer DD (2003) A retrospective analysis of hippocampal pathology in human temporal lobe epilepsy: evidence for distinctive patient subcategories. Epilepsia 44:677-687.

De Paola V, Arber S, Caroni P (2003) AMPA receptors regulate dynamic equilibrium of presynaptic terminals in mature hippocampal networks. Nature neuroscience 6:491-500.

Deo RC, Schmidt EF, Elhabazi A, Togashi H, Burley SK, Strittmatter SM (2004) Structural bases for CRMP function in plexin-dependent semaphorin3A signaling. Embo j 23:9-22.

DePaoli-Roach AA (1984) Synergistic phosphorylation and activation of ATP-Mg-dependent phosphoprotein phosphatase by F A/GSK-3 and casein kinase II (PC0.7). J Biol Chem 259:12144-12152.

Dichter MA, Ayala GF (1987) Cellular mechanisms of epilepsy: a status report. Science 237:157-164.

Dinocourt C, Gallagher SE, Thompson SM (2006) Injury-induced axonal sprouting in the hippocampus is initiated by activation of trkB receptors. European Journal of Neuroscience 24:1857-1866.

Dubinsky RM, Yarchoan R, Dalakas M, Broder S (1989) Reversible axonal neuropathy from the treatment of AIDS and related disorders with 2',3'-dideoxycytidine (ddC). Muscle and Nerve 856-860.

Dudek FE, Clark S, Williams PA, Grabenstatter HL (2006) Kainate-Induced Status Epilepticus: A Chronic Model of Acquired Epilepsy. In: Models of Seizures and Epilepsy (Pitkanen, A. et al., eds), pp 415-432 Boston, MA

San Diego, CA

London, UK: Elsevier.

Dudek FE, Hellier JL, Williams PA, Ferraro DJ, Staley KJ (2002) The course of cellular alterations associated with the development of spontaneous seizures after status epilepticus. Progress in brain research 135:53-65.

Duncan GE, Kohn H (2005) The novel antiepileptic drug lacosamide blocks behavioral and brain metabolic manifestations of seizure activity in the 6 Hz psychomotor seizure model. Epilepsy research 67:81-87.

Dyhrfjeld-Johnsen J, Berdichevsky Y, Swiercz W, Sabolek H, Staley KJ (2010) Interictal spikes precede ictal discharges in an organotypic hippocampal slice culture model of epileptogenesis. Journal of Clinical Neurophysiology 27:418-424.

Elmer E, Kokaia Z, Kokaia M, Carnahan J, Nawa H, Lindvall O (1998) Dynamic changes of brain-derived neurotrophic factor protein levels in the rat forebrain after single and recurring kindling-induced seizures. Neuroscience 83:351-362.

Endo H, Nito C, Kamada H, Nishi T, Chan PH (2006) Activation of the Akt//GSK3[beta] signaling pathway mediates survival of vulnerable hippocampal neurons after transient global cerebral ischemia in rats. J Cereb Blood Flow Metab 26:1479-1489.

Englander J, Bushnik T, Duong TT, Cifu DX, Zafonte R, Wright J, Hughes R, Bergman W (2003) Analyzing risk factors for late posttraumatic seizures: a prospective, multicenter investigation. Archives of physical medicine and rehabilitation 84:365-373.

Errington AC, Coyne L, Stohr T, Selve N, Lees G (2006) Seeking a mechanism of action for the novel anticonvulsant lacosamide. Neuropharmacology 50:1016-1029.

Errington AC, Stohr T, Heers C, Lees G (2008) The investigational anticonvulsant lacosamide selectively enhances slow inactivation of voltage-gated sodium channels. Molecular Pharmacology 73:157-169.

Esclapez M, Hirsch JC, Ben-Ari Y, Bernard C (1999) Newly formed excitatory pathways provide a substrate for hyperexcitability in experimental temporal lobe epilepsy. The Journal of comparative neurology 408:449-460.

Faden AI (2002) Neuroprotection and traumatic brain injury: theoretical option or realistic proposition. Current opinion in neurology 15:707-712.

Feng L, Molnar P, Nadler JV (2003) Short-term frequency-dependent plasticity at recurrent mossy fiber synapses of the epileptic brain. The Journal of neuroscience : the official journal of the Society for Neuroscience 23:5381-5390.

Fields RD, Neale EA, Nelson PG (1990) Effects of patterned electrical activity on neurite outgrowth from mouse sensory neurons. The Journal of neuroscience : the official journal of the Society for Neuroscience 10:2950-2964.

Fiol CJ, Haseman JH, Wang YH, Roach PJ, Roeske RW, Kowalczuk M, DePaoli-Roach AA (1988) Phosphoserine as a recognition determinant for glycogen synthase kinase-3: phosphorylation of a synthetic peptide based on the G-component of protein phosphatase-1. Archives of biochemistry and biophysics 267:797-802.

Frotscher M, Jonas P, Sloviter RS (2006) Synapses formed by normal and abnormal hippocampal mossy fibers. Cell and tissue research 326:361-367.

Frotscher M, Zimmer J (1983) Lesion-induced mossy fibers to the molecular layer of the rat fascia dentata: identification of postsynaptic granule cells by the Golgi-EM technique. The Journal of comparative neurology 215:299-311.

Frush DP, Giacchino JL, McNamara JO (1986) Evidence implicating dentate granule cells in development of entorhinal kindling. Experimental neurology 92:92-101.

Fukada M, Watakabe I, Yuasa-Kawada J, Kawachi H, Kuroiwa A, Matsuda Y, Noda M (2000) Molecular characterization of CRMP5, a novel member of the collapsin response mediator protein family. J Biol Chem 275:37957-37965.

Fukata Y, Itoh TJ, Kimura T, Menager C, Nishimura T, Shiromizu T, Watanabe H, Inagaki N, Iwamatsu A, Hotani H, Kaibuchi K (2002) CRMP-2 binds to tubulin heterodimers to promote microtubule assembly. NatCell Biol 4:583-591.

Galanopoulou AS, Gorter JA, Cepeda C (2012) Finding a better drug for epilepsy: the mTOR pathway as an antiepileptogenic target. Epilepsia 53:1119-1130.

Galimberti I, Gogolla N, Alberi S, Santos AF, Muller D, Caroni P (2006) Long-term rearrangements of hippocampal mossy fiber terminal connectivity in the adult regulated by experience. Neuron 50:749-763.

García-Pérez J, Avila J, Díaz-Nido J (1998) Implication of cyclin-dependent kinases and glycogen synthase kinase 3 in the phosphorylation of microtubule-associated protein 1B in developing neuronal cells. Journal of neuroscience research 52:445-452.

Geddes JW, Cahan LD, Cooper SM, Kim RC, Choi BH, Cotman CW (1990) Altered distribution of excitatory amino acid receptors in temporal lobe epilepsy. Experimental neurology 108:214-220.

Geschwind DH, Hockfield S (1989) Identification of proteins that are developmentally regulated during early cerebral corticogenesis in the rat. The Journal of neuroscience : the official journal of the Society for Neuroscience 9:4303-4317.

Goddard GV, McIntyre DC, Leech CK (1969) A permanent change in brain function resulting from daily electrical stimulation. Experimental neurology 25:295-330.

Golarai G, Cavazos JE, Sutula TP (1992) Activation of the dentate gyrus by pentylenetetrazol evoked seizures induces mossy fiber synaptic reorganization. Brain research 593:257-264.

Golarai G, Greenwood AC, Feeney DM, Connor JA (2001) Physiological and structural evidence for hippocampal involvement in persistent seizure susceptibility after traumatic brain injury. The Journal of neuroscience : the official journal of the Society for Neuroscience 21:8523-8537.

Golarai G, Sutula TP (1996) Functional alterations in the dentate gyrus after induction of long-term potentiation, kindling, and mossy fiber sprouting. Journal of neurophysiology 75:343-353.

Goldberg MP, Choi DW (1993) Combined oxygen and glucose deprivation in cortical cell culture: calcium-dependent and calcium-independent mechanisms of neuronal injury. The Journal of neuroscience : the official journal of the Society for Neuroscience 13:3510-3524.

Goldowitz D, Cotman CW (1980) Axonal transport and axon sprouting in the adult rat dentate gyrus: an autoradiographic study. Neuroscience 5:2163-2174.

Golgi C (1886) Sulla Fina Anatomia Degli Organi Centrali Del Sistema Nervoso. U Hoepli 215.

Gombos Z, Spiller A, Cottrell GA, Racine RJ, McIntyre Burnham W (1999) Mossy fiber sprouting induced by repeated electroconvulsive shock seizures. Brain research 844:28-33.

Gomez-Lira G, Trillo E, Ramirez M, Asai M, Sitges M, Gutierrez R (2002) The expression of GABA in mossy fiber synaptosomes coincides with the seizure-induced expression of GABAergic transmission in the mossy fiber synapse. Experimental neurology 177:276-283.

Goshima Y, Nakamura F, Strittmatter P, Strittmatter SM (1995) Collapsin-induced growth cone collapse mediated by an intracellular protein related to UNC-33. Nature 376:509-514.

Goslin K, Banker G (1989) Experimental observations on the development of polarity by hippocampal neurons in culture. The Journal of cell biology 108:1507-1516.

Graber KD, Prince DA (1999) Tetrodotoxin prevents posttraumatic epileptogenesis in rats. Annals of neurology 46:234-242.

Graber KD, Prince DA (2004) A critical period for prevention of posttraumatic neocortical hyperexcitability in rats. Annals of neurology 55:860-870.

Greenaway C, Ratnaraj N, Sander JW, Patsalos PN (2010) A high-performance liquid chromatography assay to monitor the new antiepileptic drug lacosamide in patients with epilepsy. Ther Drug Monit 32:448-452.

Griesbach GS, Hovda DA, Molteni R, Gomez-Pinilla F (2002) Alterations in BDNF and synapsin I within the occipital cortex and hippocampus after mild traumatic brain injury in the developing rat: reflections of injury-induced neuroplasticity. Journal of neurotrauma 19:803-814.

Griesemer D, Mautes AM (2007) Closed head injury causes hyperexcitability in rat hippocampal CA1 but not in CA3 pyramidal cells. Journal of neurotrauma 24:1823-1832.

Grundy PL, Patel N, Harbuz MS, Lightman SL, Sharples PM (2000) Glucocorticoids modulate BDNF mRNA expression in the rat hippocampus after traumatic brain injury. Neuroreport 11:3381-3384.

Guan RJ, Khatra BS, Cohlberg JA (1991) Phosphorylation of bovine neurofilament proteins by protein kinase FA (glycogen synthase kinase 3). Journal of Biological Chemistry 266:8262-8267.

Guidato S, Tsai LH, Woodgett J, Miller CCJ (1996) Differential cellular phosphorylation of neurofilament heavy side-arms by glycogen synthase kinase-3 and cydin-dependent kinase-5. Journal of Neurochemistry 66:1698-1706.

Guo D, Zeng L, Brody DL, Wong M (2013) Rapamycin attenuates the development of posttraumatic epilepsy in a mouse model of traumatic brain injury. PloS one 8:e64078.

Gutierrez R (2002) Activity-dependent expression of simultaneous glutamatergic and GABAergic neurotransmission from the mossy fibers in vitro. Journal of neurophysiology 87:2562-2570.

Gutierrez R, Heinemann U (2001) Kindling induces transient fast inhibition in the dentate gyrus--CA3 projection. The European journal of neuroscience 13:1371-1379.

Gutiérrez R, Romo-Parra H, Maqueda J, Vivar C, Ramìrez M, Morales MA, Lamas M (2003) Plasticity of the GABAergic Phenotype of the "Glutamatergic" Granule Cells of the Rat Dentate Gyrus. The Journal of Neuroscience 23:5594-5598.

Hanger DP, Hughes K, Woodgett JR, Brion JP, Anderton BH (1992) Glycogen synthase kinase-3 induces Alzheimer's disease-like phosphorylation of tau: Generation of

paired helical filament epitopes and neuronal localisation of the kinase. Neuroscience letters 147:58-62.

Hauser WA, Kurland LT (1975) The epidemiology of epilepsy in Rochester, Minnesota, 1935 through 1967. Epilepsia 16:1-66.

Hayes RL, Wang KK, Kampfl A, Posmantur RM, Newcomb JK, Clifton GL (1998) Potential contribution of proteases to neuronal damage. Drug news & perspectives 11:215-222.

He X-P, Kotloski R, Nef S, Luikart BW, Parada LF, McNamara JO (2004) Conditional Deletion of TrkB but Not BDNF Prevents Epileptogenesis in the Kindling Model. Neuron 43:31-42.

He XP, Minichiello L, Klein R, McNamara JO (2002) Immunohistochemical evidence of seizure-induced activation of trkB receptors in the mossy fiber pathway of adult mouse hippocampus. The Journal of neuroscience : the official journal of the Society for Neuroscience 22:7502-7508.

Hedgecock EM, Culotti JG, Thomson JN, Perkins LA (1985) Axonal guidance mutants of Caenorhabditis elegans identified by filling sensory neurons with fluorescein dyes. Dev Biol 111:158-170.

Heinrich C, Lähteinen S, Suzuki F, Anne-Marie L, Huber S, Häussler U, Haas C, Larmet Y, Castren E, Depaulis A (2011) Increase in BDNF-mediated TrkB signaling promotes epileptogenesis in a mouse model of mesial temporal lobe epilepsy. Neurobiology of disease 42:35-47.

Heng K, Haney MM, Buckmaster PS (2013) High-dose rapamycin blocks mossy fiber sprouting but not seizures in a mouse model of temporal lobe epilepsy. Epilepsia 54:1535-1541.

Hensley K, Venkova K, Christov A, Gunning W, Park J (2011) Collapsin Response Mediator Protein-2: An Emerging Pathologic Feature and Therapeutic Target for Neurodisease Indications. Molecular Neurobiology.

Herman ST (2002) Epilepsy after brain insult: targeting epileptogenesis. Neurology 59:S21-26.

Hirtz D, Thurman DJ, Gwinn-Hardy K, Mohamed M, Chaudhuri AR, Zalutsky R (2007) How common are the "common" neurologic disorders? Neurology 68:326-337.

Hisanaga S, Endo R (2010) Regulation and role of cyclin-dependent kinase activity in neuronal survival and death. J Neurochem 115:1309-1321.

Holmes GL, Gairsa JL, Chevassus-Au-Louis N, Ben-Ari Y (1998) Consequences of neonatal seizures in the rat: morphological and behavioral effects. Annals of neurology 44:845-857.

142

Holmes GL, Sarkisian M, Ben-Ari Y, Chevassus-Au-Louis N (1999) Mossy fiber sprouting after recurrent seizures during early development in rats. The Journal of comparative neurology 404:537-553.

Holtmaat AJGD, Gorter JA, Wit JD, Tolner EA, Spijker S, Giger RJ, Lopes da Silva FH, Verhaagen J (2003) Transient downregulation of sema3a mrna in a rat model for temporal lobe epilepsy: A novel molecular event potentially contributing to mossy fiber sprouting. Experimental neurology 182:142-150.

Hou ST, Jiang SX, Aylsworth A, Ferguson G, Slinn J, Hu H, Leung T, Kappler J, Kaibuchi K (2009) CaMKII phosphorylates collapsin response mediator protein 2 and modulates axonal damage during glutamate excitotoxicity. Journal of Neurochemistry 111:870-881.

Houser CR (1990) Granule cell dispersion in the dentate gyrus of humans with temporal lobe epilepsy. Brain research 535:195-204.

Houser CR, Miyashiro JE, Swartz BE, Walsh GO, Rich JR, Delgado-Escueta AV (1990) Altered patterns of dynorphin immunoreactivity suggest mossy fiber reorganization in human hippocampal epilepsy. The Journal of neuroscience : the official journal of the Society for Neuroscience 10:267-282.

Hu B, Liu C, Bramlett H, Sick TJ, Alonso OF, Chen S, Dietrich WD (2004) Changes in trkB-ERK1/2-CREB/Elk-1 pathways in hippocampal mossy fiber organization after traumatic brain injury. J Cereb Blood Flow Metab 24:934-943.

Hu BR, Fux CM, Martone ME, Zivin JA, Ellisman MH (1999) Persistent phosphorylation of cyclic AMP responsive element-binding protein and activating transcription factor-2 transcription factors following transient cerebral ischemia in rat brain. Neuroscience 89:437-452.

Hu BR, Liu CL, Park DJ (2000) Alteration of MAP kinase pathways after transient forebrain ischemia. J Cereb Blood Flow Metab 20:1089-1095.

Huang EJ, Reichardt LF (2001) Neurotrophins: roles in neuronal development and function. Annual review of neuroscience 24:677-736.

Huang X, Zhang H, Yang J, Wu J, McMahon J, Lin Y, Cao Z, Gruenthal M, Huang Y (2010) Pharmacological inhibition of the mammalian target of rapamycin pathway suppresses acquired epilepsy. Neurobiology of disease 40:193-199.

Hunt RF, Scheff SW, Smith BN (2009) Posttraumatic epilepsy after controlled cortical impact injury in mice. Experimental neurology 215:243-252.

Inagaki N, Chihara K, Arimura N, Menager C, Kawano Y, Matsuo N, Nishimura T, Amano M, Kaibuchi K (2001) CRMP-2 induces axons in cultured hippocampal neurons. Nature neuroscience 4:781-782.

Isackson PJ, Huntsman MM, Murray KD, Gall CM (1991) BDNF mRNA expression is increased in adult rat forebrain after limbic seizures: temporal patterns of induction distinct from NGF. Neuron 6:937-948.

Isokawa M, Levesque MF, Babb TL, Engel J, Jr. (1993) Single mossy fiber axonal systems of human dentate granule cells studied in hippocampal slices from patients with temporal lobe epilepsy. The Journal of neuroscience : the official journal of the Society for Neuroscience 13:1511-1522.

Janelidze S, Hu BR, Siesjo P, Siesjo BK (2001) Alterations of Akt1 (PKBalpha) and p70(S6K) in transient focal ischemia. Neurobiology of disease 8:147-154.

Jaworski J, Spangler S, Seeburg DP, Hoogenraad CC, Sheng M (2005) Control of dendritic arborization by the phosphoinositide-3'-kinase-Akt-mammalian target of rapamycin pathway. The Journal of neuroscience : the official journal of the Society for Neuroscience 25:11300-11312.

Jennett WB, Lewin W (1960) Traumatic epilepsy after closed head injuries. Journal of neurology, neurosurgery, and psychiatry 23:295-301.

Jin X, Prince DA, Huguenard JR (2006) Enhanced excitatory synaptic connectivity in layer v pyramidal neurons of chronically injured epileptogenic neocortex in rats. Journal of Neuroscience 26:4891-4900.

Kaplan DR, Miller FD (2000) Neurotrophin signal transduction in the nervous system. Current opinion in neurobiology 10:381-391.

Karin M, Liu Z-g, Zandi E (1997) AP-1 function and regulation. Current Opinion in Cell Biology 9:240-246.

Karr L, Rutecki PA (2008) Activity-dependent induction and maintenance of epileptiform activity produced by group I metabotropic glutamate receptors in the rat hippocampal slice. Epilepsy research 81:14-23.

Kater SB, Mattson MP, Cohan C, Connor J (1988) Calcium regulation of the neuronal growth cone. Trends in Neurosciences 11:315-321.

Katoh-Semba R, Takeuchi IK, Inaguma Y, Ichisaka S, Hata Y, Tsumoto T, Iwai M, Mikoshiba K, Kato K (2001) Induction of brain-derived neurotrophic factor by convulsant drugs in the rat brain: involvement of region-specific voltage-dependent calcium channels. J Neurochem 77:71-83.

Kawano Y, Yoshimura T, Tsuboi D, Kawabata S, Kaneko-Kawano T, Shirataki H, Takenawa T, Kaibuchi K (2005) CRMP-2 is involved in kinesin-1-dependent transport of the Sra-1/WAVE1 complex and axon formation. Molecular and cellular biology 25:9920-9935.

Kerokoski P, Suuronen T, Salminen A, Soininen H, Pirttila T (2004) Both N-methyl-D-aspartate (NMDA) and non-NMDA receptors mediate glutamate-induced cleavage of the cyclin-dependent kinase 5 (cdk5) activator p35 in cultured rat hippocampal neurons. Neuroscience letters 368:181-185.

Khanna R, Wilson SM, Brittain JM, Weimer J, Sultana R, Butterfield A, Hensley K (2012) Opening Pandora's jar: a primer on the putative roles of CRMP2 in a panoply of neurodegenerative, sensory and motor neuron, and central disorders. Future Neurol 7:749-771.

Kharatishvili I, Nissinen JP, McIntosh TK, Pitkanen A (2006) A model of posttraumatic epilepsy induced by lateral fluid-percussion brain injury in rats. Neuroscience 140:685-697.

Kharatishvili I, Pitkanen A (2010) Posttraumatic epilepsy. Current opinion in neurology 23:183-188.

Kimura T, Watanabe H, Iwamatsu A, Kaibuchi K (2005) Tubulin and CRMP-2 complex is transported via Kinesin-1. J Neurochem 93:1371-1382.

Kitamura K, Takayama M, Hamajima N, Nakanishi M, Sasaki M, Endo Y, Takemoto T, Kimura H, Iwaki M, Nonaka M (1999) Characterization of the human dihydropyrimidinase-related protein 2 (DRP-2) gene. DNA research : an international journal for rapid publication of reports on genes and genomes 6:291-297.

Kocsis JD, Rand MN, Lankford KL, Waxman SG (1994) Intracellular calcium mobilization and neurite outgrowth in mammalian neurons. J Neurobiol 25:252-264.

Kokaia M, Ernfors P, Kokaia Z, Elmer E, Jaenisch R, Lindvall O (1995) Suppressed epileptogenesis in BDNF mutant mice. Experimental neurology 133:215-224.

Kotti T, Riekkinen PJ, Sr., Miettinen R (1997) Characterization of target cells for aberrant mossy fiber collaterals in the dentate gyrus of epileptic rat. Experimental neurology 146:323-330.

Koyama R, Ikegaya Y (2004) Mossy fiber sprouting as a potential therapeutic target for epilepsy. Current neurovascular research 1:3-10.

Koyama R, Yamada MK, Fujisawa S, Katoh-Semba R, Matsuki N, Ikegaya Y (2004) Brain-derived neurotrophic factor induces hyperexcitable reentrant circuits in the dentate gyrus. The Journal of neuroscience : the official journal of the Society for Neuroscience 24:7215-7224.

Koyama R, Yamada MK, Nishiyama N, Matsuki N, Ikegaya Y (2002) Group II metabotropic glutamate receptor activation is required for normal hippocampal mossy fibre development in the rat. J Physiol 539:157-162.

Lahteinen S, Pitkanen A, Saarelainen T, Nissinen J, Koponen E, Castren E (2002) Decreased BDNF signalling in transgenic mice reduces epileptogenesis. The European journal of neuroscience 15:721-734.

Larner AJ (1995) Axonal sprouting and synaptogenesis in temporal lobe epilepsy: possible pathogenetic and therapeutic roles of neurite growth inhibitory factors. Seizure : the journal of the British Epilepsy Association 4:249-258.

Laurberg S, Zimmer J (1981) Lesion-induced sprouting of hippocampal mossy fiber collaterals to the fascia dentata in developing and adult rats. The Journal of comparative neurology 200:433-459.

Lee C-Y, Jaw T, Tseng H-C, Chen IC, Liou H-H (2012) Lovastatin Modulates Glycogen Synthase Kinase-3β Pathway and Inhibits Mossy Fiber Sprouting after Pilocarpine-Induced Status Epilepticus. PloS one 7:e38789.

Lee JC, Timasheff SN (1977) In vitro reconstitution of calf brain microtubules: effects of solution variables. Biochemistry 16:1754-1764.

Lee MH, Nikolic M, Baptista CA, Lai E, Tsai LH, Massague J (1996) The brain-specific activator p35 allows Cdk5 to escape inhibition by p27Kip1 in neurons. Proc Natl Acad Sci U S A 93:3259-3263.

Lei Z, Ruan Y, Yang AN, Xu ZC (2006) NMDA receptor mediated dendritic plasticity in cortical cultures after oxygen-glucose deprivation. Neuroscience letters 407:224-229.

LeTiran A, Stables JP, Kohn H (2001) Functionalized amino acid anticonvulsants: synthesis and pharmacological evaluation of conformationally restricted analogues. Bioorg Med Chem 9:2693-2708.

Lew FH, Buckmaster PS (2011) Is there a critical period for mossy fiber sprouting in a mouse model of temporal lobe epilepsy? Epilepsia 52:2326-2332.

Li L, Qu Y, Mao M, Xiong Y, Mu D (2008) The involvement of phosphoinositid 3-kinase/Akt pathway in the activation of hypoxia-inducible factor-1alpha in the developing rat brain after hypoxia-ischemia. Brain research 1197:152-158.

Licko T, Seeger N, Zellinger C, Russmann V, Matagne A, Potschka H (2013) Lacosamide treatment following status epilepticus attenuates neuronal cell loss and alterations in hippocampal neurogenesis in a rat electrical status epilepticus model. Epilepsia.

Longo BM, Mello LE (1998) Supragranular mossy fiber sprouting is not necessary for spontaneous seizures in the intrahippocampal kainate model of epilepsy in the rat. Epilepsy research 32:172-182.

Longo BM, Mello LE (1999) Effect of long-term spontaneous recurrent seizures or reinduction of status epilepticus on the development of supragranular mossy fiber sprouting. Epilepsy research 36:233-241.

Lopes MW, Soares FM, de Mello N, Nunes JC, de Cordova FM, Walz R, Leal RB (2012) Time-dependent modulation of mitogen activated protein kinases and AKT in rat hippocampus and cortex in the pilocarpine model of epilepsy. Neurochem Res 37:1868-1878.

Loscher W, Honack D, Rundfeldt C (1998) Antiepileptogenic effects of the novel anticonvulsant levetiracetam (ucb L059) in the kindling model of temporal lobe epilepsy. The Journal of pharmacology and experimental therapeutics 284:474-479.

Loscher W, Schmidt D (2011) Modern antiepileptic drug development has failed to deliver: ways out of the current dilemma. Epilepsia 52:657-678.

Lowenstein DH, Arsenault L (1996a) Dentate granule cell layer collagen explant cultures: spontaneous axonal growth and induction by brain-derived neurotrophic factor or basic fibroblast growth factor. Neuroscience 74:1197-1208.

Lowenstein DH, Arsenault L (1996b) The effects of growth factors on the survival and differentiation of cultured dentate gyrus neurons. The Journal of neuroscience : the official journal of the Society for Neuroscience 16:1759-1769.

Lowenstein DH, Thomas MJ, Smith DH, McIntosh TK (1992) Selective vulnerability of dentate hilar neurons following traumatic brain injury: a potential mechanistic link between head trauma and disorders of the hippocampus. The Journal of neuroscience : the official journal of the Society for Neuroscience 12:4846-4853.

Lucas FR, Goold RG, Gordon-Weeks PR, Salinas PC (1998) Inhibition of GSK-3β leading to the loss of phosphorylated MAP-1B is an early event in axonal remodelling induced by WNT-7a or lithium. Journal of Cell Science 111:1351-1361.

Lykissas MG, Batistatou AK, Charalabopoulos KA, Beris AE (2007) The role of neurotrophins in axonal growth, guidance, and regeneration. Current neurovascular research 4:143-151.

Lynch G, Gall C, Rose G, Cotman C (1976) Changes in the distribution of the dentate gyrus associational system following unilateral or bilateral entorhinal lesions in the adult rat. Brain research 110:57-71.

Lynch G, Stanfield B, Cotman CW (1973) Developmental differences in post-lesion axonal growth in the hippocampus. Brain research 59:155-168.

Lynch M, Sutula T (2000) Recurrent excitatory connectivity in the dentate gyrus of kindled and kainic acid-treated rats. Journal of neurophysiology 83:693-704.

Mackie K, Sorkin BC, Nairn AC, Greengard P, Edelman GM, Cunningham BA (1989) Identification of two protein kinases that phosphorylate the neural celll-adhesion molecule, N-CAM. Journal of Neuroscience 9:1883-1896.

Mandelkow EM, Drewes G, Biernat J, Gustke N, Van Lint J, Vandenheede JR, Mandelkow E (1992) Glycogen synthase kinase-3 and the Alzheimer-like state of microtubule-associated protein tau. FEBS Letters 314:315-321.

Manford M, Hart YM, Sander JW, Shorvon SD (1992a) National General Practice Study of Epilepsy (NGPSE): partial seizure patterns in a general population. Neurology 42:1911-1917.

Manford M, Hart YM, Sander JW, Shorvon SD (1992b) The National General Practice Study of Epilepsy. The syndromic classification of the International League Against Epilepsy applied to epilepsy in a general population. Archives of neurology 49:801-808.

Margerison JH, Corsellis JA (1966) Epilepsy and the temporal lobes. A clinical, electroencephalographic and neuropathological study of the brain in epilepsy, with particular reference to the temporal lobes. Brain : a journal of neurology 89:499-530.

Masukawa LM, Higashima M, Kim JH, Spencer DD (1989) Epileptiform discharges evoked in hippocampal brain slices from epileptic patients. Brain research 493:168-174.

Masukawa LM, Uruno K, Sperling M, O'Connor MJ, Burdette LJ (1992) The functional relationship between antidromically evoked field responses of the dentate gyrus and mossy fiber reorganization in temporal lobe epileptic patients. Brain research 579:119-127.

Mathern G, Babb T, Micevych P, Blanco C, Pretorius J (1997) Granule cell mRNA levels for BDNF, NGF, and NT-3 correlate with neuron losses or supragranular mossy fiber sprouting in the chronically damaged and epileptic human hippocampus. Molecular and Chemical Neuropathology 30:53-76.

Mathern GW, Adelson PD, Cahan LD, Leite JP (2002) Hippocampal neuron damage in human epilepsy: Meyer's hypothesis revisited. Progress in brain research 135:237-251.

Mathern GW, Babb TL, Leite JP, Pretorius K, Yeoman KM, Kuhlman PA (1996) The pathogenic and progressive features of chronic human hippocampal epilepsy. Epilepsy research 26:151-161.

Mathern GW, Pretorius JK, Babb TL (1995a) Quantified patterns of mossy fiber sprouting and neuron densities in hippocampal and lesional seizures. Journal of neurosurgery 82:211-219.

Mathern GW, Pretorius JK, Babb TL, Quinn B (1995b) Unilateral hippocampal mossy fiber sprouting and bilateral asymmetric neuron loss with episodic postictal psychosis. Journal of neurosurgery 82:228-233.

Mattson MP, Guthrie PB, Kater SB (1988) Components of neurite outgrowth that determine neuronal cytoarchitecture: Influence of calcium and the growth substrate. Journal of neuroscience research 20:331-345.

Mazarati A, Sankar R (2006) Status epilepticus: Danse Macabre in a ballet of subunits. Epilepsy Curr 6:102-105.

Mazarati A, Thompson KW, Suchomelova L, Sankar R, Yukiyoshi S, Nissinen J, Pitkanen A, Bertram Edward H, Wasterlain CG (2006) Status Epilepticus: Electrical Stimulation Models. In: Models of Seizures and Epilepsy (Pitkanen, A. et al., eds), pp 439-464 Burlington, MA

San Diego, CA

London, UK: Elsevier Academic Press.

McDonald JW, Garofalo EA, Hood T, Sackellares JC, Gilman S, McKeever PE, Troncoso JC, Johnston MV (1991) Altered excitatory and inhibitory amino acid receptor binding in hippocampus of patients with temporal lobe epilepsy. Annals of neurology 29:529-541.

McKinney RA, Debanne D, Gahwiler BH, Thompson SM (1997) Lesion-induced axonal sprouting and hyperexcitability in the hippocampus in vitro: implications for the genesis of posttraumatic epilepsy. Nat Med 3:990-996.

Mello LE, Cavalheiro EA, Tan AM, Kupfer WR, Pretorius JK, Babb TL, Finch DM (1993) Circuit mechanisms of seizures in the pilocarpine model of chronic epilepsy: cell loss and mossy fiber sprouting. Epilepsia 34:985-995.

Messenheimer JA, Harris EW, Steward O (1979) Sprouting fibers gain access to circuitry transsynaptically altered by kindling. Experimental neurology 64:469-481.

Minturn JE, Fryer HJ, Geschwind DH, Hockfield S (1995) TOAD-64, a gene expressed early in neuronal differentiation in the rat, is related to unc-33, a C. elegans gene involved in axon outgrowth. The Journal of neuroscience : the official journal of the Society for Neuroscience 15:6757-6766.

Molnar P, Nadler JV (1999) Mossy fiber-granule cell synapses in the normal and epileptic rat dentate gyrus studied with minimal laser photostimulation. Journal of neurophysiology 82:1883-1894.

Morales DM, Marklund N, Lebold D, Thompson HJ, Pitkanen A, Maxwell WL, Longhi L, Laurer H, Maegele M, Neugebauer E, Graham DI, Stocchetti N, McIntosh TK

(2005) Experimental models of traumatic brain injury: do we really need to build a better mousetrap? Neuroscience 136:971-989.

Morris DH, Dubnau J, Park JH, Rawls JM, Jr. (2012) Divergent functions through alternative splicing: the Drosophila CRMP gene in pyrimidine metabolism, brain, and behavior. Genetics 191:1227-1238.

Nadler JV, Perry BW, Cotman CW (1980) Selective reinnervation of hippocampal area CA1 and the fascia dentata after destruction of CA3-CA4 afferents with kainic acid. Brain research 182:1-9.

Namura S, Nagata I, Kikuchi H, Andreucci M, Alessandrini A (2000) Serine-threonine protein kinase Akt does not mediate ischemic tolerance after global ischemia in the gerbil. J Cereb Blood Flow Metab 20:1301-1305.

Nawa H, Carnahan J, Gall C (1995) BDNF protein measured by a novel enzyme immunoassay in normal brain and after seizure: partial disagreement with mRNA levels. The European journal of neuroscience 7:1527-1535.

Nguyen C, Hosokawa T, Kuroiwa M, Ip NY, Nishi A, Hisanaga S, Bibb JA (2007) Differential regulation of the Cdk5-dependent phosphorylation sites of inhibitor-1 and DARPP-32 by depolarization. J Neurochem 103:1582-1593.

Niisato E, Nagai J, Yamashita N, Nakamura F, Goshima Y, Ohshima T (2013) Phosphorylation of CRMP2 is involved in proper bifurcation of the apical dendrite of hippocampal CA1 pyramidal neurons. Dev Neurobiol 73:142-151.

Nilsson P, Ronne-Engstrom E, Flink R, Ungerstedt U, Carlson H, Hillered L (1994) Epileptic seizure activity in the acute phase following cortical impact trauma in rat. Brain research 637:227-232.

Nishimura T, Fukata Y, Kato K, Yamaguchi T, Matsuura Y, Kamiguchi H, Kaibuchi K (2003) CRMP-2 regulates polarized Numb-mediated endocytosis for axon growth. NatCell Biol 5:819-826.

Nissinen J, Lukasiuk K, Pitkanen A (2001) Is mossy fiber sprouting present at the time of the first spontaneous seizures in rat experimental temporal lobe epilepsy? Hippocampus 11:299-310.

Noshita N, Lewen A, Sugawara T, Chan PH (2001) Evidence of phosphorylation of Akt and neuronal survival after transient focal cerebral ischemia in mice. J Cereb Blood Flow Metab 21:1442-1450.

O'Dell CM, Das A, Wallace Gt, Ray SK, Banik NL (2012) Understanding the basic mechanisms underlying seizures in mesial temporal lobe epilepsy and possible therapeutic targets: a review. Journal of neuroscience research 90:913-924.

Okazaki MM, Evenson DA, Nadler JV (1995) Hippocampal mossy fiber sprouting and synapse formation after status epilepticus in rats: visualization after retrograde transport of biocytin. The Journal of comparative neurology 352:515-534.

Okazaki MM, Molnar P, Nadler JV (1999) Recurrent mossy fiber pathway in rat dentate gyrus: synaptic currents evoked in presence and absence of seizure-induced growth. Journal of neurophysiology 81:1645-1660.

Ouyang YB, Tan Y, Comb M, Liu CL, Martone ME, Siesjo BK, Hu BR (1999) Survival- and death-promoting events after transient cerebral ischemia: phosphorylation of Akt, release of cytochrome C and Activation of caspase-like proteases. J Cereb Blood Flow Metab 19:1126-1135.

Overman JJ, Carmichael ST (2014) Plasticity in the injured brain: more than molecules matter. Neuroscientist 20:15-28.

Oyesiku NM, Evans CO, Houston S, Darrell RS, Smith JS, Fulop ZL, Dixon CE, Stein DG (1999) Regional changes in the expression of neurotrophic factors and their receptors following acute traumatic brain injury in the adult rat brain. Brain research 833:161-172.

Panayiotopoulos CP (2005) In: The Epilepsies: Seizures, Syndromes and Management Oxfordshire (UK): Bladon Medical Publishing

Bladon Medical Publishing, an imprint of Springer Science+Business Media.

Park KD, Morieux P, Salome C, Cotten SW, Reamtong O, Eyers C, Gaskell SJ, Stables JP, Liu R, Kohn H (2009) Lacosamide isothiocyanate-based agents: novel agents to target and identify lacosamide receptors. Journal of Medicinal Chemistry 52:6897-6911.

Park KD, Stables JP, Liu R, Kohn H (2010) Proteomic searches comparing two (R)-lacosamide affinity baits: An electrophilic arylisothiocyanate and a photoactivated arylazide group. Organic & Biomolecular Chemistry 8:2803-2813.

Patel MN, McNamara JO (1995) Selective enhancement of axonal branching of cultured dentate gyrus neurons by neurotrophic factors. Neuroscience 69:763-770.

Patrick GN, Zukerberg L, Nikolic M, de la Monte S, Dikkes P, Tsai LH (1999) Conversion of p35 to p25 deregulates Cdk5 activity and promotes neurodegeneration. Nature 402:615-622.

Patrylo PR, Dudek FE (1998) Physiological unmasking of new glutamatergic pathways in the dentate gyrus of hippocampal slices from kainate-induced epileptic rats. Journal of neurophysiology 79:418-429.

Patrylo PR, Schweitzer JS, Dudek FE (1999) Abnormal responses to perforant path stimulation in the dentate gyrus of slices from rats with kainate-induced epilepsy and mossy fiber reorganization. Epilepsy research 36:31-42.

Piccini A, Malinow R (2001) Transient oxygen–glucose deprivation induces rapid morphological changes in rat hippocampal dendrites. Neuropharmacology 41:724-729.

Pitkänen A, Immonen RJ, Gröhn OHJ, Kharatishvili I (2009) From traumatic brain injury to posttraumatic epilepsy: What animal models tell us about the process and treatment options. Epilepsia 50:21-29.

Pitkanen A, Kharatishvili I, Nissinen J, McIntosh TK (2006) Posttraumatic Epilepsy Induced by Lateral Fluid-Percussion Brain Injury in Rats. In: Models of Seizures and Epilepsy (Pitkanen, A. et al., eds), pp 465-476 Burlington, MA

San Diego, CA

London, UK: Elsevier Academic Press.

Pitkänen A, Lukasiuk K (2009) Molecular and cellular basis of epileptogenesis in symptomatic epilepsy. Epilepsy & Behavior 14:16-25.

Pitkanen A, McIntosh TK (2006) Animal models of post-traumatic epilepsy. Journal of neurotrauma 23:241-261.

Pitkanen A, Nissinen J, Lukasiuk K, Jutila L, Paljarvi L, Salmenpera T, Karkola K, Vapalahti M, Ylinen A (2000) Association between the density of mossy fiber sprouting and seizure frequency in experimental and human temporal lobe epilepsy. Epilepsia 41 Suppl 6:S24-29.

Povlishock JT, Katz DI (2005) Update of neuropathology and neurological recovery after traumatic brain injury. The Journal of head trauma rehabilitation 20:76-94.

Qiao X, Noebels JL (1993) Developmental analysis of hippocampal mossy fiber outgrowth in a mutant mouse with inherited spike-wave seizures. The Journal of neuroscience : the official journal of the Society for Neuroscience 13:4622-4635.

Racine RJ (1972) Modification of seizure activity by electrical stimulation. II. Motor seizure. Electroencephalogr Clin Neurophysiol 32:281-294.

Rahajeng J, Giridharan SS, Naslavsky N, Caplan S (2010) Collapsin response mediator protein-2 (Crmp2) regulates trafficking by linking endocytic regulatory proteins to dynein motors. Journal of Biological Chemistry.

Ramirez JJ (2001) The role of axonal sprouting in functional reorganization after CNS injury: lessons from the hippocampal formation. Restorative neurology and neuroscience 19:237-262.

Ramirez M, Gutierrez R (2001) Activity-dependent expression of GAD67 in the granule cells of the rat hippocampus. Brain research 917:139-146.

Ramón y Cajal SR (1893) Estructura del asta de Ammon. Anal Soc Esp Hist Nat 22:53-114.

Reeves TM, Kao CQ, Phillips LL, Bullock MR, Povlishock JT (2000) Presynaptic excitability changes following traumatic brain injury in the rat. Journal of neuroscience research 60:370-379.

Reilly PL (2001) Brain injury: the pathophysiology of the first hours.'Talk and Die revisited'. Journal of clinical neuroscience : official journal of the Neurosurgical Society of Australasia 8:398-403.

Represa A, Ben-Ari Y (1992) Kindling is associated with the formation of novel mossy fibre synapses in the CA3 region. Exp Brain Res 92:69-78.

Represa A, Robain O, Tremblay E, Ben-Ari Y (1989) Hippocampal plasticity in childhood epilepsy. Neuroscience letters 99:351-355.

Ribak CE, Tran PH, Spigelman I, Okazaki MM, Nadler JV (2000) Status epilepticus-induced hilar basal dendrites on rodent granule cells contribute to recurrent excitatory circuitry. The Journal of comparative neurology 428:240-253.

Robbins RJ, Brines ML, Kim JH, Adrian T, de Lanerolle N, Welsh S, Spencer DD (1991) A selective loss of somatostatin in the hippocampus of patients with temporal lobe epilepsy. Annals of neurology 29:325-332.

Rogawski MA, Loscher W (2004a) The neurobiology of antiepileptic drugs. Nat Rev Neurosci 5:553-564.

Rogawski MA, Loscher W (2004b) The neurobiology of antiepileptic drugs for the treatment of nonepileptic conditions. Nat Med 10:685-692.

Ryu MJ, Lee C, Kim J, Shin HS, Yu MH (2008) Proteomic analysis of stargazer mutant mouse neuronal proteins involved in absence seizure. Journal of Neurochemistry 104:1260-1270.

Sabel BA (1999) Restoration of vision I: neurobiological mechanisms of restoration and plasticity after brain damage - a review. Restorative neurology and neuroscience 15:177-200.

Sahin B, Hawasli AH, Greene RW, Molkentin JD, Bibb JA (2008) Negative regulation of cyclin-dependent kinase 5 targets by protein kinase C. Eur J Pharmacol 581:270-275.

Salin P, Tseng GF, Hoffman S, Parada I, Prince DA (1995) Axonal sprouting in layer V pyramidal neurons of chronically injured cerebral cortex. The Journal of neuroscience : the official journal of the Society for Neuroscience 15:8234-8245.

Sánchez C, Tompa P, Szücs K, Friedrich P, Avila J (1996) Phosphorylation and dephosphorylation in the proline-rich C-terminal domain of microtubule-associated protein 2. European Journal of Biochemistry 241:765-771.

Santhakumar V, Ratzliff AD, Jeng J, Toth Z, Soltesz I (2001) Long-term hyperexcitability in the hippocampus after experimental head trauma. Annals of neurology 50:708-717.

Sasaki C, Hayashi T, Zhang WR, Warita H, Manabe Y, Sakai K, Abe K (2001) Different expression of glycogen synthase kinase-3beta between young and old rat brains after transient middle cerebral artery occlusion. Neurological research 23:588-592.

Sato Y, Ishida-Nakajima W, Kawamura M, Miura S, Oguma R, Arai H, Takahashi T (2011) Hypoxia–ischemia induces hypo-phosphorylation of collapsin response mediator protein 2 in a neonatal rat model of periventricular leukomalacia. Brain research 1386:165-174.

Scharfman HE, Goodman JH, Sollas AL, Croll SD (2002) Spontaneous limbic seizures after intrahippocampal infusion of brain-derived neurotrophic factor. Experimental neurology 174:201-214.

Scharfman HE, Sollas AL, Berger RE, Goodman JH (2003) Electrophysiological evidence of monosynaptic excitatory transmission between granule cells after seizure-induced mossy fiber sprouting. Journal of neurophysiology 90:2536-2547.

Schauwecker PE, McNeill TH (1995) Enhanced but delayed axonal sprouting of the commissural/associational pathway following a combined entorhinal cortex/fimbria fornix lesion. The Journal of comparative neurology 351:453-464.

Schilling K, Dickinson MH, Connor JA, Morgan JI (1991) Electrical activity in cerebellar cultures determines Purkinje cell dendritic growth patterns. Neuron 7:891-902.

Schmidt EF, Strittmatter SM (2007) The CRMP family of proteins and their role in Sema3A signaling. Advances in Experimental Medicine and Biology 600:1-11.

Schuman EM, Murase S (2003) Cadherins and synaptic plasticity: activity-dependent cyclin-dependent kinase 5 regulation of synaptic beta-catenin-cadherin interactions. Philos Trans R Soc Lond B Biol Sci 358:749-756.

Schwyzer L, Mateos JM, Abegg M, Rietschin L, Heeb L, Thompson SM, Luthi A, Gahwiler BH, McKinney RA (2002) Physiological and morphological plasticity

induced by chronic treatment with NT-3 or NT-4/5 in hippocampal slice cultures. The European journal of neuroscience 16:1939-1948.

Shapira M, Licht A, Milman A, Pick CG, Shohami E, Eldar-Finkelman H (2007) Role of glycogen synthase kinase-3beta in early depressive behavior induced by mild traumatic brain injury. Molecular and cellular neurosciences 34:571-577.

Sharma AK, Reams RY, Jordan WH, Miller MA, Thacker HL, Snyder PW (2007) Mesial temporal lobe epilepsy: pathogenesis, induced rodent models and lesions. Toxicologic pathology 35:984-999.

Shaywitz AJ, Greenberg ME (1999) CREB: a stimulus-induced transcription factor activated by a diverse array of extracellular signals. Annu Rev Biochem 68:821-861.

Sheets PL, Heers C, Stoehr T, Cummins TR (2008) Differential block of sensory neuronal voltage-gated sodium channels by lacosamide [(2R)-2-(acetylamino)-N-benzyl-3-methoxypropanamide], lidocaine, and carbamazepine. Journal of Pharmacology and Experimental Therapeutics 326:89-99.

Shelanski ML, Gaskin F, Cantor CR (1973) Microtubule assembly in the absence of added nucleotides. Proc Natl Acad Sci U S A 70:765-768.

Sholl DA (1953) Dendritic organization in the neurons of the visual and motor cortices of the cat. Journal of Anatomy 87:387-406.

Shumate MD, Lin DD, Gibbs JW, 3rd, Holloway KL, Coulter DA (1998) GABA(A) receptor function in epileptic human dentate granule cells: comparison to epileptic and control rat. Epilepsy research 32:114-128.

Silva AJ, Kogan JH, Frankland PW, Kida S (1998) CREB and memory. Annual review of neuroscience 21:127-148.

Sloviter RS (1991) Permanently altered hippocampal structure, excitability, and inhibition after experimental status epilepticus in the rat: the "dormant basket cell" hypothesis and its possible relevance to temporal lobe epilepsy. Hippocampus 1:41-66.

Sloviter RS (1992) Possible functional consequences of synaptic reorganization in the dentate gyrus of kainate-treated rats. Neuroscience letters 137:91-96.

Smith BN, Dudek FE (2001) Short- and long-term changes in CA1 network excitability after kainate treatment in rats. Journal of neurophysiology 85:1-9.

Solem M, McMahon T, Messing RO (1995) Depolarization-induced neurite outgrowth in PC12 cells requires permissive, low level NGF receptor stimulation and activation of calcium/calmodulin-dependent protein kinase. The Journal of neuroscience : the official journal of the Society for Neuroscience 15:5966-5975.

Sousa SF, Fernandes PA, Ramos MJ (2006) Protein-ligand docking: current status and future challenges. Proteins 65:15-26.

Spigelman I, Yan XX, Obenaus A, Lee EY, Wasterlain CG, Ribak CE (1998) Dentate granule cells form novel basal dendrites in a rat model of temporal lobe epilepsy. Neuroscience 86:109-120.

Stanfield BB (1989) Excessive intra- and supragranular mossy fibers in the dentate gyrus of tottering (tg/tg) mice. Brain research 480:294-299.

Statler KD, Swank S, Abildskov T, Bigler ED, White HS (2008) Traumatic brain injury during development reduces minimal clonic seizure thresholds at maturity. Epilepsy research 80:163-170.

Stein DG (1998) Brain injury and theories of recovery. Armonk, NY: Futura Publishing Co.

Stenmark P, Ogg D, Flodin S, Flores A, Kotenyova T, Nyman T, Nordlund P, Kursula P (2007) The structure of human collapsin response mediator protein 2, a regulator of axonal growth. Journal of Neurochemistry 101:906-917.

Steward O (1982) Assessing the functional significance of lesion-induced neuronal plasticity. International review of neurobiology 23:197-254.

Steward O (1992) Lesion-induced synapse reorganization in the hippocampus of cats: sprouting of entorhinal, commissural/associational, and mossy fiber projections after unilateral entorhinal cortex lesions, with comments on the normal organization of these pathways. Hippocampus 2:247-268.

Storm-Mathisen J (1974) Choline acetyltransferase and acetylcholinesterase in fascia dentata following lesion of the entorhinal afferents. Brain research 80:181-197.

Struthers RS, Vale WW, Arias C, Sawchenko PE, Montminy MR (1991) Somatotroph hypoplasia and dwarfism in transgenic mice expressing a non-phosphorylatable CREB mutant. Nature 350:622-624.

Styren SD, Miller PD, Lagenaur CF, DeKosky ST (1995) Alternate strategies in lesion-induced reactive synaptogenesis: differential expression of L1 in two populations of sprouting axons. Experimental neurology 131:165-173.

Sutula T (2002) Seizure-Induced Axonal Sprouting: Assessing Connections Between Injury, Local Circuits, and Epileptogenesis. Epilepsy Curr 2:86-91.

Sutula T, Cascino G, Cavazos J, Parada I, Ramirez L (1989) Mossy fiber synaptic reorganization in the epileptic human temporal lobe. Annals of neurology 26:321-330.

Sutula T, Harrison C, Steward O (1986) Chronic epileptogenesis induced by kindling of the entorhinal cortex: the role of the dentate gyrus. Brain research 385:291-299.

Sutula T, He XX, Cavazos J, Scott G (1988) Synaptic reorganization in the hippocampus induced by abnormal functional activity. Science 239:1147-1150.

Sutula T, Zhang P, Lynch M, Sayin U, Golarai G, Rod R (1998) Synaptic and axonal remodeling of mossy fibers in the hilus and supragranular region of the dentate gyrus in kainate-treated rats. The Journal of comparative neurology 390:578-594.

Sutula TP (2004) Mechanisms of epilepsy progression: current theories and perspectives from neuroplasticity in adulthood and development. Epilepsy research 60:161-171.

Tan M, Ma S, Huang Q, Hu K, Song B, Li M (2013) GSK-3alpha/beta-mediated phosphorylation of CRMP-2 regulates activity-dependent dendritic growth. J Neurochem 125:685-697.

Tang H, Long H, Zeng C, Li Y, Bi F, Wang J, Qian H, Xiao B (2012) Rapamycin suppresses the recurrent excitatory circuits of dentate gyrus in a mouse model of temporal lobe epilepsy. Biochemical and biophysical research communications 420:199-204.

Tang SJ, Reis G, Kang H, Gingras AC, Sonenberg N, Schuman EM (2002) A rapamycin-sensitive signaling pathway contributes to long-term synaptic plasticity in the hippocampus. Proc Natl Acad Sci U S A 99:467-472.

Tauck DL, Nadler JV (1985) Evidence of functional mossy fiber sprouting in hippocampal formation of kainic acid-treated rats. The Journal of neuroscience : the official journal of the Society for Neuroscience 5:1016-1022.

Temkin NR (2009) Preventing and treating posttraumatic seizures: The human experience. Epilepsia 50:10-13.

Thompson HJ, Lifshitz J, Marklund N, Grady MS, Graham DI, Hovda DA, McIntosh TK (2005) Lateral fluid percussion brain injury: a 15-year review and evaluation. Journal of neurotrauma 22:42-75.

Tian FF, Zeng C, Ma YF, Guo TH, Chen JM, Chen Y, Cai XF, Li FR, Wang XH, Huang WJ, Wang YZ (2010) Potential roles of Cdk5/p35 and tau protein in hippocampal mossy fiber sprouting in the PTZ kindling model. Clinical laboratory 56:127-136.

Timm F (1958) Zur Histochemie der Schwermetalle Das Sulfid-Silberverfahren. Dtsch Z ges gerichtl Med 46:706-711.

Tomizawa K, Cai XH, Moriwaki A, Matsushita M, Matsui H (2000) Involvement of cyclin-dependent kinase 5/p35(nck5a) in the synaptic reorganization of rat hippocampus during kindling progression. Jpn J Physiol 50:525-532.

Toth Z, Hollrigel GS, Gorcs T, Soltesz I (1997) Instantaneous perturbation of dentate interneuronal networks by a pressure wave-transient delivered to the neocortex. The Journal of neuroscience : the official journal of the Society for Neuroscience 17:8106-8117.

Tran LD, Lifshitz J, Witgen BM, Schwarzbach E, Cohen AS, Grady MS (2006) Response of the contralateral hippocampus to lateral fluid percussion brain injury. Journal of neurotrauma 23:1330-1342.

Turski WA, Cavalheiro EA, Bortolotto ZA, Mello LM, Schwarz M, Turski L (1984) Seizures produced by pilocarpine in mice: a behavioral, electroencephalographic and morphological analysis. Brain research 321:237-253.

Turski WA, Cavalheiro EA, Schwarz M, Czuczwar SJ, Kleinrok Z, Turski L (1983) Limbic seizures produced by pilocarpine in rats: behavioural, electroencephalographic and neuropathological study. Behavioural brain research 9:315-335.

Uchida Y, Ohshima T, Sasaki Y, Suzuki H, Yanai S, Yamashita N, Nakamura F, Takei K, Ihara Y, Mikoshiba K, Kolattukudy P, Honnorat J, Goshima Y (2005) Semaphorin3A signalling is mediated via sequential Cdk5 and GSK3beta phosphorylation of CRMP2: implication of common phosphorylating mechanism underlying axon guidance and Alzheimer's disease. Genes to Cells 10:165-179.

Uchida Y, Ohshima T, Yamashita N, Ogawara M, Sasaki Y, Nakamura F, Goshima Y (2009) Semaphorin3A signaling mediated by Fyn-dependent tyrosine phosphorylation of collapsin response mediator protein 2 at tyrosine 32. J Biol Chem 284:27393-27401.

Ueno Y, Chopp M, Zhang L, Buller B, Liu Z, Lehman NL, Liu XS, Zhang Y, Roberts C, Zhang ZG (2012) Axonal outgrowth and dendritic plasticity in the cortical peri-infarct area after experimental stroke. Stroke 43:2221-2228.

Vaidya VA, Siuciak JA, Du F, Duman RS (1999) Hippocampal mossy fiber sprouting induced by chronic electroconvulsive seizures. Neuroscience 89:157-166.

van den Bogaart G, Meyenberg K, Diederichsen U, Jahn R (2012) Phosphatidylinositol 4,5-bisphosphate increases Ca2+ affinity of synaptotagmin-1 by 40-fold. J Biol Chem 287:16447-16453.

Van Ooyen A, Van Pelt J, Corner MA (1995) Implications of activity dependent neurite outgrowth for neuronal morphology and network development. Journal of Theoretical Biology 172:63-82.

van Pelt J, van Ooyen A, Corner MA (1996) Growth cone dynamics and activity-dependent processes in neuronal network development. Progress in brain research 108:333-346.

Varrin-Doyer M, Vincent P, Cavagna S, Auvergnon N, Noraz N, Rogemond V, Honnorat J, Moradi-Ameli M, Giraudon P (2009) Phosphorylation of collapsin response mediator protein 2 on Tyr-479 regulates CXCL12-induced T lymphocyte migration. J Biol Chem 284:13265-13276.

Vezzani A, Ravizza T, Moneta D, Conti M, Borroni A, Rizzi M, Samanin R, Maj R (1999) Brain-derived neurotrophic factor immunoreactivity in the limbic system of rats after acute seizures and during spontaneous convulsions: temporal evolution of changes as compared to neuropeptide Y. Neuroscience 90:1445-1461.

Vincent P, Collette Y, Marignier R, Vuaillat C, Rogemond V, Davoust N, Malcus C, Cavagna S, Gessain A, Machuca-Gayet I, Belin MF, Quach T, Giraudon P (2005) A role for the neuronal protein collapsin response mediator protein 2 in T lymphocyte polarization and migration. Journal of immunology (Baltimore, Md : 1950) 175:7650-7660.

Volman V, Bazhenov M, Sejnowski TJ (2011) Pattern of trauma determines the threshold for epileptic activity in a model of cortical deafferentation. Proc Natl Acad Sci U S A 108:15402-15407.

Vuaillat C, Varrin-Doyer M, Bernard A, Sagardoy I, Cavagna S, Chounlamountri I, Lafon M, Giraudon P (2008) High CRMP2 expression in peripheral T lymphocytes is associated with recruitment to the brain during virus-induced neuroinflammation. Journal of neuroimmunology 193:38-51.

Walker MC, Ruiz A, Kullmann DM (2001) Monosynaptic GABAergic signaling from dentate to CA3 with a pharmacological and physiological profile typical of mossy fiber synapses. Neuron 29:703-715.

Wang B, Dawson H, Wang H, Kernagis D, Kolls BJ, Yao L, Laskowitz DT (2013) Lacosamide improves outcome in a murine model of traumatic brain injury. Neurocrit Care 19:125-134.

Wang LH, Strittmatter SM (1996) A family of rat CRMP genes is differentially expressed in the nervous system. J Neurosci 16:6197-6207.

Wang LH, Strittmatter SM (1997) Brain CRMP forms heterotetramers similar to liver dihydropyrimidinase. J Neurochem 69:2261-2269.

Wang QM, Roach PJ, Fiol CJ (1994) Use of a Synthetic Peptide as a Selective Substrate for Glycogen Synthase Kinase 3. Analytical Biochemistry 220:397-402.

Wang Y, Brittain JM, Jarecki BW, Park KD, Wilson SM, Wang B, Hale R, Meroueh SO, Cummins TR, Khanna R (2010a) In silico docking and electrophysiological characterization of lacosamide binding sites on collapsin response mediator protein 2 (CRMP-2) identifies a pocket important in modulating sodium channel slow inactivation. Journal of Biological Chemistry.

Wang Y, Brittain JM, Wilson SM, Hingtgen CM, Khanna R (2010b) Altered Calcium Currents and Axonal Growth in Nf1 Haploinsufficient Mice. Translational Neuroscience 1:106-114.

Wang Y, Park KD, SalomeY C, Wilson SM, Stables JP, Liu R, Khanna R, Kohn H (2010c) Development and Characterization of Novel Derivatives of the Antiepileptic Drug Lacosamide That Exhibit Far Greater Enhancement in Slow Inactivation of Voltage-Gated Sodium Channels. ACS Chemical Neuroscience 2:90-106.

Wang Y, Wilson SM, Brittain JM, Ripsch MS, SalomeÝ• C, Park KD, White FA, Khanna R, Kohn H (2011) Merging Structural Motifs of Functionalized Amino Acids and +Ý-Aminoamides Results in Novel Anticonvulsant Compounds with Significant Effects on Slow and Fast Inactivation of Voltage-Gated Sodium Channels and in the Treatment of Neuropathic Pain. ACS Chemical Neuroscience 2:317-332.

Wasterlain CG, Stohr T, Matagne A (2011) The acute and chronic effects of the novel anticonvulsant lacosamide in an experimental model of status epilepticus. Epilepsy research 94:10-17.

Wayman GA, Impey S, Marks D, Saneyoshi T, Grant WF, Derkach V, Soderling TR (2006) Activity-Dependent Dendritic Arborization Mediated by CaM-Kinase I Activation and Enhanced CREB-Dependent Transcription of Wnt-2. Neuron 50:897-909.

Wei FY, Tomizawa K, Ohshima T, Asada A, Saito T, Nguyen C, Bibb JA, Ishiguro K, Kulkarni AB, Pant HC, Mikoshiba K, Matsui H, Hisanaga S (2005) Control of cyclin-dependent kinase 5 (Cdk5) activity by glutamatergic regulation of p35 stability. J Neurochem 93:502-512.

Wenzel HJ, Woolley CS, Robbins CA, Schwartzkroin PA (2000) Kainic acid-induced mossy fiber sprouting and synapse formation in the dentate gyrus of rats. Hippocampus 10:244-260.

West JR (1984) Age-dependent sprouting in the dentate gyrus demonstrated with anterograde HRP. Brain research bulletin 12:323-330.

Wienken CJ, Baaske P, Rothbauer U, Braun D, Duhr S (2010) Protein-binding assays in biological liquids using microscale thermophoresis. Nat Commun 1:100.

Wieser HG, Hane A (2004) Antiepileptic drug treatment in seizure-free mesial temporal lobe epilepsy patients with hippocampal sclerosis following selective amygdalohippocampectomy. Seizure : the journal of the British Epilepsy Association 13:534-536.

Williams AJ, Hartings JA, Lu XC, Rolli ML, Dave JR, Tortella FC (2005) Characterization of a new rat model of penetrating ballistic brain injury. Journal of neurotrauma 22:313-331.

Williams AJ, Hartings JA, Lu XC, Rolli ML, Tortella FC (2006) Penetrating ballistic-like brain injury in the rat: differential time courses of hemorrhage, cell death, inflammation, and remote degeneration. Journal of neurotrauma 23:1828-1846.

Willmore LJ (1992) Posttraumatic epilepsy. Neurologic clinics 10:869-878.

Wilson SM, Xiong W, Wang Y, Ping X, Head JD, Brittain JM, Gagare PD, Ramachandran PV, Jin X, Khanna R (2012) Prevention of posttraumatic axon sprouting by blocking collapsin response mediator protein 2-mediated neurite outgrowth and tubulin polymerization. Neuroscience 210:451-466.

Witgen BM, Lifshitz J, Smith ML, Schwarzbach E, Liang SL, Grady MS, Cohen AS (2005) Regional hippocampal alteration associated with cognitive deficit following experimental brain injury: a systems, network and cellular evaluation. Neuroscience 133:1-15.

Wolff C, Carrington B, Varrin-Doyer M, Vandendriessche A, Van der Perren C, Famelart M, Gillard M, Foerch P, Rogemond V, Honnorat J, Lawson A, Miller K (2012) Drug Binding Assays do not Reveal Specific Binding of Lacosamide to Collapsin Response Mediator Protein 2 (CRMP-2). CNS Neuroscience & Therapeutics 18:493-500.

Wong M (2010) Mammalian target of rapamycin (mTOR) inhibition as a potential antiepileptogenic therapy: From tuberous sclerosis to common acquired epilepsies. Epilepsia 51:27-36.

Wu P, Hu YZ (2010) PI3K/Akt/mTOR pathway inhibitors in cancer: a perspective on clinical progress. Current medicinal chemistry 17:4326-4341.

Wuarin JP, Dudek FE (1996) Electrographic seizures and new recurrent excitatory circuits in the dentate gyrus of hippocampal slices from kainate-treated epileptic rats. The Journal of neuroscience : the official journal of the Society for Neuroscience 16:4438-4448.

Wuarin JP, Dudek FE (2001) Excitatory synaptic input to granule cells increases with time after kainate treatment. Journal of neurophysiology 85:1067-1077.

Wuarin JP, Peacock WJ, Dudek FE (1992) Single-electrode voltage-clamp analysis of the N-methyl-D-aspartate component of synaptic responses in neocortical slices from children with intractable epilepsy. Journal of neurophysiology 67:84-93.

Wullschleger S, Loewith R, Hall MN (2006) TOR signaling in growth and metabolism. Cell 124:471-484.

Xerri C, Merzenich MM, Peterson BE, Jenkins W (1998) Plasticity of primary somatosensory cortex paralleling sensorimotor skill recovery from stroke in adult monkeys. Journal of neurophysiology 79:2119-2148.

Xiong T, Tang J, Zhao J, Chen H, Zhao F, Li J, Qu Y, Ferriero D, Mu D (2012) Involvement of the Akt/GSK-3β/CRMP-2 pathway in axonal injury after hypoxic–ischemic brain damage in neonatal rat. Neuroscience 216:123-132.

Xu GF, O'Connell P, Viskochil D, Cawthon R, Robertson M, Culver M, Dunn D, Stevens J, Gesteland R, White R, et al. (1990) The neurofibromatosis type 1 gene encodes a protein related to GAP. Cell 62:599-608.

Yakovlev AG, Knoblach SM, Fan L, Fox GB, Goodnight R, Faden AI (1997) Activation of CPP32-like caspases contributes to neuronal apoptosis and neurological dysfunction after traumatic brain injury. The Journal of neuroscience : the official journal of the Society for Neuroscience 17:7415-7424.

Yamashita N, Ohshima T, Nakamura F, Kolattukudy P, Honnorat J, Mikoshiba K, Goshima Y (2012) Phosphorylation of CRMP2 (collapsin response mediator protein 2) is involved in proper dendritic field organization. The Journal of neuroscience : the official journal of the Society for Neuroscience 32:1360-1365.

Yan Q, Radeke MJ, Matheson CR, Talvenheimo J, Welcher AA, Feinstein SC (1997) Immunocytochemical localization of TrkB in the central nervous system of the adult rat. The Journal of comparative neurology 378:135-157.

Yang K, Perez-Polo JR, Mu XS, Yan HQ, Xue JJ, Iwamoto Y, Liu SJ, Dixon CE, Hayes RL (1996) Increased expression of brain-derived neurotrophic factor but not neurotrophin-3 mRNA in rat brain after cortical impact injury. Journal of neuroscience research 44:157-164.

Yang L, Afroz S, Michelson HB, Goodman JH, Valsamis HA, Ling DS (2010a) Spontaneous epileptiform activity in rat neocortex after controlled cortical impact injury. Journal of neurotrauma 27:1541-1548.

Yang T, Zhou D, Stefan H (2010b) Why mesial temporal lobe epilepsy with hippocampal sclerosis is progressive: uncontrolled inflammation drives disease progression? Journal of the neurological sciences 296:1-6.

Yano S, Morioka M, Fukunaga K, Kawano T, Hara T, Kai Y, Hamada J, Miyamoto E, Ushio Y (2001) Activation of Akt/protein kinase B contributes to induction of ischemic tolerance in the CA1 subfield of gerbil hippocampus. J Cereb Blood Flow Metab 21:351-360.

Yoneda A, Morgan-Fisher M, Wait R, Couchman JR, Wewer UM (2012) A collapsin response mediator protein 2 isoform controls myosin II-mediated cell migration and matrix assembly by trapping ROCK II. Molecular and cellular biology 32:1788-1804.

Yoshimura T, Kawano Y, Arimura N, Kawabata S, Kikuchi A, Kaibuchi K (2005) GSK-3[beta] Regulates Phosphorylation of CRMP-2 and Neuronal Polarity. Cell 120:137-149.

Zeng LH, Rensing NR, Wong M (2009) The mammalian target of rapamycin signaling pathway mediates epileptogenesis in a model of temporal lobe epilepsy. The Journal of neuroscience : the official journal of the Society for Neuroscience 29:6964-6972.

Zhang X, Chen Y, Ikonomovic MD, Nathaniel PD, Kochanek PM, Marion DW, DeKosky ST, Jenkins LW, Clark RS (2006) Increased phosphorylation of protein kinase B and related substrates after traumatic brain injury in humans and rats. J Cereb Blood Flow Metab 26:915-926.

Zhang X, Cui SS, Wallace AE, Hannesson DK, Schmued LC, Saucier DM, Honer WG, Corcoran ME (2002) Relations between brain pathology and temporal lobe epilepsy. The Journal of neuroscience : the official journal of the Society for Neuroscience 22:6052-6061.

Zhang Z, Majava V, Greffier A, Hayes RL, Kursula P, Wang KK (2009) Collapsin response mediator protein-2 is a calmodulin-binding protein. Cell MolLife Sci 66:526-536.

Zhao S, Fu J, Liu X, Wang T, Zhang J, Zhao Y (2012) Activation of Akt/GSK-3beta/beta-catenin signaling pathway is involved in survival of neurons after traumatic brain injury in rats. Neurological research 34:400-407.

Zhou Y, Bhatia I, Cai Z, He Q-Y, Cheung P-T, Chiu J-F (2008) Proteomic Analysis of Neonatal Mouse Brain: Evidence for Hypoxia- and Ischemia-Induced Dephosphorylation of Collapsin Response Mediator Proteins. Journal of Proteome Research 7:2507-2515.

Zhu H, Nie L, Maki CG (2005) Cdk2-dependent Inhibition of p21 stability via a C-terminal cyclin-binding motif. J Biol Chem 280:29282-29288.

Zhu LQ, Zheng HY, Peng CX, Liu D, Li HL, Wang Q, Wang JZ (2010) Protein phosphatase 2A facilitates axonogenesis by dephosphorylating CRMP2. The Journal of neuroscience : the official journal of the Society for Neuroscience 30:3839-3848.

Zimmer J (1973) Changes in the Timm sulfide silver staining pattern of the rat hippocampus and fascia dentata following early postnatal deafferentation. Brain research 64:313-326.

CURRICULUM VITAE

Sarah Marie Wilson

A. Education

INDIANA UNIVERSITY
Indianapolis, Indiana
Ph.D. Medical Neuroscience 2014
Mentor: Dr. Rajesh Khanna

INDIANA UNIVERSITY
Bloomington, Indiana
Bachelor of Science with Honors, High Distinction – Psychology, 2009

B. Positions and Honors

Position	Year(s)	Field	Institution
Undergraduate Research Assistant	2006-2009	Psychology	Indiana University, Bloomington
Undergraduate Teaching Intern	2007-2009	Biology	Indiana University, Bloomington
Post-baccalaureate Research Assistant	2009	Pharmacology	Stark Neurosciences Research Institute
PhD Candidate	2010-2014	Medical Neuroscience	Indiana University School of Medicine
Graduate Teaching Assistant	2012	Biochemistry	Indiana University School of Medicine

Dean's List, College of Arts and Sciences – Indiana University, May 2006 – May 2009
Phi Beta Kappa Honors Society – Indiana University, May 2009
Founder's Scholar – Indiana University, May 2009
Paul and Carole Stark Pre-doctoral Fellowship – Indiana University School of Medicine, August 2010
2nd place, Sigma Xi Research Competition – Indiana University School of Medicine, August 2011
IUSM Travel Grant – Indiana University School of Medicine, December 2011
Travel Bursary, 4th International Congress on Neuropathic Pain – NeupSIG, Toronto, May 2013
Larry Kays, M.D. Student Fellowship – Indiana University School of Medicine, August 2013
2nd Place, Gill Thesis Award – Indiana University, September 2013

C.   Publications

1. **Wilson SM**, Park KD, and Khanna R. Differential regulation of CRMP2 phosphorylation following TBI: implications for mossy fiber sprouting. Translational Neuroscience. 2014. [in preparation].
2. **Wilson SM** and Khanna R. CRMP2 and Lacosamide: Strange bedfellows or complete strangers? Molecular Neurobiology. 2014. [in preparation].
3. **Wilson SM** and Khanna R. Activity-dependent changes in CRMP2 phosphorylation contribute to neurite outgrowth following chronic depolarization. Journal of Neurochemistry. 2014 [in preparation].
4. Due MR, **Wilson SM,** Ripsch MS, Khanna R, White FA. Novel pharmacotherapy for neuropathic pain in the rodent: the effects of morphine in combination with carbamazepine. PAIN. 2013 [in review].
5. Quach TT, **Wilson SM**, Rogemond V, Chounlamountri N, Kolattukudy PE, Martinez S, Khanna M, Belin MF, Khanna R, Honnorat J, Duchemin AM. Mapping CRMP3 domains involved in dendrite morphogenesis and voltage-gated calcium channel regulation. Journal of Cell Science. 2013 Jul 18 [Epub ahead of print].
6. Dustrude ET, **Wilson SM,** Ju W, Xiao Y, Khanna R. CRMP2 SUMOylation modulates NaV1.7 trafficking. Journal of Biological Chemistry. 2013 Jul 8. [Epub ahead of print]
7. Lee H, Park KD, Yang XF, Dustrude ET, **Wilson SM**, Khanna R, Kohn H. (Biphenyl-4-yl)methylammonium chlorides: potent anticonvulsants that modulate Na^+ channels. Journal of Medicinal Chemistry. 2013 Jul 3 [Epud ahead of print].
8. Mowery TM, **Walls SM**, Garraghty PE. AMPA and $GABA_{A/B}$ receptor subunit expression in the cortex of adult squirrel monkeys during peripheral nerve regeneration. Brain Research. 2013 May 2. [Epub ahead of print]
9. Ju W, Li Q, **Wilson SM**, Brittain JM, Meroueh L, Khanna R. SUMOylation alters CRMP2 regulation of calcium influx in sensory neurons. Channels (Austin). 2013 Mar 19;7(3). [Epub ahead of print]
10. Khanna R, **Wilson SM**, Brittain JM, Weimer J, Sultana R, Butterfield A, Hensley K. Opening Pandora's jar: a primer on the putative roles of CRMP2 in a panoply of neurodegenerative, sensory and motor neuron, and central disorders. Future Neurology. 2012 Nov 1;7(6):749-771.
11. King AM, Yang XF, Wang Y, Dustrude ET, Barbosa C, Due MR, Piekarz AD, **Wilson SM**, White FA, Salomé C, Cummins TR, Khanna R, Kohn H. Identification of the benzylprowyophenyl pharmacophoreL a structural unit that promotes sodium channel inactivation. ACS Chemical Neuroscience. 2012 Dec 19;3 (12):1037-49.
12. **Wilson SM,** Schmutzler BS, Brittain JM, Dustrude ET, Ripsch MS, Pellman JJ, Yeum TS, Hurley JH, Hingtgen CM, White FA, Khanna R. Inhibition of transmitter release and attenuation of AIDS therapy-induced and tibial nerve injury-related painful peripheral neuropathy by novel synthetic Ca2+ channel peptides. Journal of Biological Chemistry. 2012 Oct 12;287(42):35065-77.
13. **Wilson SM**, Xiong W, Wang Y, Ping X, Head JD, Brittain JM, Gagare PD, Ramachandran V, Jin X, and Khanna R.   Prevention of posttraumatic axon

sprouting by blocking CRMP2-mediated neurite outgrowth and tubulin polymerization. Neuroscience. 2012 Mar; 210: 451-66.

14. Brittain JM, Wang Y, **Wilson SM**, Khanna R. Regulation of CREB signaling through L-Type Ca^{2+} channels by Nipsnap-2. Channels (Austin). 2012 Mar.

15. Khanna M, Wang F, Jo I, Knabe WE, **Wilson SM,** Li L, Bum-Erdene K, Li J, W. Sledge G, Khanna R, Meroueh SO. Targeting multiple conformations leads to small molecule inhibitors of the uPAR.uPA protein-protein interaction that blocks cancer cell invasion. ACS Chem Biol. 2011 Sep 29; 6 (11): 1231-43.

16. **Wilson SM**, Brittain JM, Piekarz AD, Ballard CJ, Ripsch MS, Cummins TR, Hurley JH, Khanna M, Hammes NM, Samuels BC, White FA, Khanna R. Further insights into the antinociceptive potential of a peptide disrupting the N-type calcium channel-CRMP-2 signaling complex. Channels (Austin). 2011 Sep 1;5(5).

17. Brittain JM, Chen L, **Wilson SM**, Brustovetsky T, Gao X, Ashpole NM, Molosh AI, You H, Hudmon A, Shekhar A, White FA, Zamponi GW, Brustovetsky N, Chen J, Khanna R. Neuroprotection against traumatic brain injury by a peptide derived from the collapsin response mediator protein 2 (CRMP2). J Biol Chem. 2011 Aug 9. [Epub ahead of print]

18. Wang Y, **Wilson SM**, Brittain JM, Ripsch MS, Salomé C, Park KD, White FA, Khanna R and Kohn H. Merging Structural Motifs of Functionalized Amino Acids and α-Aminoamides Results in Novel Anticonvulsant Compounds with Significant Effects on Slow and Fast Inactivation of Voltage-gated Sodium Channels and in the Treatment of Neuropathic Pain. ACS Chemical Neuroscience. 2011 Jun 15;2(6):317-322

19. Brittain JM, Duarte DB, **Wilson SM**, Zhu W, Ballard C, Johnson PL, Liu N, Xiong W, Ripsch MS, Wang Y, Fehrenbacher JC, Fitz JD, Khanna M, Park CK, Schmutzler BS, Cheon BM, Due MR, Brustovetsky T, Ashpole NM, Hudmon A, Meroueh SO, Hingtgen CM, Brustovetsky N, Ji RR, Hurley JH, Jin X, Shekhar A, Xu XM, Oxford GS, Vasko MR, White FA, Khanna R. Suppression of inflammatory and neuropathic pain by uncoupling CRMP-2 from the presynaptic Ca^{2+} channel complex. Nature Medicine. 2011 Jun 5;17(7):822-9.

20. Wang Y, Park KD, Salome C, **Wilson SM,** Stables JP, Liu R, Khanna R, Kohn H. Development and characterization of novel derivatives of the antiepileptic drug lacosamide that exhibit far greater enhancement in slow inactivation of voltage-gated sodium channels. ACS Chemical Neuroscience. 2010. 2(2):90-106.

21. Wang Y, Brittain JM, **Wilson SM**, Hingtgen CM, Khanna R (2010) Altered calcium currents and axonal growth in Nf1 haploinsufficient mice. *Translational Neuroscience* **1:** 106-114

22. Wang Y, Brittain JM, Jarecki BW, Park KD, **Wilson SM**, Wang B, Hale R, Meroueh SO, Cummins TR, Khanna R (2010) In silico docking and electrophysiological characterization of lacosamide binding sites on collapsin response mediator protein 2 (CRMP-2) identifies a pocket important in modulating sodium channel slow inactivation. The Journal of biological chemistry 285:25296-307.

23. Wang Y, Brittain JM, **Wilson SM**, Khanna R (2010) Emerging roles of collapsin response mediator proteins (CRMPs) as regulators of voltage-gated calcium channels and synaptic transmission. Communicative and Integrative Biology 3:58-61.

D.   Abstracts

Wilson SM, Schmutzler B, Brittain J, Dustrude E, Ripsch M, Pellman J, Yeum T-S, Hurly J, Hingtgen C, White F, Khanna R (2013). Inhibition of transmitter release and attenuation of painful peripheral neuropathy by novel synthetic Ca^{2+} channel peptides. 4th International Congress on Neuropathic Pain, NeupSIG, Toronto, ON, Canada.

Due MR, Feldman P, **Wilson SM**, Allette YM, Ripsch MS, Grych H, Cheng K, Yin H, Khanna R, White F. (2013). The time dependent role of neuronal RAGE (receptor for advanced glycosylation end-products) in a rat model of neuropathic pain. 4th International Congress on Neuropathic Pain, NeupSIG. Toronto, ON, Canada

Wilson SM, Xiong W, Head J, Brittain J, Gagare P, Singh I, Ramachandran P, Jin X, Khanna R (2012) Targeting CRMP2-mediated sprouting in posttraumatic epileptogenesis. Gordon Research Conference: Mechanisms of epilepsy and neuronal synchronization. Waterville Valley, New Hampshire.

Khanna R, Brittain JM, Duarte DB, **Wilson SM**, Zhu W, Ballard C, Johnson PL, Lui N, Xiong W, Ripsch MS, Wang Y, Fehrenbacher JC, Khanna M, Park CK, Brustovetsky N, Ji RR, Hurler JH, Jin X, Shekhar A, Xu X, Oxford GS, Vasko MR, White FA. Suppression of inflammatory and neuropathic pain by uncoupling collapsin response mediator protein 2 (CRMP2) from the presynaptic calcium channel complex. (2012). FASEB, San Diego, CA.

Wilson SM, Xiong W, Head J, Brittain J, Gagare P, Ramachandran P, Jin X, Khanna R. (2011) The   anticonvulsant Lacosamide inhibits CRMP2 mediated neurite outgrowth in vitro and prevents enhanced   excitatory connectivity in an animal model of posttraumatic epileptogenesis. Society for Neuroscience.   Washington D.C.

Wilson SM, Schmutzler BS, Brittain JM, Garcia AS, Hingtgen CH, Khanna R. (2011). Differential lipid raft targeting of neurofibromin and CRMP-2 and regulation of transmitter release by CRMP-2 in sensory neurons from *Nf1* haploinsufficient mice. Gill Symposium. Bloomington, Indiana.